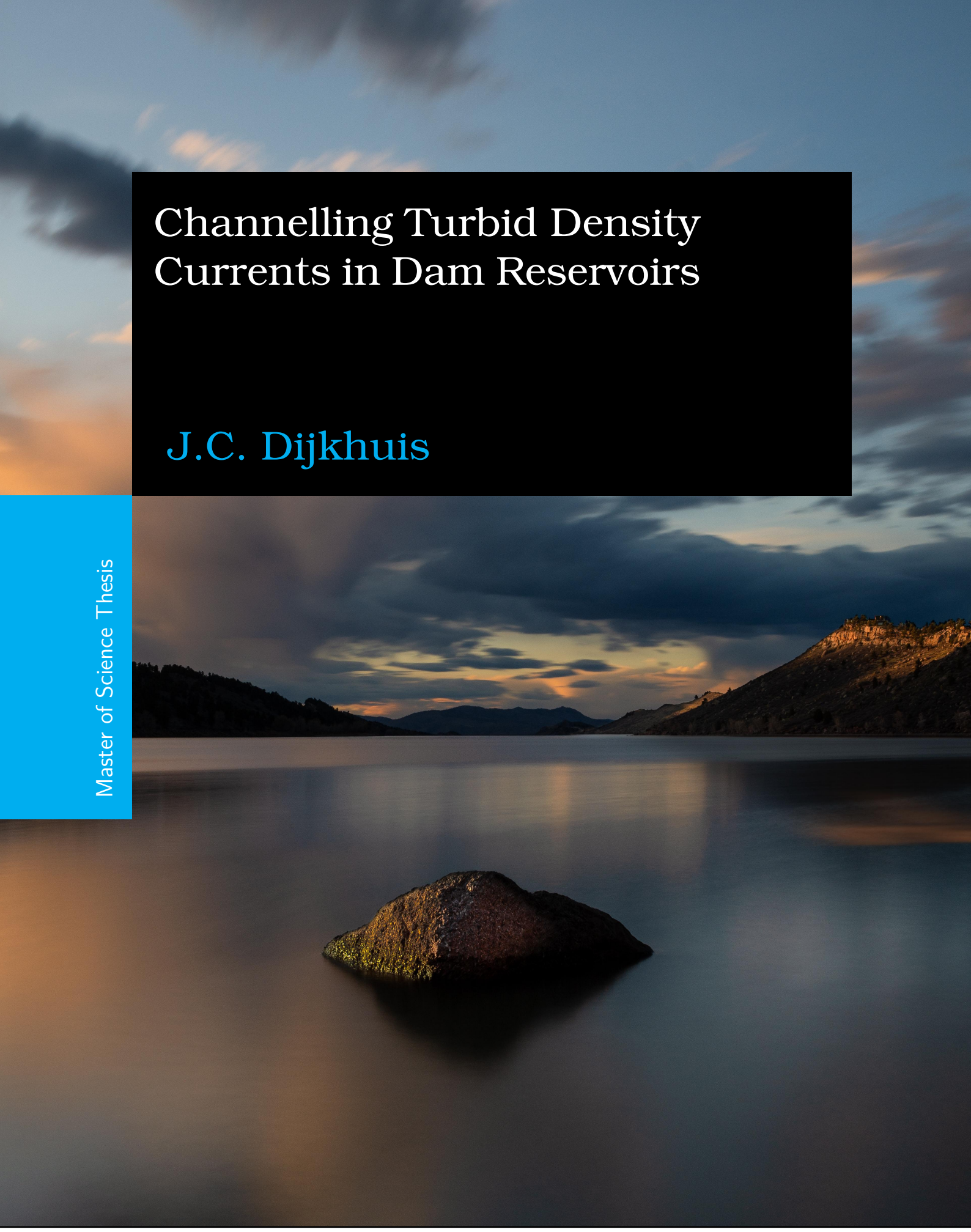

Channelling Turbid Density Currents in Dam Reservoirs

J.C. Dijkhuis

Master of Science Thesis

TU Delft Delft University of Technology

Hydraulic Engineering and Offshore & Dredging Engineering

Channelling Turbid Density Currents in Dam Reservoirs

by

J.C. Dijkhuis

to obtain the degree Master of Science
at Delft University of Technology,
to be defended publicly on July 15th, 2019 at 13:30.

Student number: 4257308
Project duration: September 17, 2018 – Juli 8, 2019
Thesis committee:

Prof. dr. ir. C. van Rhee	TU Delft
Dr. Ir. C. J. Sloff	TU Delft, Deltares
Dr. Ir. G. H. Keetels	TU Delft
Dr. Ir. J. C. Goeree	Royal IHC, TU Delft

TU Delft Delft University of Technology

IHC

"In a gentle way you can shake the world"

Mahatma Gandhi

Preface

The report In front of you is my Master Thesis project. This thesis not only marks the end of a nine-month project where I had the opportunity to integrate knowledge and skills I have gained throughout my academic career, but it also marks the end of my student time at the TU Delft.

This thesis has been a great and exciting challenge in which I had to broaden and deepen my knowledge continuously. This thesis would not have been so pleasant without the people I have gathered around me. I want to take the opportunity to thank those who have supported me through this process.

First, I want to express my gratitude to my daily supervisors from the TU Delft; Prof. Dr. Ir. C. van Rhee, Cees, and Dr. Ir. C.J. Sloff, Kees. Whom both are outstanding researchers and engineers that have a lot of experience in dredging and reservoir engineering. It was a great pleasure and opportunity to work with, and learn from, their knowledge and expertise. Our discussion that sometimes went far beyond the project scope were very encouraging.

Secondly, I want to thank Royal IHC for allowing me to do this project. It was a great pleasure to work with so many experienced and intelligent people at Royal IHC.

Thirdly, I would like to especially thank my daily supervisor at Royal IHC, Dr. Ir. J.C. Goeree, Joep, who has been available for guidance throughout the process.

Fourthly, a warm thank you go to R.W. Sen, Rick, my fellow graduate student, an experienced programmer and friend, with whom I spend many hours, working, discussing, improving my coding skills, playing table tennis and walking the same round time after time.

Further, I want Dr. Ir. G.H. Keetels, Geert, for taking the time to read my manuscript, sharing his knowledge and for being part of my thesis committee.

Finally, I want to thank my parents, sisters, friends and (old)roommates who have supported and motivated me throughout my entire studies.

J.C. Dijkhuis
Delft, Juli 2019

Abstract

Dam reservoirs form a crucial part for human society storing water, controlling floods, providing hydropower, water for irrigation and drinking. Annually 1% of the worldwide dam reservoirs storage capacity is lost, caused by sedimentation. The inflow of sediment and reduction of flow velocity and turbulence in the reservoir provides favourable conditions for settling. Several sediment transport mechanisms are responsible for this, one of these is the turbid density current. The turbid density currents settle as the reservoir becomes wider, and it is affected by forces along the top and the bottom of the current. Recently, focus on reservoir engineering has shifted from primarily structural dam design towards complete sediment management strategies. In order to improve the sustainability of dam reservoirs, many management techniques are developed that inhibit or mitigate sedimentation. However, the effectiveness of these techniques is not yet known. This thesis provides an additional concept for sediment management in dam reservoirs consisting of channelling of turbid density currents in dam reservoirs. The channel provides controllable parameters. The aim is to study the effects of channelling turbid density currents.

The study starts with a literature review, to describe sedimentation, sediment transport, and turbid density currents in dam reservoirs, including their analytical and numerical descriptions.

Two computational models study the concept: a steady-state model and a numerical model. The steady-state solution and is based upon an equation for open channel flows modified for turbid density currents. This model is used to investigate the effects of hydraulic radii and slope of the channel on the turbid density current — secondly, the dynamic numerical solution. An analytical description is provided using the one-dimensional shallow water equations, consisting of the continuity, momentum and particle conservation equations. The solution includes four sources: deposition, erosion, gravity and friction. It omits water entrainment and bed deformation. The model is discretised using the Generalised Lax Friedrichs method. First validation and investigation of the quality of the source terms are done. Subsequently, the model, including the four source terms, is used to study the effect of slope, hydraulic radii, concentration and sediment size in the channel. Expanding the numerical study by a Water Injection Dredging case in which local velocity, concentration and height are increased along a certain length to study possible effects.

To conclude, channelling turbid density currents is a viable solution to improve sediment transport. The slope and depth of the channel have the most significant effects. The generalised Lax Friedrichs method provides a valid and straightforward discretisation method for the numerical model. Furthermore, the model provides an easy, quick and simple to use tool to make first estimations of the effects of channel dimensions.

Contents

Nomenclature

α	0 = non-hindered settling, 1 = hindered settling	[−]
α	Angle bottom corner of trapezoidal channel	[−]
β	Angle top corner of trapezoidal channel	[−]
Δp	Pressure drop	$[kPa]$
Δ	Dimensionless density ($=\frac{\rho_s - \rho_w}{\rho_w}$)	[−]
δ	Dilatancy	[−]
κ	Permeability parameter	[−]
κ	von Karman constant	0.40 [−]
μ	dynamic viscosity($1.3 \cdot 10^{-3}$ at $10 \cdot C$)	$1.3 \cdot 10^{-3}$ $[kg/ms]$
∇	Vector operator	[−]
∂	Partial derivative	[−]
ϕ	Concentration	[−]
ϕ_{in}	Incoming concentration	[−]
ρ_a	Density ambient fluid	$[kg/m^3]$
ρ_c	Channel density	$[kg/m^3]$
ρ_f	Density of fluid	$[kg/m^3]$
ρ_m	Mixture density	$[kg/m^3]$
ρ_{rw}	Reservoir density	$[kg/m^3]$
ρ_r	River density	$[kg/m^3]$
ρ_s	Sediment density	2650 $[kg/m^3]$
ρ_w	Water density	1000 $[kg/m^3]$
τ_b	Bed shear stress	$[N/m^2]$
τ_c	Critical shear stress	$[N/m^2]$
τ_s	Effective shear stress	$[n/m^2]$
θ	Dimensionless shields number	[-]
θ_{cr}	Dimensionless critical shields number	[−]
A	Cross-sectional surface area	$[m^2]$
A	Diffusion term for the Generalised Lax Friederich Scheme	0.1 [−]
A_i	Exposed surface areas of particle	$[m^2]$
A_{nozzle}	Nozzle area	$[m^2]$

A_{rect}	Cross sectional area rectangular channel	$[m^2]$
A_{tot}	Total nozzle area	$[m^2]$
A_{trap}	Cross sectional area trapezoidal channel	$[m^2]$
B	Diffusion term for the Generalised Lax Friederich Scheme	1.0 [−]
b	Rouse number	[-]
C	Chézy coefficient	$m^{1/2}/s$
C	Concentration	[−]
C	Diffusion term for the Generalised Lax Friederich Scheme	0.1 [−]
C_1	Ferguson and church parameter	18 [-]
C_2	Ferguson and church parameter	1(particles) 0.44(spheres) [-]
C_a	Reference concentration	[−]
C_D	Drag coefficient	[−]
C_i	Coefficient of proportionality depending on the shape	[−]
C_k	Angularity of the grains	[−]
c_{max}	Maximum near bed concentration	[−]
c_{nb}	Near bed concentration	[−]
C_{wid}	Reduction factor by schierck	0.96[−]
D	Deposition flux	$[m/s]$
d	Sediment/particle diameter	$[m]$
D_*	Dimensionless grain/particle size	[−]
D_{10}	Sediment size 10% is smaller	$[m]$
d_{50}	Median particle diameter	$[m]$
D_n	Nozzle diameter	$[m]$
E	Erosion	$[m/s]$
E_h	Hindered erosion	$[m/s]$
E_p	Erosion flux	$[kgm/s]$
f	Darcy Weisbach friction factor	0.025 [−]
f	External force term	[−]
F_{drive}	Driving forces in fluid flow	$[N]$
F_D	Drag forces on a particle	$[N]$
F_f	Friction forces on a particle	$[N]$
f_f	Friction term (Darcy Weisbach)	[−]
f_g	Gravity source term	$[m/s]$
F_L	Lift forces on a particle	$[N]$

F_{res}	Resulting forces in fluid flow	$[N]$
F_s	Shear forces on a particle	$[N]$
F_w	Submerged weight of a particle	$[N]$
f_x	Source term	$[-]$
g	Gravitational acceleration	$[m/s^2]$
g'	Reduced gravity	$[m/s^2]$
H	Horizontal forces	$[N]$
h	Height	$[m]$
h_d	Height bottom section of the dam break	$[m]$
h_g	Starting height top of dam break	$[m]$
h_{in}	Incoming height	$[m]$
h_m	Height middle section of the dam break	$[m]$
i	Numerical space step	$[m]$
k	Non dimensional shear-stress parameter	$[-]$
K_s	Eddy diffusivity	$[-]$
k_s	Nikuradse roughness	$[-]$
L	Length	$[m]$
L_{beam}	Beam length of the water injection dredge	$[m]$
M	Momentum forces	$[N]$
n	Manning's Roughness coefficient	$[-]$
n	Rowe parameter	$[-]$
n	numerical space step	$[m]$
n_0	Porosity	$[-]$
n_i	Porosity	$[-]$
N_{nozzle}	Number of nozzles	$[-]$
nt	Number of time steps	$[-]$
nx	Number of steps steps in x direction	$[-]$
P	Wetted perimeter	$[m]$
P_{rect}	Wetted perimeter rectangular channel	$[m]$
P_{trap}	Wetted perimeter trapezoidal channel	$[m]$
Q	Discharge	$[m^3/s]$
Q_c	Channel discharge	$[m^3/s]$
Q_{rw}	Reservoir return flow discharge	$[m^3/s]$
Q_r	River discharge	$[m^3/s]$

Q_{wid}	Discharge for Water Injection Dredge	$[m^3/s]$
q_{wid}	specific discharge for Water Injection Dredge	$[m^2/s]$
R	Hydraulic radius	$[m]$
R_{rect}	Hydraulic radius rectangular channel	$[m]$
R_{trap}	Hydraulic radius trapezoidal channel	$[m]$
Re	Reynolds number	$[-]$
Re_p	Particle Reynolds number	[-]
S	Slope	$[-]$
S_0	Slope of the channel	$[-]$
S_{intr}	Intrusion depth of water injection dredge	$[m]$
S_{nozzle}	Nozzle spacing	$[m]$
t	Time	$[s]$
T_{settle}	Settling time of particle over height	$[s]$
TE	Trap Efficiency	$[-]$
u	Velocity	$[m/s]$
u_c	Critical velocity	m/s
u_*	Shear velocity	[m/s]
u_c	Channel flow velocity	$[m/s]$
u_{in}	Incoming velocity	$[m/s]$
u_{nozle}	Nozzle velocity	$[m/s]$
u_{rw}	Reservoir flow velocity	$[m/s]$
u_r	River flow velocity	$[m/s]$
V	Vertical forces	$[N]$
v	Kinematic viscosity	$1.3 \cdot 10^{-6}$ $[m^2/s]$
V_c	Shock velocity of the dam break	$[m/s]$
$V_{entered}$	Volume of Sediment that enters the reservoir	$[m^3]$
v_e	Sediment erosion term for high velocity erosion	$[m/s]$
v_s	Particle settling velocity	$[m/s]$
$V_{trapped}$	Volume of Sediment trapped by the reservoir	$[m^3]$
V_{wid}	Erosion (height) velocity for Water Injection Dredge	$[m^2/s]$
W_b	Bottom width trapezoidal channel	$[m]$
x	Horizontal coordinate	$[m]$
x_L	End of numerical domain	$[m]$
z	Height	$[m]$
z_0	Bed roughness height	$[m]$
z_a	Reference height for concentration	$[m]$

List of Figures

List of Tables

I

Introduction

1 Introduction

1.1. Background

The oldest dam reservoir in operation is the 100 Mm^3 Afengtang reservoir west of Shanghai build between 589 - 581 B.C. Originally the dam has been constructed of alternating layers of earth and straw, kept together by chestnut piles[46]. Since then 2500 years have passed, and dam reservoir construction has developed significantly in cooperation with engineers, governments and society. Dams now consist of well-engineered concrete walls. The number of reservoirs and their size have increased over time. Currently, dam reservoirs are responsible for 40% of the total irrigation and water supply, and 20% of the total energy supply worldwide [46][50]. Until recently, governments could suffice with building new dam reservoirs within rivers, but space is becoming scarce and this solution is not longer considered sustainable. The increased growth and development of the last 100 years resulted in a sedimentation problems that have grown so large that this can no longer be ignored.

Rivers transport more water than sediment, the time it takes to fill a reservoir with sediment is significantly longer. Due to this, the gradual accumulation of sediment has only been recognised recently. The reduced rate of dam construction throughout the world, combined with reservoir sedimentation results in more storage being lost yearly [23]. Studies show an annual worldwide storage loss of approximately 1%[46]. Currently, dam reservoirs are one of the most unsustainable factors in the modern water supply system[40]. With over 45,000 large dams (size > 7000km^3) and increased attention, the need for sustainable dam reservoir management is acknowledged by governments, engineers and supported by the world bank.

The sedimentation problem is caused by the influence of dam reservoirs on the natural sediment balance within rivers. From the upstream river, sediment enters the dam reservoir by several types of sediment transport, such as turbid density currents. Dam reservoirs provide favourable conditions for particle settling as the flow velocity is reduced. In recent years several management techniques have been developed to reduce sedimentation. These techniques consist of reduction, rerouting, removing, and redistribution of sediment [5].

1.2. Problem statement

The problem is that within dam reservoirs sediment accumulation harms function. Compared to the river, the flow velocity in a dam reservoir reduces due to increasing width, depth and stagnant water. The reduced velocity and turbulence result in a reduction of sediment transport capacity contributing to sedimentation.

Sediment transport is divided into bed-, suspended, and wash-load transport, which is associated with different sediment particle sizes. Suspended- and wash-load mainly transports finer sediment fractions. Within Bed-load transport the sediment fractions are larger. Within suspended-and wash-load transport, sediment is also as transported in the form of turbid density currents. The sediment is then transported over the bottom of the reservoir utilising a turbid density current. Within a reservoir the turbid density currents diverge and are influenced by the bottom and top friction, resulting in velocity and transport capacity reduction causing sedimentation.

To solve for the adverse effects of sedimentation, many different management approaches have been developed to reclaim dam reservoir space. Within this thesis, a concept is proposed to improve turbid density

current transport in dam reservoirs. The concept consists of dredging a channel in the dam reservoir. The channel could ensure that the density current does not diverge, preventing it from losing its flow velocity and sediment transport capacity. Within the channel specific parameters (dimensions) can be altered which ensure optimal sediment transport. The idea is that sediment is kept in suspension as the channel can maintain higher flow velocities. It is yet unknown if the channel is capable to transport density currents that are coming from the upstream river. In addition to this sediment transport could be improved or maintained with Water Injection Dredging. A model is developed to describe and study the phenomena and the concept.

1.3. Objective

The primary objective of this thesis is to investigate and answer the main research question:

Is channelling of turbid density currents an effective measure to transport sediment through dam reservoirs?

To answer this main research question, the following six sub-questions(SQ) are formulated:

SQ1. What mechanisms are responsible for sedimentation of dam reservoirs?
SQ2. Which management techniques are currently available to mitigate negative effects?
SQ3. What are the characteristics of a turbid density current and why do these settle in dam reservoirs?
SQ4. How to prevent settling of turbid density currents in dam reservoirs?
SQ5. How can turbid density currents be mathematically described and is there a simple method, either analytically or numerically, to model this?
SQ6. Can Water Injection Dredging within a channelled reservoirs improve the transport of turbid density currents?

The answers to the sub-questions are given throughout the thesis: SQ1 in chapter 2 and chapter 3, SQ2 in chapter 2, SQ3 in chapter 3 and further elaborated on in chapter 4, SQ5 is introduced in chapter 4 and further elaborated on through chapter 5 and chapter 6, SQ6 in chapter 5 and chapter 6. First the results are discussed in chapter 7, the answers to the sub question and main research question are summarised in chapter 8, further recommendations are given in chapter 9.

1.4. Methodology

The aim is to study the concept of channelling turbid density currents in dam reservoirs through computational modelling. The channel dimensions and current parameters can be adjusted to asses their influence on the density current. To reduce sedimentation and stimulate erosion is the ultimate goal. Sediment is kept in suspension if sufficient turbulence is available. Characteristics that determine if there is sufficient turbulence are velocity, slope, concentration, sediment particle size and the hydraulic radius.

The section methodology describes the available methodologies and reason for the particular strategy applied within this research.

Limited data on channelling turbid density currents in dam reservoirs are available. First, a literature study as provided in Part II and then an experimental study that follows this. There are approximately three experimental methods available to study the effects of the channelling of a dam reservoir. Either large life-sized experiments, scaled experiments or numerical/computational modelling. First, within a life-sized experiment, one can experiment by trial and error and try to extract data from this experiment to asses its effectiveness. A reason to use such a method is that one can immediately observe the effects of the channelling of a reservoir. Usually, these experiments are expensive, labour intensive and will generate data for one reservoir which are hard to generalise.

Second, a scaled experiment in a laboratory provides a representation of reality. Within such an experiment, one tries to reproduce as many parameters from reality as possible. These experiments will provide visualisations of the concept. It is harder to quantify the effects of the measures, and the set up of an experiment is labour intensive and expensive,as repeating the experiment, changing it several times is required to obtain valid results.

Third, a computational model experiment. One can choose to use readily available software and create a numerical model. For first estimations modelling is the cheaper option of the three modalities mentioned. The complicated part of modelling is grasping physical processes in analytic and numerical equations. For a problem considering sediment transport, it has been proven to be complicated.

It is impossible to do life-sized experiments; a laboratory experiment has been considered but seemed too complicated to set up. The decision was made to choose for a computational modelling study using

analytical and numerical solutions of turbid density currents. In previous studies, it is has been proven to be an effective method to simulate turbid density currents. One can refer to chapter 7 for more detail.

The model, as presented in chapter 4, offers a solution for the modelling of the turbid density current in a channel. The model represents the characteristics of the flow and the channel, and it is one dimensional, subdivided into two sections: a steady-state solution and a numerical solution.

The steady-state solution of the turbid density current is used to obtain information on the influence of hydraulic radii, slope and velocity of the current. The steady-state is an iteration step that provides insights on the effects of hydraulic radii and slopes on the current velocity.

The numerical model provides information on the development of the turbid density current over a part of the assumed channel length. It is modelling the steady middle part of the current, not accounting for the front of the current and the plunging of the flow. Initial and boundary conditions are stated in subsection 4.3.2. The numerical model is then validated and assessed through a dam break experiment, settling model, grid size experiment and evolution experiment. In subsection 5.3.5 several scenarios are proposed. The results are shown and discussed in Part IV.

At last, the modelling of a Water Injection Dredging(WID) by doing a case study. WID is a proven technique to erode and move sediment in rivers and ports. The sediment transported downstream by WID could positively influence the proposed concept. The results are provided in Part IV, section 6.3.

1.5. Outline

To counteract the sedimentation of dam reservoirs this thesis proposes a conceptual idea of channelling turbid density currents in dam reservoirs. The conceptual idea is investigated based on natural, physical, (empirical) mathematical and numerical principles. The report is subdivided into five parts the I. Introduction, II. Literature Study, III. Methodology, IV. Results, V. Discussion, Conclusions and Recommendation and VI. Appendices.

Part I, Introduction: Provides background information, the problem statement, objective, methodology and the structure of the report.

Part II, Literature Review: Provides a literature study of the methodology and is divided into three chapters, Sedimentation and Management of Dam Reservoirs (chapter 2), Sediment Transport Principles (chapter 3) and Turbidity Currents in Dam Reservoirs(chapter 4). First dam reservoirs, sedimentation and management techniques(chapter 2) are discussed. Second, chapter 3 sediment transport principles include, types of sediment transport, the behaviour of grains in currents and open channel flows. Third, chapter 4 the turbidity currents in dam reservoirs which compromises the available theory (section 4.1), a mathematical derivation and description of turbidity current in one dimension (section 4.2). Lastly the numerical method is proposed and discretisation, including initial and boundary conditions of the model section 4.3.

Part III, Modelling: Provides the proposed concept and modelling approach (chapter 5). Two research methods are proposed consisting of a steady-state and numerical approach. The numerical model is used to asses a Water Injection Dredging case that can positively influence sediment transport in the channel.

Part IV, Results and Discussion: First, provides the Results(Part IV) and is divided into three sections the steady-state solution(section 6.1), numerical approach(section 6.2) and Case Study for Water Injection Dredging (section 6.3). Each section includes graphs that are accompanied by analysis. The discussion(chapter 7), discusses the meaning, significance of the results and comparing it to expectations obtained from literature, noting any unexpected behaviour — further, an analysis of strengths, weaknesses, precision and validity. At last, it is assessing the patterns and evaluation.

Part V, Conclusion and Recommendations: is divided into two chapters, Conclusions(chapter 7) and Recommendations (chapter 9). Finally, the conclusion, relating to the original problem statement, answering the research question and assessing the success of the study. In the end, recommendations are provided for further studies.

Part VI, Appendices: Provides in depth information on this thesis together width python scripts used for modelling.

II

Literature Review

2

Sedimentation and Management of Dam Reservoirs

This chapter provides an introduction to dam reservoirs, management thereof and sedimentation therein.

2.1. Introduction

The main function of dam reservoirs is to store water to either control floods, for hydropower or to provide (drinking) water. Other less regular functions are recreation, navigation and safety.

Dam reservoir consists of three main areas, regardless of their function, as can be seen in Figure 2.1: Dead-, active-and maximum-storage area. Dead storage does not affect the function of the dam and is thus usually located below the dam outlet. The active area determines the functional capacity of the dam, either one of the functions listed above. The maximum storage is used to delay large amounts of water(floods) that come from upstream in short periods, in the downstream direction.

Two function types exist for dam reservoirs, either run-of-river or storage reservoirs as can be seen Figure 2.2. The main function of Run of river types are hydropower generation; they consist of relatively small active storage and relative large dead storage areas[5]. In contrast to this, storage reservoirs have a large active storage area and small dead storage area. Using active storage water for hydropower generation, irrigation or water supply[5]. The vast majority of large dam reservoir in the world are storage reservoirs.

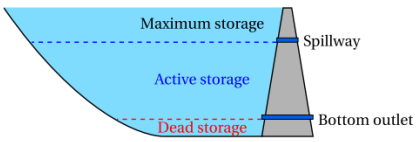

Figure 2.1: Three storage areas in dam reservoirs with arbitrary sizes [25]

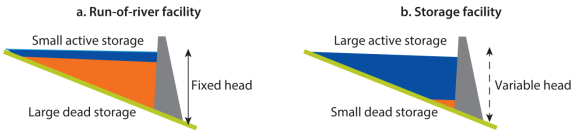

Figure 2.2: Storage and the run of river type reservoir[5]

Besides their function, characterising reservoirs is also done by shape and size. Four different shapes of reservoirs are identified by Borland and Millers[11], based upon reservoir sedimentation data in the United States. The data obtained indicates a connection between reservoir shape and the percentage of deposited sediment at different depths. Relating it to a shape factor that results in a distinction between four types[5]:

- Type I: Lake ($M = 3.5 - 4.5$), more sediment in upstream part of reservoir
- Type II: Floodplain-foothill ($M = 2.5 - 3.5$)
- Type III: Hill ($M = 1.5 - 2.5$)
- Type IV: Gorge ($M = 1.0 - 1.5$), more sediment in dead storage area of reservoir

The types are compared in a graph, plotting the percent of reservoir depth against the percent sediment deposited[5]. Knowing the type of reservoir is a crucial tool in reservoir management. The shape of the reservoir influences the velocity profile, effecting turbulence and sediment transport. Geometrical knowledge of reservoirs allows for the prediction of the sedimentation zones [60].

The sediment management aims and techniques differ within reservoirs different reservoir types. For run-of-river reservoirs, the purpose is to improve operational efficiency to limit abrasion and clogging impact of turbines. For storage reservoir, sediment management aims to ensure large amounts of storage area to provide water supply during droughts or too attenuated floods. [5] More details on sediment management techniques within dam reservoirs are discussed in section 2.3.

With over 45,000 large dams in the world, the need and availability of data are immense. The largest most and comprehensive database is the Global Reservoir and Dam (GRanD) database. It is a combined effort of two projects. The world Register of Dams built by the International Commission of Larg Dams(ICOLD) listing more than 33,000 large dam reservoirs. Secondly, Earth System Science Partnership(ESSP) who noticed inconsistencies in the database and assisted in building the new corrected GRanD. The database is freely available for non-commercial use.

2.2. Sedimentation of Dam Reservoirs

Recently focus within reservoir engineering has shifted from primarily structural dam design towards a complete sediment management strategy. Placing a dam on a natural watercourse forms reservoirs. Depending on the size, shape and inflow, all dam reservoirs will be subject to some degree of sedimentation during their lifetime. The remainder of this section discusses, consequences, sedimentation patterns and trap efficiency.

2.2.1. Consequences

Currently, the average age of reservoirs is 30-40 years, losing approximately 1% of the worldwide storage capacity yearly[26]. Loss of storage due to sedimentation has both upstream and downstream impacts. Downstream retrogression occurs and on the upstream side aggregation and flooding occurs. Upstream consequences of sediment trapping are storage loss, delta deposition, river navigation problems, abrasion, erosion, energy loss, obstruction of intake and outlets and landslides. Downstream consequences of dams are environmental impacts, stream morphology changes and reduction of suspended sediment concentration. For a more detailed explanation on up-and downstream impact see Morris and Fan (1998)[46]. Further, the influence of sediment on the hydropower generation is significant. It causes clogging of cooling intakes and abrasion, resulting in a reduction of power[5].

2.2.2. Sedimentation Patterns

The unified view of the spatial distribution of deposited sediment in the dam reservoir is that sediment is deposited near the dam in horizontal layers slowly filling up the reservoir[5][47]. This idea assumes that sediment only deposits within the dead storage area and active storage area remains available for the reservoir lifetime. The incorrect assumption of sedimentation causes over-prediction of reservoir lifetime and results in an early loss reservoir capacity.

Sediment transported by rivers consists of grains with different properties(e.g. size, density), resulting in the spatial distribution of sediment particles along the reservoir. As the reservoir becomes, wider and deeper water velocity decreases downstream. The larger sediment particles deposit in the first part of the reservoir and the smaller particle deposit further into the reservoir. Leading to a process referred to as segregation that results in different settling types: Delta, Tapering, Wedge and Uniform shapes, as shown in Figure 2.3 [46]. It is a simple representation of reality, as these types coincide. The wedge shape rarely occurs; it is a result of regular occurring density currents and lack of coarse sediment. Density currents do explain the transport and distribution of sediment particles within reservoirs; providing more detail on this in chapter 4. The other shapes are an effect of by particle size distribution, flood occurrence, density currents and reservoir operation.

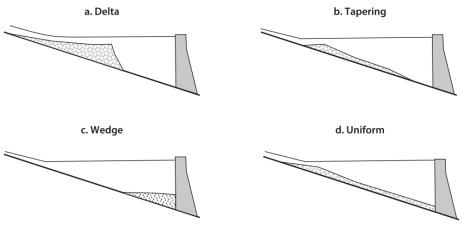

Figure 2.3: Shapes of deposited sediment in dam reservoirs[46]

2.2.3. Trap efficiency

Within reservoirs accumulation of sediment is caused by a reduction of water velocity as forces exerted by the flow forces are insufficient and thus unable to transport sediment particles after some time sediment interferes with sediment inflow from the river.

The definition of trap efficiency is the retaining of the amount or part of the incoming sediment load within a reservoir. Using both the formula for trap efficiency, Equation 2.1, and sediment inflow, one can determine the amount deposited sediment. Larger reservoirs trap more sediment and thus have higher trapping efficiency. Many slightly different empirical methods have been developed to determine trap efficiency; the most widely used is the one provided by Brune (1953)[14], see Figure 2.4. It is a relatively simple method with the volume trapped($V_{trapped}$) and volume entered($V_{entered}$) yielding the Trapp Efficiency(TE)[14]:

$$TE = (\frac{V_{trapped}}{V_{entered}}) \cdot 100 \tag{2.1}$$

The trap efficiency curve by Brune, as shown in Figure 2.4, results in over or underestimation of the Trap Efficiency due to it being relatively straightforward. Its low precision is caused by not taking into account the variable inflow of water and sediment, and it is advised to use it for a rough estimate only. A more recent empirical relation with better prediction capacity is provided by van Rijn (2013)[71].

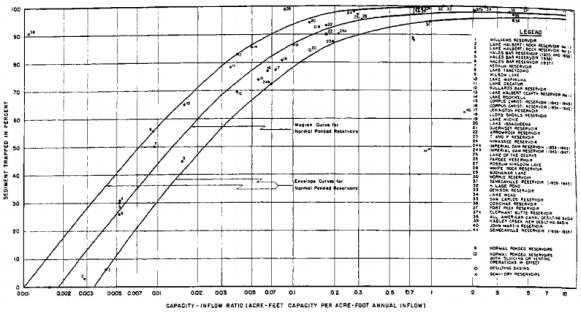

Figure 2.4: Trap efficiency as related to capacity inflow ratio type of reservoir and method of operation Source: Brune (1953)[14]

2.3. Sediment Management of Dam Reservoirs

Reservoir storage is crucial for human society, with the sedimentation of the dam reservoir, there is a need for sustainable management techniques[40]. Many techniques are available to counteract and control the adverse impacts of sedimentation on reservoirs. To achieve successful dam reservoir management is only possible integral dynamic combination of active and adaptive strategies. Figure 2.5 provides an overview of effectively used techniques[46]. Although the effectiveness of the techniques is not (yet) scientifically supported, the techniques are used many reservoirs.

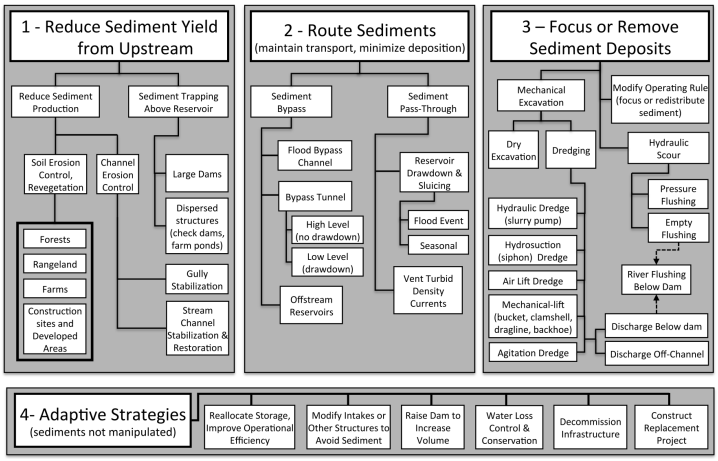

Figure 2.5: Classification system for sediment management techniques [47]

The management techniques, as provided in Figure 2.5, for sustainable reservoirs are classified by Morris (2015) [47]:

1. Reduce yield from upstream: Subdivided into "Control at the source" and "trapping eroded sediment upstream", as can be obtained from the top left Figure 2.5, further details are provided in subsection 2.3.1.
2. Route Sediments: Subdivided into "Bypass" and "Pass-Through" system, as can be obtained from the top middel in Figure 2.5 further details are provided in subsection 2.3.2.
3. Focus, redistribute or remove sediment deposits, as can be obtained from the top right in Figure 2.5 further details are provided in subsection 2.3.3.
4. Adaptive strategies, as can be obtained from the bottom in Figure 2.5, further details are provided in subsection 2.3.4.

2.3.1. Reduce Sediment Yield

To reduce the sediment yield from upstream two strategies are used, reduction of sediment production at its source and sediment trapping upstream of the reservoirs.

The reduction of sediment production is achieved in two ways. Sediment will come from upstream if the soil at forests, range-land, farms or construction areas as they do not provide enough structure. A protective vegetative cover can control soil erosion. The cover provides structure to the soil due to a physical and chemical binding, improving soil structure, porosity and permeability[47]. When channel erosion occurs, it is an effect of surface runoff water that forms concentrated flow creating channels. The concentrated flow increases erosion capacity and results in a meandering channel, mainly eroding the outer bank. To slow down, this process, gully and stream stabilisation and restoration of the land area is needed. Although it is a straight forward solution, stabilising natural meandering streams is hard in practice[47]. Sediment trapping upstream of the reservoir as not all sediment that enters a channel will reach the dam reservoir. Trapping occurs by large dams or structures or by Sometimes small farm ponds, or small (natural-)structures can be very effective to reduce sediment yield[71] [47].

2.3.2. Route Sediment

Routing sediment has two main goals, maintain transport capacity and minimise deposition; either by a bypass or a pass-through system.

First, the sediment bypass solution: a flood bypass channel, bypass tunnel or off-stream reservoir. A Sediment Bypass Tunnel(SBT) has an entrance upstream of the reservoir and transports both suspended, and bedload transport is discharging it downstream of the dam. An SBT should have a size that fits a flood and should be able to operate for long and multiple periods per year. There is a distinction between high-level, no drawdown, and low-level, drawdown, bypass tunnel system. This classification depends on the location of the tunnel inlet.

A high-level tunnel is installed upstream, combined with a check dam, during a flood flow the tunnel entrance submerges by the backwater induced by the check dam and will create an orifice flow. Due to the low flow velocity in front of the SBT, course sediment cannot enter the tunnel.

A low-level, which cannot go without drawdown of the reservoir, SBT has an entrance below the average pool elevation. It can bypass suspended load, including turbidity currents(chapter 4), without reservoir drawdown. However, in practice, to control the moving and developing delta, the reservoir is drawn down for flushing[37]. The flushing discharge may pass through the SBT or low-level outlets at the dam[46][47].

Another option, to bypass sediment, is to create an off-stream reservoir storage area outside the natural river channel. Clearwater diverted into the off-stream reservoir. Water with sediment will pass beyond the entrance. Although it is a highly effective method in reducing sedimentation, the off-streams reservoirs need sediment management too as these filling up with sediment from upstream too[46].

Second, sediment pass-through system aims to maintain transport minimising deposition and subdividing the pass-through system in reservoir drawdown and sluicing and the venting of turbid density currents.

Reservoir drawdown and sluicing timed with flood flow events and seasonally. Using drawdown when a flood occurs with high sediment inflow causes a reduction of residence time and enhances sediment discharge.

Sluicing is a technique reducing the water level of the reservoir before a flood event. Operating the gates so that impounded reach can transport both sediment and water downstream. Sediment sluicing is the operation during which the reservoir levels are lowered at high inflow, maintaining flow velocity keeping sediment in suspension [36][47]. Sluicing the dam is causes high flow velocities that erode deposited sediment.

Table 2.1: Difference between sluicing and flushing based upon there common parameters. Source: [47]

Differences: Sluicing and Flushing		
Parameter	Sluicing	Flushing
Timing	Occuring with natural flood flow	Does not occur with natural flood
Reservoir inlet	Operated during sluicing	Not able to be used, due to sediment concentration or low water
Outlet capacity	Can pass large floods with minimum backwater	Discharge may be limited by low level outlet capacity
Sediment discharge	Sediment Outflow ≈ Inflow	Sediment Outflow > Inflow
Erosion pattern	No retrogressive erosion	Retrogressive erosion of fine sediments moving upstream the channel
Gate placement	Set and operate to achieve desired hydraulic profile during drawdown	Set gates at lowest possible level to maximise erosion in an empty reservoir

Sluicing is often mistaken for flushing the differentiation between these techniques can be ambiguous. To provide insight in Table 2.1 a the differentiating factors between sluicing and flushing is made. More details on the flushing management technique is provided in subsection 2.3.3. [29][37][65][60]

2.3.3. Focus, Redistribute or Remove Sediment

The focus, redistribution and removal of sediment comprise several techniques that are intertwined. This section highlights, the aspects of mechanical excavation, modification of operating rule and hydraulic scour.

Mechanical excavation focusses on the removal of sediment rather than the redistribution of it: a separation between dry excavation and dredging. When the reservoir is drawn down dry excavation is possible, the open excavation will recover coarse sediment from the delta. If sediment is submerged, dredging can be applied. There are many techniques available such as hydraulic dredging with a slurry pump, water injection dredging, hydro suction dredging using a siphon, airlift dredge, mechanical lift such as bucket clamshell, dragline and backhoe and agitation dredge[5]. Dredging is a very cost-effective method for removal of large volumes of sediment as the drawdown of the reservoir is not required[47][25]. Hydropower dams can even use self-produced energy to dredge the reservoir.

The modification of operating rule focusses on redistribution of sediment limiting the advancing delta within the reservoir. When a reservoir has a consistent water level, the delta(see Figure 2.5) has a stable profile, and sediment is deposited and focused on the front of the delta[47]. The delta gradually advances towards the dam. Raising the minimum operating level retards this advance. Sedimentation occurs within the upstream part of the reservoirs. On the other hand, the reservoir can be drawn down during flood events to eroding and redistributing sediment, focusing the delta deeper into the impoundment[47]. It reduces the backwater and upstream flood levels.

Hydraulic scour/erosion is focused on the redistribution of sediment along the reservoir and is done by flushing and within the flushing technique, divided into pressure and empty flushing. Pressure flushing is when an outlet is still submerged and opened to release sediment while the reservoirs water level is high [29]. It results in a local cone shape caused by erosion, above the reservoir outlet only removing sediment close to the dam. Empty flushing is the opening of an outlet to empty the reservoir eroding sediment deposits and releasing water completely.

They are reaching maximum flushing capacity when the outlets are placed at the lowest level. Due to a higher potential energy level, the most sediment is removed. Flushing is a technique that mostly erodes the fine fractions in the dam reservoir [47]. The release of the high concentration of sediment below the dam will result in the accumulation of sediment in the river channel. It is essential to provide sufficient clearwater release to transport released sediment downstream to make it a sustainable solution[47]

2.3.4. Adaptive Strategies

In the previous paragraphs, active strategies were highlighted to manage sedimentation impact within reservoirs. Within this paragraph, adaptive strategies are provided; these adaptive strategies are actions that do not involve active handling of sediment[47]:

- Reallocating storage and improving operational efficiency: Reservoirs on several water levels and improvement of operations of the reservoir.

- Change inlets or other structural measures to avoid adverse effects of sedimentation; accomplished by improving the structures to withstand more sediment load.
- Increasing volume by raising the dam: by heightening the dam it increases the surface area and thus the amount of available storage space. Also, the building of a dam downstream of the 'old' dam reservoir is one of the options.
- Water loss control and conservation: implies more efficient use of water within the reservoir. Reducing physical water loss by improving irrigation systems.
- Decommission infrastructure: If a dam is no longer economical or sustainable to operate and the development of an end of life strategy should be considered.
- Construction of replacement project

3

Sediment Transport Principles

Hydraulic transport of sediment is both theoretically and experimentally a difficult problem due to the nature of the fluid flow — the interaction between liquid and solid phase and complicated phenomena of turbulence. Many studies have been done and are still done to provide formulations and approximations for sediment transport principles. Within this chapter the main aspects of sediment transport are discussed. This provides a basis for both turbid density currents(chapter 4) and modelling(section 4.2, section 4.3) decisions. For this study assessing transport of the coarser silt(0.02-0.063mm) and smaller fractions of fine sand (0.063-0.2) in dam reservoirs is considered.

This chapter introduces the types of sediment transport, the behaviour of sediment grains in a current and open channel flow.

3.1. Types of Sediment Transport

Transport of sediment takes place due to current (gravity-, wind-, wave-, tide-and density-driven currents), waves (deformation of short waves with decreasing water depth; shoaling) or by both waves and currents[73][61]. For current flowing over a river bed, the transport is devided into three types: bed-, suspended-and wash-load transport. With right conditions, a combination of these can result in turbid density currents, chapter 4. The predominant transport mode depends on size, shape and density of sediment particles in respect to the velocity and turbulence field of the water body[20].

Bed-load transport, is transport of particles by rolling sliding and saltating and is dominated by flow induced drag forces and by gravity forces acting on the particles [73],section 3.2. Unfortunately bed-load transport is not universally agreed upon. Several definitions are available such as Bagnold (1966)[7] and Einstein 1950 [24], the definitions are provided in Appendix A section A.1.

When particles are removed from the bed when bed shear velocity exceeds the particle fall velocity, referring to suspended-load transport, particles are push upwards to a point where turbulent forces are equal or higher than the submerged particle weight. A result of the random particle motions due to velocity fluctuations[73]. Suspended sediment concentrations decrease with the height in the water column, subsection 3.3.1. Bagnold (1966)[7] defines suspended-load transport as supporting the excess weight of the particles is by random successions of upward impulses imported by turbulent eddies.

Wash-load transport is very fine sediment(<0.05 mm) that is supplied from upstream in suspension and is barely found in the river bed. Hardly any exchange with the bed occurs, with little effect on channel slope and bed surface texture. Fine sediment particles enhance suspended sand transport as it increases the viscosity and the density. Reducing fall velocity of suspended particles and transport capacity of flow will increase [72].

Turbid density current is a combination of bed-, suspended-and wash-load transport and are essential in describing erosion and deposition processes in reservoirs [49]. The supporting mechanism for the flow is turbulence, moving the particles through the water column. A turbidity current is a form of gravity current, and the driving force is the horizontal difference in density due to sediment particles and the ambient fluid. Gravity pulls the current and accelerates downslope. It erodes sediment from the bottom and entrains fluid(water) from above.

3.2. Grains in a Current

This section includes the theory of threshold of motion, critical shield number, deposition and erosion.

3.2.1. Threshold of Motion

A submerged grain is in equilibrium, stable or in balance when the driving forces(F_{drive}) due to flowing fluid are equal with the resisting forces(F_{res}) from the grain, Figure 3.1. The driving forces acting on a grain are lift(F_L), drag(F_D) and shear(F_s) forces. The resisting forces are the submerged weight(F_w) and friction forces(F_f) consisting of contact and friction forces along the surface of the grain. A grain is stable if both lift force and submerged weight counterbalance and when drag, shear and friction forces counterbalance. As soon as the driving forces are larger than the resistance forces($F_{drive} > F_{res}$) a grain can starts moving.

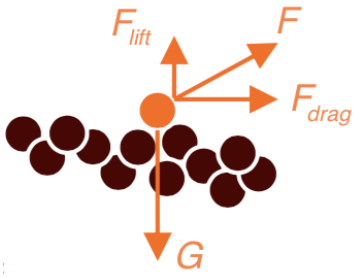

Figure 3.1: Forces on a grain

The driving forces are expressed as[59]:

$$F_{drive} = F_{res} \tag{3.1a}$$
$$F_{drive} = F_l + F_D + F_g \tag{3.1b}$$
$$F_{res} = F_w + F_f \tag{3.1c}$$

$$\left.\begin{aligned} \text{Drag force: } F_D &= \frac{1}{2} C_D \rho_w u^2 A_D \\ \text{Shear force: } F_S &= \frac{1}{2} C_F \rho_w u^2 A_s \\ \text{Lift force: } F_L &= \frac{1}{2} C_L \rho_w u^2 A_L \end{aligned}\right\} F_{drive} \propto \rho_w u^2 d^2 \tag{3.2}$$

with ρ_w water density, u the velocity, C_D, C_f, C_L is the coefficient of proportionality for drag, friction and lift forces respectively(depending on the shape) and A_D, C_f, C_L the exposed surface areas for drag, friction and lift of the particle. All forces are proportional to the square velocity defined near the grain, and the proportionality of the surface is proportional to the square of a size "d"(a function of d^2). The resultant load is expressed a function of u^2 and d^2.

The same holds for resisting forces that ensure a grain stays in its equilibrium position. Lift forces balance with submerged weight. Shear and drag are balanced by momentum around arbitrary contact point A or by friction force. The balance is independent of the type of equilibrium; either horizontal, vertical or momentum forces. Only the proportionality of load and strength remains, expressed as[61][59]:

$$F_l + F_W = 0 \tag{3.3a}$$
$$F_d + F_s + F_f = 0 \tag{3.3b}$$

$$\left.\begin{aligned} \textstyle\sum H = 0 &: F_D = f \cdot W = F_f \\ \textstyle\sum V = 0 &: F_L = W \\ \textstyle\sum M = 0 &: F_D \cdot O(d) = W \cdot O(d) \end{aligned}\right\} \rho_w u_c^2 d^2 \propto (\rho_s - \rho_w) g d^3 \tag{3.4}$$

With the horizontal forces H, the vertical forces V, momentum forces M, the weight of the particle W, the friction f, the distance towards rotation point O(d) The equation above can be rewritten with a dimensionless parameter k:

$$\rho_w u^2 d^2 \propto (\rho_s - \rho_w) g d^3 k \tag{3.5}$$

Rewriting Equation 3.5 above provides:

$$k = \frac{u_c^2}{\Delta g d} \tag{3.6}$$

with the critical velocity u_c, dimensionless density Δ Equation 3.6 leads to the non-dimensional shear stress, referred to as the shields parameter θ. Shields considers the friction force caused by the water on the bed on an area larger than one grain. When the driving force exceeds a particular critical value, the bed starts

to erode, and grains start to move. It should be noted that the Shields curve does not predict the exact moment at which single grains start to move. Grains could start to move at a lower or higher Shields parameter due to different exposure levels and the influence of turbulence[8]. Shields provides the relation between a dimensionless shears stress and the Particle Reynolds number in the following form[59]:

$$\theta = \frac{\tau_c}{(\rho_s - \rho_w)gd} = \frac{u_{*c}^2}{\Delta g d} = f(Re_*) = f(\frac{u_* d}{\nu}) \tag{3.7}$$

Shields plotted a curve by hand through the limited amount of data on the threshold of motion for currents available to him in the 1930s [61]. An updated version of this line by Soulsby(1997)[61] is provided in Figure 3.2. The threshold implies that grains start to lose stability and start moving, which is called the critical moment.

The bed shear stresses one of the flow-induced driving forces acting on the area of the grain determines the threshold of motion. The total shear stress is equal to skin friction and drag. If sediment transport is not too intense, the total bed shear stress is equal to the skin friction. With τ_b the bed shear or bottom friction exerted on the bed by current flowing over it. And u_* is the friction velocity related to ($\tau_b = \tau_c$):

$$\tau_b = \rho_w C_D u^2 \tag{3.8}$$

with the drag coefficient C_D. Several expression for the hydraulic roughness are provided below, the Darcy Weisbach resistance coefficient(f), the Chezy coefficient(C) and Mannings coefficient(n). Those are related C_D for current flow in the following[61]:

$$C_D = \frac{f}{8} = \frac{g}{C^2} = \frac{g n^2}{h^{1/3}} \tag{3.9}$$

Empirical relations are available to determine the coefficients of Darcy-Weisbach, Chézy and Manning. The choice of friction coefficients is not entirely arbitrary. The Darcy-Weisbach friction coefficient seems to give a great resemblance to the flow in a pipe or open channel flow; it is for this reason used within this thesis[61]:

$$\tau_c = \rho_w \frac{f}{8} u^2 \tag{3.10}$$

$$u_* = \sqrt{(\frac{\tau_c}{\rho_w})} = \sqrt{C_D u^2} \tag{3.11}$$

With Darcy-Weisbach f, the drag coefficient C_D, There are many empirical relations available to determine the friction factor although one can choose to use a constant friction coefficient, that approximates the coefficient closely, which is assumed as $f = 0.025$.

3.2.2. Critical shields

The moment that a particle starts moving is called the critical moment. This critical moment corresponds to a critical shields parameter. There are many functions available to determine this critical shields parameter, such as the one provided by Brownlie (1981)[13] that is based upon the particle Reynolds number:

$$\theta_{cr} = 0.22 Re_p^{-0.6} + 0.06 exp(-17.77 Re_p^{-0.6}) \tag{3.12}$$

With particle Reynolds number(Re_p) defined as:

$$Re_p = \frac{d\sqrt{\Delta g d}}{\nu} \tag{3.13}$$

With dimensionless density Δ, grain/particle diameter d, kinematic viscosity ν.

Shields originally plotted a curve, by hand, through the data available to him in the form of θ_{cr} versus the particle Reynolds number, not shown. However, this is inconvenient since shear velocity u_* appears on both axes. A direct mathematical transformation can be made to plot the critical shield number θ_{cr} versus dimensionless particle diameter D_*, Equation 3.15, which is easier to use in practical applications, as shown in Figure 3.2. An algebraic expression using the dimensionless particle diameter (D_*) that fits the Shields curve is given by Soulsby and Whitehouse (1997) [61]:

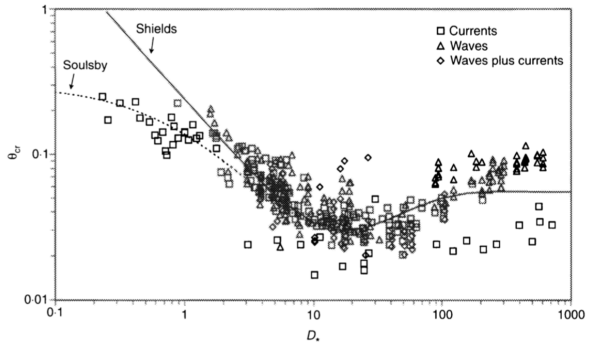

Figure 3.2: Updated version of the shields curve providing the threshold of motion of sediment beneath waves and currents [61]

$$\theta_{cr} = \frac{0.24}{D_*} + 0.055[1 - exp(-0.020D_*)] \tag{3.14}$$

with:

$$D_* = (\frac{\Delta g}{\nu^2})^{1/3} d \tag{3.15}$$

The curve plots well through waves and waves and current data, as well as the extensive set of current data available. However for very fine grains, the equation over predicts. Force consideration by Bagnold 1966[7] showed that the critical shields θ_{cr} could not exceed a value of approximately 0.30 because this exerts a sufficient force on the grains to overcome the weight of every grain in the topmost layer of the bed. Corrected by Soulsby and Whitehouse (1997), see Figure 3.2, to give an improved threshold bed shear-stress formula[61]:

$$\theta_{cr} = \frac{0.30}{1 + 1.2D_*} + 0.055[1 - exp(-0.020D_*)] \tag{3.16}$$

The dimensionless grain size D_* defined in Equation 3.15. Equation 3.16 gives good approximations for small particle sizes but approximates constant values for large grains $D_* > 200$ with $\theta_{cr} = 0.055$. For these larger grains correspond with d > 10 mm formula for the threshold for grain diameter is derived. Equation 3.16 is intended for a horizontal bed, and it can be altered to provide initiation of motion on a sloping bed. However, assuming the angles of the reservoir channels are small, this effect is insignificant and as a result not accounted for within this study. Also, this study does not account for the influencing effect of ripples.

3.2.3. Erosion

If the threshold of motion, critical shields number, is exceeded particles start to erode. Many studies have been done to quantify the process of pick up and erosion of sediment bed. Many pick up functions are available such as those by Cao (2004)[18], Hu Cao (2008)[33] Van Rhee (2010)[69], van Rijn (1984)[72]. The focus of these studies is to improve the pick up functions for certain flow regimes. The van Rijn (1984)[72] pick up function seems to make good predictions and is used within this study[8]:

$$E_p = 0.00033 D_*^{0.3} (\frac{\theta - \theta_{cr}}{\theta_{cr}})^{1.5} \rho_s \sqrt{\Delta g d_{50}} \tag{3.17}$$

With the pick up E_p in [kgm/s], shields number θ, the critical shields θ_{cr}, the sediment density, ρ_s, dimensionless density Δ, gravitational acceleration g and median diameter d_{50}.

Rewriting the equation by dividing van ρ_s for implementation in the model(section 4.2):

$$E = 0.00033 D_*^{0.3} (\frac{\theta - \theta_{cr}}{\theta_{cr}})^{1.5} \sqrt{\Delta g d_{50}} \tag{3.18}$$

With the median diameter of the grains d_{50}. With dimensionless grain size D_* defined as in Equation 3.15, the critical shield number in Equation 3.16 as proposed by Soulsby and Whitehouse (1997)[61]. The data of van Rijn (1984) [72] was based upon a flow velocity of 0.5-1 m/s, $\theta = 0.3 - 1.0$ and $d_{50} = 130 - 1500$ and no near bed concentration. This is in good resemblance with the flow velocities within the experimental model.

3.2.4. Hindered Erosion

Hindered erosion occurs due to high concentrations of sediment at the bed, the near-bed concentration c_{nb}, and turbulent eddies hindering pick up by pushing sediment particles back to the bed and particle-particle interactions [8]. Besides this turbulence is suppressed by sediment as an effect of high bed concentrations. First, Winterwerp et al. (1992)[76] determined that erosion is limited by the concentration, with higher concentrations lower erosion occurred. Winterwerp et al. (1992)[76] only considered the reduction of entrainment by the influence of suspended particles on eroding particles, which is similar to the effect of hindered settling. Secondly, van Rhee and Talmon (2010)[69] followed up on hindered erosion and included a reduction factor for the near-bed concentration on the "net erosion flux". The approach included an assumption made by Cao (1997)[19] on turbulent burst. Meaning particles are picked up and transported back to the bed hindering and causing reduced pickup. van Rhee and Talmon 2010[70] checked validity of Equation 3.19(Although the The equation did not fit data of Winterwerp et al. 1992[76]), van Rhee (2010)[69] also suggested similar relation:

$$E_h = E \cdot \frac{1 - n_i - c_{nb}}{1 - n_i} \tag{3.19}$$

With c_{nb} the near-bed concentration, n_i porosity of the bed. Equation 3.19 provides that a maximum amount of particles can be eroded from the bed according to $1 - n_i$ and particles are transported back by turbulent eddies is limited by the near bed concentration c_{nb}. If c_{nb} = 0 pick up is equal to regular erosion, if c_{nb} >0 pick up is reduced by hindered erosion.

Another approach to include effects of concentration sediment is the reverse formulation of the hindered settling provided in Equation 3.19, according to the reversed concept of hindered settling by Richardson and Zaki (1954)[55]:

$$E_h = E \cdot (1 - \frac{1}{1 - c_{max}})^n \tag{3.20}$$

With pick up function E, and n equal to 1.38 that correlates with the data of Winterwerp (1992)[76] Particles start to move at lower and higher critical shields value due to different exposure to the flow. Miedema (2012a)[44] made a theoretical model including exposure, velocity profile close to the bed, drag, lift and turbulent velocity fluctuations and showed that almost all particles at the top bed are mobile(100-1000 moving grains per m2). When the shields parameter has exceeded the pick up flux increases up to ~1 m/s($\theta_{cr} = 0.5$), until this point, the erosion is dominated by the erosion of single grains which are entrained into the flow "grain by grain". Exceeding the shields parameters, the pick-up increases. The empirical pick-up flux as the one proposed by van Rijn (1984a)[72] in Equation 3.17 is applicable in combination with hindered erosion as proposed in Equation 3.20 . When higher flow velocities and shields parameters occur, bulk properties of sand such as porosity and permeability start to play a role a strategy as proposed by van Rhee(2010) [69] could be applied. Unfortunately, no theoretical models are available. Cao (1997) [19] includes the effect of turbulent bursting in a pick-up function. Also the pick up for values beyond u = 1 m/s and $\theta_{cr} = 0.5$ is not yet understood [8].

3.2.5. Deposition

Deposition of sediment grains depends on the current velocity, grain settling velocity and turbulence. For a single grain the settling velocity in a stationary water column can be determined with:

$$v_s = \sqrt{\frac{4\Delta g d}{3C_D}} \tag{3.21}$$

With the particle settling velocity v_s, gravitation acceleration g, diameter d, drag coefficient C_D.
Within river flow the water is not stationary, and settling depends on the turbulence regime. The drag coefficient C_D is depended on the flow regime and is related to the particle Reynolds number. There are three different turbulence regimes described for the particle Reynolds number(Re_p)[55][28]:

$$Re_p = \frac{v_s d}{\nu} \tag{3.22}$$

$$C_D = \begin{cases} \frac{24}{Re_p} & Re_p < 1 \quad \text{Laminar regime} \\ \frac{24}{Re_p} + \frac{3}{\sqrt{Re_p}+0.34} & 1 < Re_p < 2000 \quad \text{Transition regime} \\ 0.34 & Re_p > 2000 \quad \text{Turbulent regime} \end{cases} \tag{3.23}$$

To determine the settling velocity, one should determine if the flow is laminar, transitional or turbulent. Within the transitional regime, requires an iteration step. One should account for that particles have a particular grain size distribution over different diameters. Within this study, it is assumed that particles have a median diameter(d_{50}). The iterative process is avoided by using the settling velocity by Ferguson and Church 2004[28], which is valid for a wide range of particle Reynolds numbers(Re_p):

$$v_s = \frac{\Delta g d_{50}^2}{C_1 \upsilon + \sqrt{0.75 C_2 \Delta g d_{50}^3}} \tag{3.24}$$

In which $C1 = 18$, $C2 = 1$ for natural sands(0.44 for spheres) Ferguson and Church (2004) found these values for sediment as an intermediate relation for grains of varied shape as fitted to there data[28]. Gravitation acceleration(g), kinematic viscosity υ, median sedimentsize d_{50}, relative density Δ

Within the current, a specific concentration of particles is present. Due to sediment concentration interaction with both the fluid and other particles, the settling velocity decreases, referring to the phenomenon as hindered settling. Richardson & Zaki(1954)[55] proposes a relation for hindered settling:

$$v_{s,h} = v_s (1-\phi)^n \tag{3.25}$$

Where v_s is the settling velocity of a single grain, the concentration ϕ, the hindered settling velocity $v_{s,h}$ and approximating n with the method of Rowe (1987)[57](or a value assumed between 2-4 if one wants to simplify calculations):

$$n = \frac{4.7 + 0.41 Re_p^{0.75}}{1 + 0.175 Re_p^{0.75}} \tag{3.26}$$

The Deposition flux D can now be defined when hindered settling occur:

$$D = \rho_s \phi v_s (1 - \alpha\phi)^n \tag{3.27}$$

With $\alpha = 0$ for non-hindered settling, $\alpha = 1$ for hindered settling. The Deposition flux D when non-hindered settling occurs is:

$$D = \rho_s v_s \phi \tag{3.28}$$

in which ρ_s is the sediment density.

3.3. Open Channel Flow

3.3.1. Types

One refers to open channel flow when the free surface flow is subject to atmospheric pressure on the surface. River flow is an obvious example of open channel flow. The balance of forces in open channel flow determine if and how much sediment is eroded and transported. A channel is prismatic when the cross-section of a channel is constant in shape, size and bottom slope. The most common shapes of prismatic channels are rectangular, trapezoidal, triangular and circular. There are four general types of flow in prismatic channels[15][67]:

1. Steady and unsteady flow: The steady-state flow, the depth and discharge velocity do not change with time. Unsteady if this is not the case.
2. Uniform and non-uniform flow: Flow depth along the channel does not change; for every cross-section, the flow is uniform. Non-uniform if flow changes in the direction of the flow for a certain time.
3. Uniform steady flow: Flow depth is not changing with time at every cross-section and is constant along the flow direction, the free surface is parallel to the bed.
4. Non-uniform flow: Changing water depth along the channel cross-section.

3.3.2. Turbulence

Flow is laminar, turbulent or in an intermediate regime. Laminar flow occurs when viscous forces are dominant compared to inertial forces; the flow is smooth and has constant fluid motion. Inertial forces dominate turbulent flow compared to viscous forces; the flow has eddies and vortexes and other instabilities(turbulence).

Open channel flows experience resistance due to friction; the velocity at the bottom is zero. It implies that in laminar flow viscous forces should be dominant throughout the entire height of the flow. It has a smooth velocity profile and follows a parabolic shape. Within the turbulent flow of a channel, a tiny boundary layer occurs in which the viscosity dominates the flow. The upper part of the flow is inviscid, neglecting viscosity, shear is small, and velocity is almost constant. The velocity profile shape is logarithmic and at the top maximum velocity occurs in which shear is zero.

The Reynolds number provides a measure for the amount of turbulence, and it is used to determine if the flow is turbulent or not, defined as:

$$Re = \frac{\rho_f u L}{\mu} = \frac{uL}{\nu} \tag{3.29}$$

In which ρ_f(1000 kg/m^3 for water) is the density of the fluid, u the velocity of the fluid, L the characteristic linear dimension, μ the dynamic viscosity(1.3$\cdot$ 10^{-3} for water of 10 degrees Celsius) of the fluid and v the kinematic viscosity(1.3$\cdot$ 10^{-6} for water of 10 degrees Celsius) of the fluid. In the case of open channel flow, L is equal to the hydraulic radius$R$:

$$R = \frac{A}{P} \tag{3.30}$$

In which the hydraulic radius R, cross-sectional area A and wetted perimeter$P$. As a general rule in open channel flow based on the hydraulic radius there are conditions for turbulent and laminar flow:

- Re < 500 laminar
- 500 <Re <1000 transitional
- Re >1000 turbulent

Using Equation 3.29 to determine turbulence regime Re. From this, one can obtain that for very low velocities the flow in a river/open/prismatic channel is almost always turbulent. For this study, flow is always in the turbulent regime.

3.3.3. Velocity and Shear Stress

When the current in a prismatic channel flows over a solid boundary, the channel bed, it experiences friction shear stress. It will form a boundary layer. The boundary layer may take the complete depth in shallow water or a part of the water column in deeper water. The no-slip condition dictates that the velocity of the flow at the boundary is zero[15]. Within the boundary layer, the current velocity increases with height. At a certain height above the boundary, the velocity is maximum. How the current velocity increases with the height is the velocity profile. Between the boundary layer and top, one can use the depth-averaged current velocity. A schematic representation of the velocity profile, shear stress and concentration profile is given in Figure 3.3.

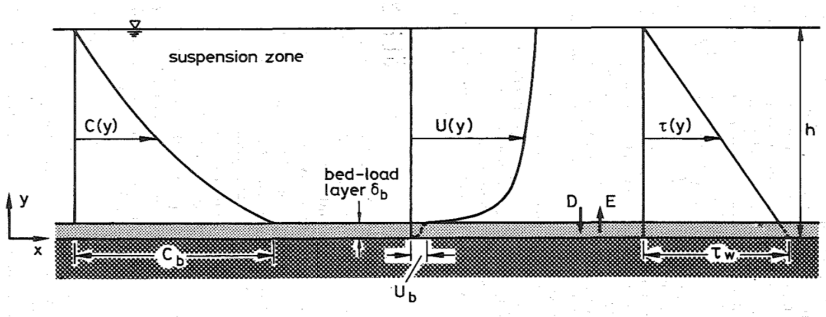

Figure 3.3: Schematic representation of sediment transport over a lose bed [20]. With U_b the bed layer velocity.

In an open channel with bottom friction the logarithmic velocity profile holds, see Figure 3.3 and Equation 3.31:

$$u(z) = \frac{u_*}{\kappa} \ln \frac{z}{z_0} \tag{3.31}$$

$$u_* = \sqrt{\frac{\tau_b}{\rho}} \tag{3.32}$$

With u(z) velocity at height z, the von Karman constant κ (0.40), bed roughness height z_0 and the bed shear stress τ_b. For the bed roughness height, according to Nikuradse (1933), that used smooth and rough pipes for the experiments, and fitted by Christoffersen and Jonsson (1985)[61]:

$$z_0 = \frac{k_s}{30}(1 - \exp(\frac{-u_* k_s}{27\nu})) + \frac{\nu}{9u_*} \tag{3.33}$$

With kinematic viscosity ν and the Nikuradse roughness k_s. The Nikuradse roughness depends on the viscosity of water, current velocity and dimensions of the physical roughness of the bed. The most widely used simple approximation is[61]:

$$k_s = 2.5d_{50} \tag{3.34}$$

Roughness coefficient k_s, median diameter d_{50}. Mud and sand are smooth or transitional, and coarse sands and gravels are rough. If a flat bed is assumed: no ripples, dunes or sand waves and sediment transport small. The total bed shear stress is equal to skin friction. It is assumed that bed shear stress is related to the depth-averaged current velocity through the drag coefficient as given in Equation 3.8 ($\tau_b = \rho_w C_D u^2$). With C_D being the drag coefficient, for drag coefficient approximations refer to Equation 3.9. In many cases, the bed is not flat and will have ripples, dunes and sand-waves. The total bed shear stress is referred to τ_t and is composed of the skin friction(effective shear-stress) τ_s and τ_b due to drag on individual grains:

$$\tau_t = \tau_s + \tau_b \tag{3.35}$$

There are several methods available to calculate the skin friction developed by Einstein (1950) and Wilson (1989). The bed is assumed to be flat within this study.

3.3.4. Concentration Profile

For currents in prismatic channels, suspended sediment concentration decreases when moving higher into the water column, Figure 3.3. The rate of change depends on the balance between fall velocity v_s and bed-shear velocity u_*. Balancing settling by turbulent diffusion. The equation that governs this balance is[61]:

$$v_s C = -K_s \frac{dC}{dz} \tag{3.36}$$

With settling velocity v_s from Ferguson and Church(2004)[28] see Equation 3.24, Volume concentration C of sediment at height z above the bed and eddy diffusivity K_s of the sediment.

Equation 3.36 can be solved using different assumptions to give the vertical distribution of the concentration of suspended sediment in the flow. The difference is eddy diffusivity K_s, it depends on turbulence in the flow and height above the bed. The Rouse number determines the profile shape:

$$b = \frac{v_s}{\kappa u_*} \tag{3.37}$$

When the eddy diffusivity(K_s) increases parabolic with the height:

$$K_s = \kappa u_* (1 - (\frac{z}{h})) \tag{3.38}$$

The rouse profile is obtained, see Figure 3.4, derivation is provided in Appendix A section A.2:

$$C(z) = C_a(\frac{z}{z_a}(\frac{h - z_a}{h - z}))^{-b} \tag{3.39}$$

In which height above seabed z, reference height near the seabed z_a, concentration at height z $C(z)$, reference concentration C_a at height z_a and the water depth h [61]. Many other assumptions on the distribution of the eddy diffusivity are available in Soulsby 1997[61].

The following types of transport hold for, Equation 3.37, Rouse number(b):

- $0 < b < 0.8$ wash load transport
- $0.8 < b < 1.2$ suspended sediment transport
- $1.2 < b < 2.5$ 50% suspended sediment transport
- $b > 2.5$ bed load transport

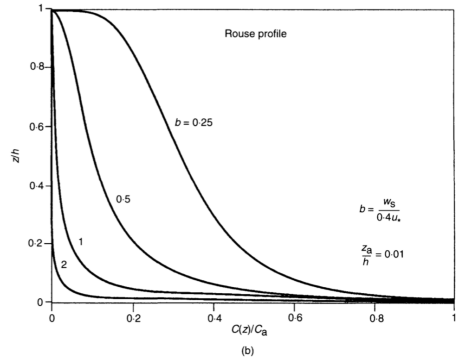

Figure 3.4: Rouse profile providing variation of grain size and current velocity with linear axes showing difference

4

Turbid Density Currents in Dam Reservoirs

4.1. Theory

"If turbid density currents can be entirely stopped or influenced in such a way that the sediments do not deposit in critical locations, then the sustainability of the reservoir operation may be increased considerably [60]."

This chapter provides a theoretical introduction of turbidity currents, mathematical description and the translation to a numerical approach.

4.1.1. Introduction

When a fluid with a given density moves into another stagnant fluid of a different density, the flow stratifies [53]. The flow either moves under, through or over the ambient fluid depending on density. Density difference is caused by temperature, chemical composition(e.g. salinity), pressure and suspended matters(e.g. sediment)[53]. The stratified flows occur in oceans, lakes and reservoirs and stratification occurs by waves, continental shelf collision, turbid water, mining and dredging. In literature, many expressions exist for stratified flow such as density current, gravity current and turbidity current, each having a slightly different meaning. The focus of this study is on turbid density currents(Turbidity currents).

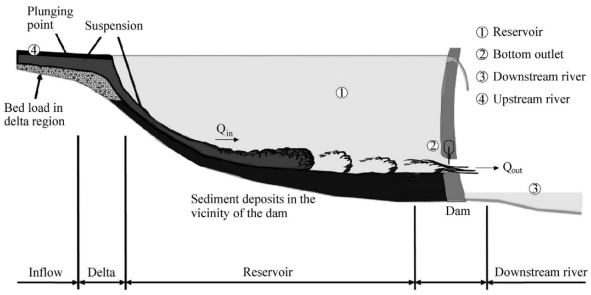

Figure 4.1: Turbid density current travelling along a bed slope of a dam reservoir vented through the bottom outlet [21]

First a clarification of what is meant by a turbid density current: The adjective "turbid" means cloudy, opaque or thick with suspended matter. 1. "Turbidity transported in reservoirs by temperature-induced density currents are density currents transporting turbidity[47]." 2. "Density currents caused primarily or entirely by the presence of the turbidity are turbidity currents as stated by Middleton and Hampton, 1973[47]." The term turbid density current applies to both.

Turbidity currents contain sediment and are denser than the ambient fluid; gravity pulls the solid particles in the mixture, causing downslope flow. The fluids turbulence supports the suspension of particles. Density and gravity are the driving forces having a dual role in in the control of velocity, thickness and underflow characteristics[1]. Gravity currents are either conservative (temperature or dissolved substances) or non-conservative (turbidity current on a mobile bed with erosion and deposition). The non-conservative turbidity

currents are subdivided in low velocity, low density and high-velocity high-density currents. Characterising the turbid density currents by a distinctive raised head, followed by quasi-uniform flow [35]. Figure 4.1 provides an example of a vented turbid density current in a reservoir. A Turbid density current will continue to flow if[22]:

1. Shear stress-induced by downslope gravity is larger than the frictional resistance.
2. Sediment particles stay in suspension by the support mechanisms. The current need to generate sufficient turbulence to keep sediment in suspension.
3. A turbidity current can only be sustained if inflow continues. When the duration of the inflow is less than the travel time to reach the reservoir end the current will dissipate[46]. The maximum concentration for a turbid density current is approximately 8-9 % [6] [35].

The occurrence of turbidity currents impact water quality and sedimentation of lakes and reservoirs. Under favourable conditions, the current transports through the submerged thalweg towards the dam. The defined channel facilitates the current as it can not spread out. After the successive occurrence, the thalweg is filled up[49]. The turbidity current starts to spread out, becoming wide and shallow with more significant top and bottom surface areas. It increases frictional resistance, and also facilitates both sediment deposition plus dilution from above with clear water[35]. Both processes lower the current's density and velocity, allowing more sediment to deposit, and eventually causing the current to stop.

As mentioned in section 2.3, turbid density currents are used in dam reservoir management strategies and are usually vented or flushed through low-level outlets[46]. It reduces the accumulation of sediment within the impoundment. Empty flushing can scour out and maintain a submerged channel which will help sustain turbidity current motion[47].

The aim of is to see the effects of channelling a dam reservoir. By analytical and numerical modelling it provides insight into the possible solution to keep a turbid density currents 'alive' and let it reach beyond the dam.

4.1.2. Development in a Reservoir

Turbidity currents can exchange sediment with the bed over which they flow and are affecting their dynamics. Pantin (1986)[51] and Parker (1987)[52] proposed that under certain circumstances, turbidity currents may ignite or self-accelerate to higher velocities by sediment entrainment from the bed. This section discusses the development of a turbid density current in a dam reservoir.

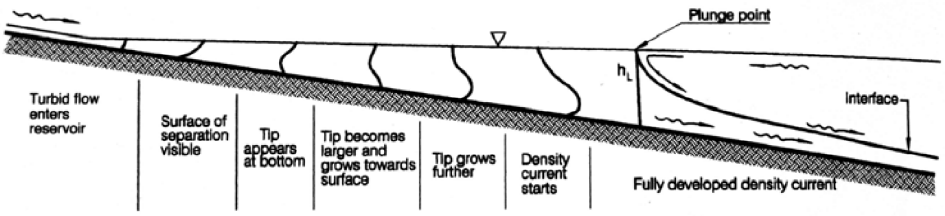

Figure 4.2: Transition from non-stratified to stratified flow as provided by Morris and Fan 1998 [46]

The turbidity currents plunge beneath the impounded water in the reservoir due to a higher density than the ambient fluid and can transport large quantities of sediment towards the dam. The developing current moves along the lower sloping boundary of the receiving water, see Figure 4.2. As previously mentioned in subsection 4.1.1 the turbidity current focuses into the deepest part of the cross-section, referred to as the thalweg. The current can travel long distances if it flows through a defined channel, and if inflow from upstream continues; otherwise, it will dissipate. Close to the dam it can either accumulate as a muddy lake when outlets are closed, or it could be released when opened [47] [4].

The characteristics of a turbid density current in a dam reservoir consist of entering-, plunging-, separating- and inter-flow. The following is a summary of the article by Alavian and Jirka (1992)[1]. Figure 4.3 show the five possible characteristic flow zones within a turbid density current, explained in the following:

1 Initial flow from riverine with density ρ_m, is described as suspended sediment transport and can be described with single-layer flow hydraulics using subsection 3.3.3 and subsection 3.3.4.

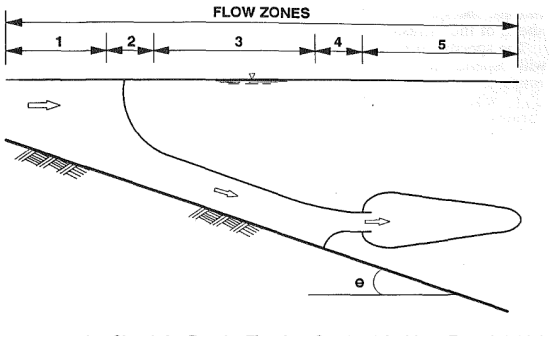

Figure 4.3: Turbid density current into Stratified Ambient; Zone 1: Initial flow, Zone 2: Plunge, Zone 3: Density Current, Zone 4: Seperation, Zone 5: Interflow. [1]

2 The plunge point: the area where the inflowing turbid water enters the reservoir and plunges beneath the clear water resulting in stratified flow. The plunging of the current is an effect of temperature and turbidity differences, in which the turbidity aspect is most important. The balance between momentum and baroclinic pressure caused by density differences determines the plunging location[75]. Baroclinic pressure gradients driving the current downslope is formulated as: $g' \sin\alpha$, in which α is the slope angle and g' the reduced gravity Equation 4.1. Reduced gravity is the driving force of a turbid density current:

$$g^{'} = g\frac{\rho_m - \rho_w}{\rho_w} \tag{4.1}$$

With the reduced gravity acceleration $g^{'}$, the gravitational acceleration g, the density of the mixture of the turbidity current ρ_m and ambient fluid density ρ_w. The density of the ambient fluid depends on the salinity and temperature [2]. In case of uniform under-flows, baroclinic pressure gradient force is balanced by the boundary and interfacial shear stresses[1]. Due to this two-layer flow occurs and mixing across the density interface and dilution of the underflow takes place. Within narrow reservoirs plunging flow forms a line across the top width of the reservoir, the surface water is turbid upstream of the line and clear downstream. Within a wide reservoir, the turbid surface is more irregular, and tongue like that shifts from side to side. There are many empirical relations available to calculate the plunge point in Knoblauch (1999)[35].

3 The flow is stratified: At this point, the flow separates into two layers, mixing occurs across the top and bottom of the current. The bottom and ambient water influence the propagation velocity and thickness of the head and thickness of the flow. The middle part of the current is in quasi-steady state. The velocity must be sustained to keep sediment in suspension by turbulence and travel long distances. It will maintain the density differences between the gravity current and surrounding fluid.
Turbidity currents contain a wide range of sediment particles. Even particles that are in theory not able to be maintained in suspension are kept in suspension because the current hinders these. When particles do settle, it reduces the currents density and gravitational acceleration force as gravitational force maintains the velocity. Lower velocity implies less turbulence and energy and thus less sediment in suspension.

4 Reduced density: Either the gravity and turbulent forces are in balance, and after the passage of the head, a steady-state current forms. Alternatively, the underflow becomes buoyant due to entrainment of water and settling of particles. The current move up into the reservoir, separating it from the reservoir bed and resulting in inter-flow.

5 Intrusion or inter-flow: The intrusion will slowly dissipate due to frictional forces and water entrainment.

4.1.3. Characteristics

Turbidity currents have low density, are Newtonian and have a low turbulent regime and have sequence type deposits called turbidites[41]. Within a turbidity current, both dynamical and deposition processes coincide in space and time. The flow transforms by sediment transport, erosion, deposition, mixing and water entrainment. When buoyancy is maintained, and there is no interaction with the bed throughout the movement, it

is called a conservative turbidity current. For non-conservative turbidity currents, there is an interaction with the bed; there is an open boundary in which erosion and sedimentation take place. Figure 4.4 show the processes that take place in a turbid density current. Erosion, deposition, the mixing zone, entrainment of water, the inner layer, and the front force and the force of the ambient fluid.

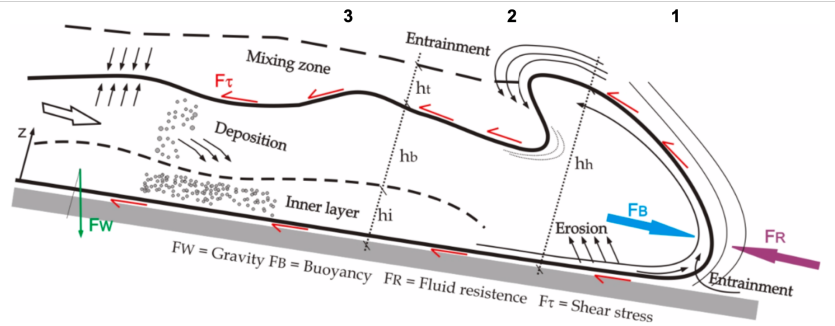

Figure 4.4: Schematic of a turbid density current. Source: [41]

A turbid density current can be divided into three parts: 1. The Head, 2. The Body and 3. The Tail see Figure 4.4[41]:

1. The head is the front of the turbid density current and has a semi-ellipse form. It is generally thicker compared to the body and tail caused by the resistance of the ambient fluid. There are strong three dimensional effects and mixing taking place, which are important for the flow dynamics. The front of the head is the nose, which is just above the bottom — caused by the no-slip condition at the bottom and the shear resistance of the surface Britter & Simpson (1978)[41].

   Within the head, two types of instabilities are responsible for mixing with the ambient fluid. The first type is an intricate pattern of lobes and clefts caused by second-order gravitational instabilities at the fronts surface[41]. The second type of instabilities is a series of billows closely related to Kelvin-Helmholtz instabilities[41], occurring occur behind the head and are an effect of viscous shear at the surface of the head and body. The zone behind it is the neck of the current and creates large turbulent mixing dividing the head from the body[41].

2. The body: the velocity is approximately 30-40% higher compared to the head. The head is slower due to a large billow causing entrainment of ambient fluid, referred to as a diluted zone. For the flow to maintain and advance the body current increases to compensate for the loss of sediment. The body divides into two zones: near body zone and upper body zone. Within the near body zone, the density is higher. In the upper body zone mixing with the ambient fluid occurs. Between these two zones, an interface called the bipartite flow provides a discontinuity in the body, which is stratification in the flow. It results in a gradient of velocity, concentration and viscosity.

3. The tail: is the back part of the current in which the flow decelerates and final dilution of the current takes place.

As discussed, the turbidity currents have a body velocity and a head velocity. These velocities differ significantly from open channel flow. The body has a quasi-steady velocity profile and can characterise the current in terms of velocity and height. The head of the turbidity current is turbulent. Due to entrainment of clear water and sediment, that increases the height and decreases the velocity in the head, explained in point 2 above. The velocity profile is significantly modified, see Figure 4.5. The velocity and concentration profile of open channel flow on the left and that of a (subcritical) turbid density current on the right. For supercritical flow, the velocity is greater and more peaked closer to the bottom. Velocity change is an effect of shear effects on the upper surface; turbid density current profile has zero values at the top and bottom surfaces and increases towards the middle of the flow. It is resulting in the balance of drag forces on the surfaces. The front has a maximum value that lies at approximately 0.2-0.3 times the height of the current[41], which depended on the concentration and en-trained sediment. The profile is complex due to matrix strength and cohesive forces. The typical velocity, shear and concentration profiles for open channel flow, turbid density currents and debris flow are given in Figure 4.6.

Typical values for the velocity of a turbid density current are approximately 0.3 m/s. Larger velocities have been measured by Brown(1943) and are approximately 0.9-1 m/s[41][35]. The concentration of the turbid denstiy current range between 0.002 % and 9% [35]. With a height going up to approximately 30m [35].

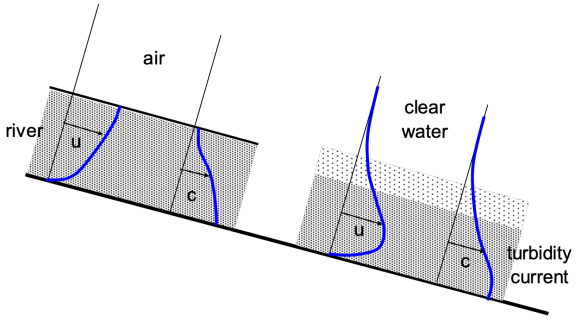

Figure 4.5: Streamwise velocity and concentration profile of suspended sediment transport(left) and a turbid density current(right)

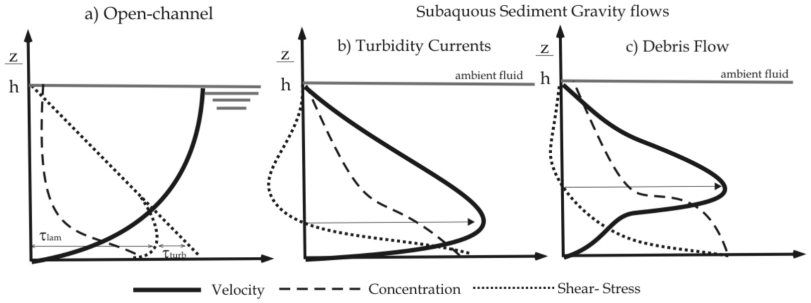

Figure 4.6: Stream wise vertical profiles of velocity, concentration and shear stress for a. open channel flow, b. turbidity currents and c. debris flow

4.2. Mathematical Model

A turbid density current is complex due to the processes of erosion, entrainment and deposition coinciding and in different directions. It is complicated and computationally intensive to model a turbid density current in three dimensions. One can decide to model in one dimension to make first assumptions, leading to simplifications of physical phenomena and aspects that have little influence on the current. It is a proven method to model turbid density currents in one dimension with shallow water equations by [10][16][18][63][75].

In this section, the Navier-Stokes equations are used to derive the Shallow Water Equations. After the derivation of the shallow water equations, one can make several assumptions. These assumptions lead to the one-dimensional single-layer shallow water equations. As turbid density current is particle driven, this leads particle conservation equation. Within the turbid density current, several source terms are incorporated; including deposition, erosion, friction and omitting gravity and the entrainment of water and bed change.

4.2.1. Derivation

This section provides a summary of the derivation of the 1D Shallow Water Equations for particle driven flow from the Navier-Stokes, a complete derivation is provided in Appendix B. For further reference one can refer to [31], [3] and [63].

The general form of the Navier-Stokes can be derived from Newton's second law. The density differences within the flow are small the Boussinesq approximation. The assumption implies $\frac{densitycurrent}{densityambientfluid} \approx 1$ [34]. The variation of the density does not affect the flow field, except for buoyancy forces. Physically this can be interpreted as that the density difference entering the system are in the form of gravitational forces. Deriving from this, the Navier-Stokes equations for an incompressible Newtonian fluid with a conservative external field:

$$\underbrace{\rho(\frac{\partial \vec{v}}{\partial t} + \vec{v} \cdot \nabla \vec{v})}_{1} = \underbrace{-\nabla p}_{2} + \underbrace{\mu \nabla^2 \vec{v}}_{3} + \underbrace{\vec{f}}_{4} \tag{4.2}$$

With 1.Inertial forces of the fluid. 2. The volumetric stress tensor: Pressure forces inhibit motion due to normal stresses and enlarging or reducing the size of the body. 3. The stress deviator tensor: shear stress and horizontal friction. Shear stress induces viscous flow and turbulence. 4. The external force term: such as friction and gravity.

Equation 4.2 can be written in the form of partial differential equations(PDE's). The PDE's can be simplified by several assumption for Turbid Density currents. Below a summary is given of the assumption made, detailed derivation can be found in Appendix B, section B.2, subsection B.2.1. For further reference consider [30][63] .

1. Height and width of current are much smaller than the length.
2. Flow is one dimensional and parallel to bottom and wall of the channel.
3. Hydrostatic pressure: Flow is varying slowly in time and horizontal(x)-direction and changes in the vertical direction is small.
4. Inviscid flow: Reynolds number is 'high', inertial forces dominate the current compared to viscous forces.

Using the above assumption yields the one dimensional Shallow Water Equation:

$$\frac{\partial uh}{\partial t} + \frac{\partial u^2 h}{\partial x} + g\frac{1}{2}\frac{\partial h^2}{\partial x} = f_x \tag{4.3}$$

In which f_x is a source term that in this study is equal to gravity f_g and friction forces f_f:

$$f_x = f_g - f_f \tag{4.4a}$$
$$f_g = g'(\phi) So \tag{4.4b}$$
$$f_f = -\frac{f}{8R}u^2 \tag{4.4c}$$

With gravity term f_g, reduced gravity g', volume concentration ϕ, slope S_o, Darcy Weisbach friction factor f, hydraulic radius R and velocity u. A Turbid density current is driven by density differences it results in hydrostatic pressure differences between the fluid and the turbidity current. This results in the reduced gravity. For the derivation Appendix B subsection B.2.1 and for reference [34] [10]. The reduced gravity is in the form:

$$g^{'}(\phi) = g\frac{\rho_m(\phi) - \rho_a}{\rho_a} \tag{4.5}$$

With the mixture density ρ_m depending on the volume concentration ϕ and the ambient fluid density ρ_a (in this study assumed as the density of freshwater ρ_w = 1000 kg/m3) The particles are assumed to be distributed homogeneously over height and length of the current. The density of the ambient fluid is assumed constant. The density of the current varies over time and length in the following form:

$$\rho_m(\phi) = \phi(x,t)\rho_s + (1 - \phi(x,t))\rho_a \tag{4.6}$$

The 1D Shallow Water equation assuming a Newtonian fluid for a current with density differences yields the momentum equation [10][17]:

$$\frac{\partial uh}{\partial t} + \frac{\partial u^2 h}{\partial x} + g'(\phi)\frac{1}{2}\frac{\partial h^2}{\partial x} = f_x \tag{4.7}$$

The momentum equation is solved together with the continuity equation, the mass conservation equation)[18]:

$$\frac{\partial h}{\partial t} + \frac{\partial uh}{\partial x} = 0 \tag{4.8}$$

The driving force behind the current is the variety of particles in suspension this requires an equation for the conservation of particles. Accounting for entrainment and deposition and omitting water entrainment and bed deformation. Assuming that the velocity and turbulence within the current are sufficient to keep particles in suspension. The Particle conservation equation:

$$\frac{\partial \phi h}{\partial t} + \frac{\partial u \phi h}{\partial x} = E - D \tag{4.9}$$

With the source terms erosion E in Equation 4.10a derived in subsection 3.2.3, subsection 3.2.4 and deposition D in Equation 4.10b , derived in subsection 3.2.5. The source terms for the 1D shallow water equation describing the turbid density currents contain; friction, gravity, erosion and depositions. The derivation of the friction and erosion source terms is provided in Appendix B, section B.5. For reference on the derivation of gravity and friction refer to [67][39]. For reference on the Deposition term, refer to subsection 3.2.5. For the erosion term refer to subsection 3.2.3 for non-hindered erosion and to subsection 3.2.4 for hindered erosion. An overview of the source terms is provided below:

The Source terms:

$$\text{Erosion:} \quad E = 0.00033 D_*^{0.3} \left(\frac{\theta - \theta_{cr}}{\theta_{cr}}\right)^{1.5} \sqrt{\Delta g d_{50}} \cdot \left(1 - \frac{\phi}{1 - c_{max}}\right)^n \tag{4.10a}$$

$$\text{Deposition:} \quad D = \rho_s v_s \phi (1 - \alpha \phi)^n \tag{4.10b}$$

$$\text{Friction:} \quad f_f = -\frac{f}{8R} u^2 \tag{4.10c}$$

$$\text{Gravity:} \quad f_g = g'(\phi) So \tag{4.10d}$$

- u in [m/s]
- h in [m]
- f = 0.025 [-]
- R = Hydraulic radius [m]
- S_o = slope [-]
- D_* = $(\frac{g\Delta}{\nu^2})^{1/3} d$
- θ = $\frac{u_{*c}^2}{\Delta g d}$
- θ_{cr} = $\frac{0.30}{1+1.2D_*} + 0.055[1 - exp(-0.020 D_*)]$
- Δ = $\frac{\rho_s - \rho_w}{\rho_w}$ = 1.65
- ρ_s = 2650 [kg/m3], sediment density
- v_s = $\frac{\Delta g d_{50}^2}{C_1 \nu + \sqrt{0.75 C_2 \delta g d_{50}^3}}$
- ϕ = particle concentration
- n = exponent by Richardson and Zaki (1954) [55]
- α = 0 non-hinder settling, 1 hindered settling
- ρ_m = the mixture density

4.2.2. Mathematical Model Overview

The summary and complete analytical description of a turbid density current moving down a slope based upon the 1D Shallow Water Equations derived in subsection 4.2.1 and Appendix B include the mass, moment and the particle conservation equation. The four source terms incorporate erosion, deposition, friction and gravity.

The complete description of the system is given below:

$$\text{Continuity equation:} \quad \frac{\partial h}{\partial t} + \frac{\partial u h}{\partial x} = 0 \tag{4.11a}$$

$$\text{Momentum equation:} \quad \frac{\partial u h}{\partial t} + \frac{\partial u^2 h}{\partial x} + g'(\phi) \frac{1}{2} \frac{\partial h^2}{\partial x} = f_g - f_f \tag{4.11b}$$

$$\text{Particle equation:} \quad \frac{\partial \phi h}{\partial t} + \frac{\partial u \phi h}{\partial x} = E - D \tag{4.11c}$$

$$\text{Reduced gravity:} \quad g'(\phi) = g \frac{\rho_m(\phi) - \rho_w}{\rho_w} \tag{4.12a}$$

$$\text{Current density:} \quad \rho_m(\phi) = \phi \rho_s + (1 - \phi) \rho_w \tag{4.12b}$$

Source terms: (4.13a)

Erosion: $$E = 0.00033 D_*^{0.3} \left(\frac{\theta - \theta_{cr}}{\theta_{cr}}\right)^{1.5} \sqrt{\Delta g d_{50}} \cdot \left(1 - \frac{\phi}{1 - c_{max}}\right)^n \tag{4.13b}$$

Deposition: $$D = \rho_s v_s \phi (1 - \alpha\phi)^n \tag{4.13c}$$

Friction: $$f_f = -\frac{f}{8R} u^2 \tag{4.13d}$$

Gravity: $$f_g = g'(\phi) S_o \tag{4.13e}$$

4.3. Numerical Model

4.3.1. Discretisation method

There is no analytical solution for the 1D shallow water equations with particle driven current, erosion, sedimentation, gravity and friction. The equations are solved numerically. The numerical method has to cope with hyperbolic equations with shocks and jumps and preset boundary and initial conditions. The Generalised Lax Friederich Scheme is used to discretise the continuity, momentum and particle conservation equation. It method used in previous studies that it is a good tool to model a comparable system of equations[63]. The scheme is a transformation of an unconditionally unstable scheme, the Forward in Time and Central in Space (FTCS) scheme. It is a cell centred finite difference method as shown in Figure 4.7, cell centres are located between the boundaries that are located on $i - \frac{1}{2}$ and $i + \frac{1}{2}$. There is numerical diffusion within the equation. The amplitude of the solution will decrease.

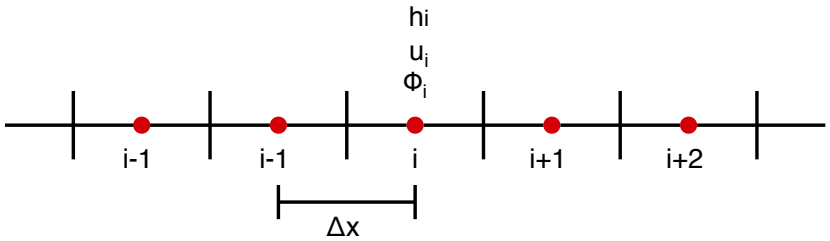

Figure 4.7: Cell centred finite difference scheme

Before the method is applied to the system of equations, this section describes which aspects are taken into account before the scheme is applied. First the Generalised Lax Friederich Scheme with an arbitrary value u:

$$u_i^{n+1} = \frac{A u_{i-1}^n + B u_i^n + C u_{i+1}^n}{A + B + C} - v \frac{\Delta t}{2\Delta x} (u_{i-1}^n - u_{i+1}^n) \tag{4.14}$$

The Generalised Lax Friederich Scheme is a form of the Forward in Time and Central in Space(FTCS) scheme. It is an explicit method that determines the state of the system in the next time step$(n+1)$ based on the current time step(n)[78]. The scheme is 1^{st} order accurate in space and 2^{nd} order accurate in time. Let us denote the 1D advection equation:

$$\frac{\partial u}{\partial t} + v \frac{\partial u}{\partial x} = 0 \tag{4.15}$$

The above equation is a hyperbolic partial differential equation that describes the advection of scalar u(x,t) transported by the flow at a constant speed v and its solution is wave-like as the analytical problem described in section 4.2 [78]. Within a wave-like equation, disturbances are moved though the domain and are not in every location. Equation 4.15 is almost similar to the continuity equation, Equation 4.11a. Let us first discretise Equation 4.15 with the FTCS scheme:

$$\frac{u_i^{n+1} - u_i^n}{\Delta t} = -v \frac{u_{i-1}^n - u_{i+1}^n}{2\Delta x} \tag{4.16}$$

Rewriting the Equation 4.16 yields:

$$u_i^{n+1} = u_i^n - v\frac{\Delta t}{2\Delta x}(u_{i-1}^n - u_{i+1}^n) \tag{4.17}$$

Within numerical modelling, one aims to find a numerical recipe or algorithm that leads to a solution that is close to the exact or analytical solution of the differential equation. Although convergence is somewhat apparent, proof of convergence is far from trivial[78]. Instead, one aims to find a numerical solution with consistency and stability. In which consistency provides a relation between the numerical scheme and the differential equation. So where stability provides a relation between the computed solution and exact solution of the numerical scheme[78]. The stability criterion is only for the numerical scheme and does not contain a condition on the differential equation. The von Neumann stability analysis, a necessary condition but not sufficient, due to incomplete analysis, shows that the FTCS is unconditionally unstable, for details refer to Zijlema (2015)[78]: The amplification factor is greater than unity(1) for all values implying the scheme is unconditionally unstable. A finite difference scheme is stable in the limit of $\Delta t- > 0$ and $\Delta x- > 0$, if the amplification made at on time step of the calculation does not cause errors to increase too large as the computation continues.

One can also apply the Courant-Friedrichs-Lewy(CFL) condition, which is a necessary condition for convergence of a finite difference scheme to a (non-)linear hyperbolic Partial Differential equation is based on the domain of dependence. The CFL condition states:

$$\frac{|u|\Delta t}{\Delta x} \leq 1 \tag{4.18}$$

"The CFL condition means that the distance Δx covered during Δt with speed/velocity u must be smaller or equal to Δx. While the CFL condition is a necessary condition for convergence, it does not guarantee convergences while not meeting it does guarantee non-convergence. Convergence implies CFL condition, usually referring to an explicit scheme. According to the CFL condition, there is no explicit unconditionally stable finite difference scheme for solving a hyperbolic PDE[78]." It proves that the FTCS scheme is unconditionally unstable.The Lax-Friedrichs discretisation of the advection-diffusion equation [66]:

$$u_i^{n+1} = \frac{1}{2}(u_{i-1}^n + u_{i+1}^n) - v\frac{\Delta t}{2\Delta x}(u_{i+1}^n - u_{i-1}^n) \tag{4.19}$$

The Lax-Friedrichs numerical method does not consider the point that is updated. The generalised Lax-Friedrichs(LxF) scheme does consider the point and is formulated in the following, for reference Tong(2012) [66]:

$$u_i^{n+1} = \frac{Au_{i-1}^n + Bu_i^n + Cu_{i+1}^n}{A+B+C} - v\frac{\Delta t}{2\Delta}(u_{i+1}^n - u_{i-1}^n) \tag{4.20}$$

With A = 1, B = 0, C = 1, one obtains the Lax-Frierichs method [66]. Values of A= 0.1, B = 1 and C = 0.1 are chosen for convenience and provide good solutions. When A = 0, B = 1, C = 0 is applied the FTCS scheme is obtained as in Equation 4.16.

4.3.2. Initial and Boundary Conditions

For the problem to be well posed sufficient initial and boundary conditions should be imposed to solve for the different equations and variables[78].

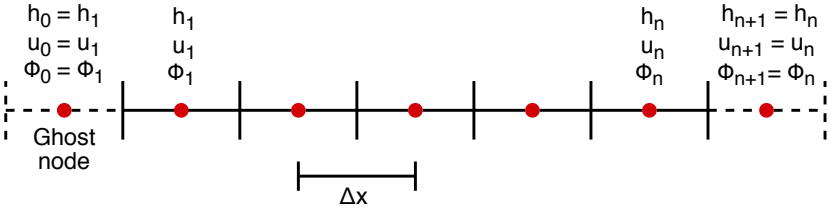

Figure 4.8: Cell centred finite difference scheme with ghost cells and nodes

The ghost nodes are needed at the start and end of the domain to represent the boundaries as shown in Figure 4.8, a central space scheme needs information on the left and right of the point of interest. The schematic representation is provided in Figure 4.8. The walls of the system are located on $i - \frac{1}{2}$ and $i + \frac{1}{2}$. To solve the system of equations boundary conditions are set at the starting point(x=0) and end(x=L) point. For

the system of equations provided in subsection 4.2.2, Neumann and Dirichlet boundary conditions are used. The initial inflow values are a height, velocity and concentration coming from upstream(x=0), the Neumann boundary. At the end of the domain, Dirichlet boundary conditions as there is flow out of the system. As the central space scheme is used, both ghost cells left of the boundary and right of the boundary are needed. Height, velocity and concentration are assumed to be equal to the cells centre. The initial condition is set to ensure the numerical scheme is not divided by zero and to solve for incoming concentration.

The boundary conditions:

$$\begin{aligned} h(x=0,t) &= h_{in} \quad \text{and} \quad (\tfrac{\partial h}{\partial x})_{L,t} = 0 \\ u(x=0,t) &= v_{in} \quad \text{and} \quad (\tfrac{\partial h}{\partial x})_{L,t} = 0 \\ \phi(x=0,t) &= \phi_{in} \quad \text{and} \quad (\tfrac{\partial h}{\partial x})_{L,t} = 0 \end{aligned}$$

The initial conditions:

$$h(x, t=0) = 0.001 \text{ for } 0 \leq x \leq x_L$$

4.3.3. Numerical Model Overview

This section gives a model overview of; the discretised numerical 1D Shallow Water Equations for a Turbid Density Current with gravity, friction, Particle Settling and Erosion. The equations are discretised using the Generalised Lax Friedrichs Method, as discussed in subsection 4.3.1. The diffusion term values are: A = 0.1, B = 1.0, C = 0.1.

Continuity equation:

$$h_i^{n+1} = \frac{Ah_{i-1}^n + Bh_i^n + Ch_{i+1}^n}{A+B+C} - \frac{\Delta t}{2\Delta x}([uh]_{i+1}^n - [uh]_{i-1}^n) \tag{4.21}$$

Momentum equation:

$$\begin{aligned} [uh]_i^{n+1} = \frac{A[uh]_{i-1}^n + B[uh]_i^n + C[uh]_{i+1}^n}{A+B+C} - \Delta t \frac{u_{i+1}^n [uh]_{i+1}^n - u_{i-1}^n [uh]_{i-1}^n}{2\Delta x} - \\ \frac{1}{2}\Delta t \frac{g'(\phi)_{i+1}^n h_{i+1}^n h_{i+1}^n - g'(\phi)_{n-1}^n h_{i-1}^n h_{i-1}^n}{2\Delta x} + \Delta t g'(\phi)_i^n S_o - \Delta t \frac{f}{8R} u_i^n u_i^n \end{aligned} \tag{4.22}$$

Particle conservation equation:

$$[\phi h]_i^{n+1} = \frac{A[\phi h]_{i-1}^n + B[\phi h]_i^n + C[\phi h]_{i+1}^n}{A+B+C} - \Delta t \frac{u_{i+1}^n [\phi h]_{i+1}^n - u_{i-1}^n [\phi h]^n + i - 1}{2\Delta x} - \Delta t D_i^n + \Delta t E_{s,i}^n \tag{4.23}$$

$$\text{Reduced gravity:} \quad g'(\phi)_i^n = \frac{\rho_m(\phi)_i^n - \rho_w}{\rho_w} \tag{4.24a}$$

$$\text{Current density:} \quad \rho_{m,i}^n = (1-\phi_i^n)\rho_w + \phi_i^n \rho_s \tag{4.24b}$$

$$\text{Source terms:} \tag{4.24c}$$

$$\text{Erosion:} \quad E_{s,i}^n = 0.00033 D_*^{0.3} (\frac{\theta_i^n - \theta_{cr}}{\theta_{cr}})^{1.5} \sqrt{\Delta g d_{50}} \cdot (1 - \frac{\phi_i^n}{1-c_{max}})^n \tag{4.24d}$$

$$\text{Deposition:} \quad D_i^n = v_{s,i}^n \phi (1-\alpha\phi)^n \tag{4.24e}$$

$$\text{Friction:} \quad f_{f,i}^n = \frac{f}{8R} u_i^n u_i^n \tag{4.24f}$$

$$\text{Gravity:} \quad f_{g,i}^n = g'(\phi)_i^n S_o \tag{4.24g}$$

$$\text{Parameters:} \tag{4.24h}$$

$$\text{To obtain } u\text{:} \quad u_i^{n+1} = \frac{[uh]_i^{n+1}}{h_i^{n+1}} \tag{4.24i}$$

$$\text{To obtain } \phi\text{:} \quad \phi_i^{n+1} = \frac{[\phi h]_i^{n+1}}{h^{n+1}} \tag{4.24j}$$

$$\text{Shields } (\theta)\text{ :} \quad \theta_i^n = \frac{C_d [u_i^n]^2}{\Delta g d_{50}} \tag{4.24k}$$

$$\text{Critical shields } (\theta_{cr})\text{:} \quad \theta_{cr} = \frac{0.30}{1+1.2D_*} + 0.055[1 - exp(-0.020 D_*)] \tag{4.24l}$$

$$\text{Dimensionless grainsize } D_*\text{:} \quad D_* = (\frac{g\Delta}{\nu^2})^{1/3} d_{50} \tag{4.24m}$$

$$\text{Fall velocity } (v_s) \quad v_s = \frac{\Delta g d_{50}^2}{C_1 \nu + \sqrt{0.75 C_2 \Delta g d_{50}^3}} \tag{4.24n}$$

$$\text{Hydraulic radius:} \quad R = \frac{A}{P} \qquad \text{P: wett perimeter, A: Cross sectional area} \tag{4.24o}$$

Physical parameters																		
d_{50} [μm]	h [m]	u [m/s]	ϕ [-]	L [m] ϕ [-]	W_b [m]	t[s]	S [-]	m [-]	v_s [m/s]	Δ	D_*	R [m]	ν	θ	θ_{cr}	g	C1	C2
50 - 200	5-30	0.3-2.0	0.01-0.09	700-2000	10	variable	0.001-0.05	4	variable	1.65	variable	variable	1.310^{-6}	variable	variable	9.81	18	1

Table 4.1: Physical parameters to test the influence of grid size on the numerical model

h = water depth
Δt = time step size
Δx = space step size
u = velocity
κ = 0.4 von Karman constant
C_D = Drag coefficient
u_* = friction velocity
E_s = erosion capacity
$g'(\phi)$ = reduced gravity $[m/s^2]$
S_o = slope of the channel
R = Hydraulic radius of trapezoidal channel
ρ_m = mixture density depended on concentration
ρ_s = 2650 kg/m3 (density sand)
ρ_w = 1000 kg/m3 (density water)
$\nu = 1.3 \cdot 10^{-6}$ kinematic viscosity
$\phi_{initial}$ = 0.02 (2 % vol.)
z_0 = 0.06
c = 0.6
d_{50} = 50 - 200 μm median sediment diameter(??)
g = 9.81
Δ = 1.65
C_1 = 18
C_2 = 1
P = wett perimeter [m]
A = area of the channel

III

Modelling

5
Modelling

5.1. Introduction

This chapter provides the concept and modelling approach for this study.

First, in this section, summarising the literature study in subsection 5.1.1. Followed by an explanation of the concept on channelling turbid density currents in dam reservoirs in subsection 5.1.2 and the channel properties in subsection 5.1.3. The materials and apparatus for modelling in subsection 5.1.4 and preliminary modelling of the rouse profiles in subsection 5.1.5.

Secondly, in section 5.2 and section 5.3, the two modelling approaches respectively the steady-state solution and the numerical approach are discussed. The steady-state model, section 5.2, is derived from the analytical model in section 4.2. The numerical model, in section 5.3, derived in section 4.3 is used to model the dynamic behaviour of the turbid density current in the channel. Before the model is applied: the model is validated by a dam break experiment(subsection 5.3.1), influence of the grid size(subsection 5.3.3) and choosing a settling model(subsection 5.3.2). After this, the scenarios and parameters for the source terms and the the full model are provided in subsection 5.3.5.

The results of the steady-state solution and numerical scenarios are given in chapter 6. There meaning is discussed in chapter 7.

5.1.1. Summary

Sedimentation in dam reservoirs is a major problem that finally receives the necessary attention as is apparent from chapter 2. Reconsider the flow and sediment dynamics in a dam reservoir, as discussed in chapter 3 and chapter 4. The upstream river transports both water and sediment into the dam reservoir. Sediment is transported utilizing different transport mechanisms; bed-, suspended- and wash-load transport, see section 3.1. In some cases, a turbid density current is formed, see chapter 4, from suspended- and wash-load transport that enters the reservoir. This density current moves towards the lowest point in the river, assuming density is higher than the ambient fluid, referred to as the thalweg. Density differences and gravity drive the current as an effect of the sloping bed. Over time the thalweg is filled up due to sedimentation. As the density currents can no longer flow through the thalweg, the current starts to be affected by the change of depth and width in the reservoir. Friction increases at the top, bottom and front of the turbid density current, see subsection 4.1.3. The increased friction reduces the velocity resulting in increased water entrainment and settling of sediment, reducing the dam reservoirs water capacity.

5.1.2. The Concept

The concept is to dredge a channel, that efficiently transports the density current downstream with minimal sedimentation occurring. The concept is provided in an artist impression in Figure 5.1.

The current situation in a dam reservoir illustrated in Figure 5.1a; the turbid density current enters the dam reservoirs, plunges below the surface and moves downslope while spreading and settling, causing sedimentation of the dam reservoir.

The new situation is illustrated in Figure 5.1b. A channel is created, the turbid density current plunges into the channel and is no longer affected by width changes. The hydraulic radius and slope can be controlled to increase velocity and turbulence, improving the transport of sediment.

The aim is to investigate the effectiveness of the channelling concept. The dimensions of the channel chosen in such a way that the turbid density current fits in it. The impact of different hydraulic radii, slopes and shapes on turbid density current transport are studied. The primary focus is on sediment particles with sizes in a range of 50 μm - 200 μm.

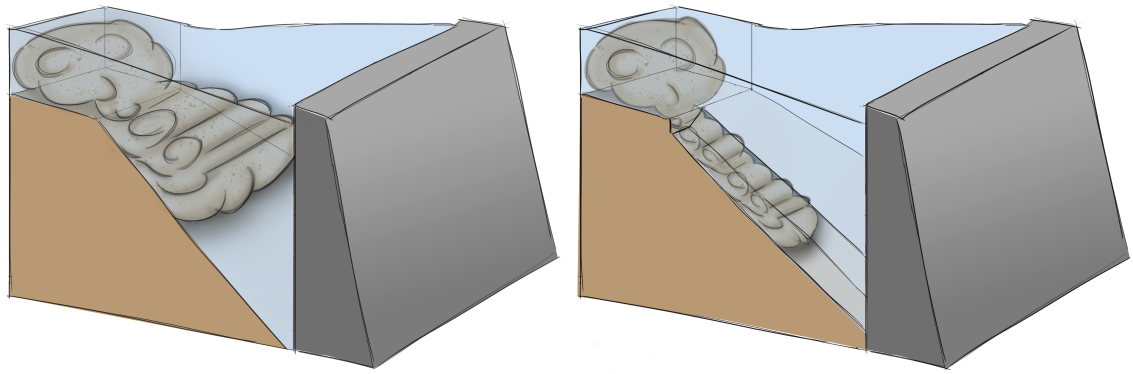

(a) Turbid density current entering a reservoir from an upstream river

(b) Turbid density current entering a reservoir through a channel

Figure 5.1: The concept: Channelling a turbid density currents in dam reservoirs. An artist impression specially made for this study by B.C. van Schaik

5.1.3. Channel Properties

Both the steady-state and dynamic model include a hydraulic radius of the channel in the calculations. The hydraulic radius depends on the area and the wetted perimeter of the channel. The wetted perimeter consists of the walls on which the fluid acts upon with shear stress; this depends on channel type.

In open channel flow for a rectangular channel, the upper boundary is omitted due to zero shear, and the wetted perimeter consists of the two walls and the bottom. The channel in the reservoir is created "underwater" the top of the flow should now experience shear stresses from the upper water layer too. But from studies it is found that the shear and friction along the top is very minimal provided in Figure 4.6 and subsection 4.1.3. The open channel flow characteristics are assumed.

The channel dimensions ensure that the turbid density current is captured within the channel. The loss of sediment that would occur due to turbulent mixing, not accounting for water entrainment and overflow of the channel. Within the first modelling approach a rectangular channel,Figure 5.2a, is used as it provides an easy starting point for estimations, Equation 5.1. In the numerical model and the steady-state model, a trapezoidal channel Figure 5.2b, is assumed as sediment in the dredged channel will settle under a natural angle of repose; when sediment is submerged in the water, this is approximately 30 °. To simplify calculations, the ratio of the slope of the rectangular channel is chosen to be 2:1, the natural angle of repose approximately 26.5 °. Dredging a channel will most certainly provide such a trapezoidal channel due to the earlier mentioned natural angle of repose. It will affect the hydraulic radius of the channel. The hydraulic radius, cross-sectional area and wetted perimeter are calculated with equations for the Trapezoidal channel below, Equation 5.3, Equation 5.1, Equation 5.2. A given depth and width will result in a certain assumed channel shape. Next, to this, the natural slope in a river is approximately 0.001[-]. Within calculations, the minimum slope is 0.001[-] and is gradually increase towards a maximum of 0.05[-]. The maximum slope strongly depends on the length and depth of the available reservoir.

Rectangular Channel	Trapezoidal Channel	
$R_{rect} = \frac{A_{rc}}{P_{rc}}$	$R_{trap} = \frac{A_{trap}}{P_{trap}}$	(5.1)
$A_{rect} = Wh$	$A_{trap} = W_b h + 2h^2$	(5.2)
$P_{rect} = W + 2h$	$P_{trap} = W_b + 2h\sqrt{5}$	(5.3)

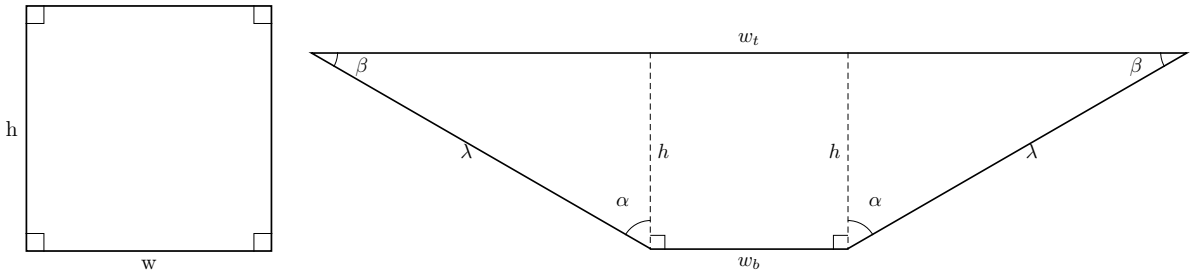

(a) Rectangular channel (b) Trapezoidal channel

Figure 5.2: Frontview sketch of the rectangular channel and trapezoidal channel providing height(h), width(w), slope length(λ) and angles(α and β)

5.1.4. Materials and Apparatus

The model for this thesis is written in Python 3, a general-purpose, open-source programming language. The scripts(for rouse profiles, Steady State and Numerical model are provided in Appendix C. Any computer with Python 3 can be used to run the model, installing can be done through "anaconda", the processing time depends on numerical detail and processor capacity. The scripts did successfully run on multiple computers: Windows 10 and OSX 10.14.5 with a 2,3 GHz Intel Core i5 processors. Editing of the code is done with Spyder 3.3.2. The needed packages are stated within the scripts and should be sufficient to make the model work. Copying and pasting the code it into a ".py" file from the appendix should work, note that both simulator and plotting file is needed. If one wants to understand the script, one can follow the notes and comments within it(marked by a # and "' signs). Plots are printed to both '.png' and '.pdf' formats within the directory.

5.1.5. Preliminary Modelling

The preliminary modelling is done to obtain insight in the rouse profiles induced by open channel flow at different average flow velocities and particle sizes. The figures provide an overview of the concentration over the height. The results are provided in section A.3.

5.2. The Steady State Model

The steady-state model is derived from the analytical model from section 4.2 including all source terms set equal to zero. It yields the simplest form of the equations and describes the velocity of the turbid density current based upon gravity, friction, density, hydraulic radius and slope. The mass balance is used for the river, reservoir and current. By using the mass balance 3 scenarios are studied: Reservoirs With Return Flow subsection 5.2.2, Reservoir Without Return Flow in subsection 5.2.3 and Reservoir Without Return Flow: Simplified subsection 5.2.4.

5.2.1. The Steady State Model

Turbid density currents are unsteady for discharge, sediment concentration, grain size distribution, velocity, and thickness[46]. The steady-state solution for a turbid density current holds when there are no changes over time and length of the flow, a kinematic wave. The flow is uniform, and the friction slope is equal to the slope of the channel. The kinematic wave equation holds when the change in height and velocity along the channel are negligible, the shallow water equations. With Friction and gravity as proposed in section 4.2: Simplifying the continuity, Equation 4.11a, momentum, Equation 4.11b and particle conservation, Equation 4.11c, with the assumptions above, this yields:

$$f_g - f_f = 0 \tag{5.4}$$

For friction and gravity:

$$\text{Friction:} \qquad f_f = -\frac{f}{8R}u^2 \tag{5.5}$$

$$\text{Gravity:} \qquad f_g = g'(\phi)S_o \tag{5.6}$$

Combining Equation 5.4, Equation 5.5 and Equation 5.6 yields:

$$g'(\phi)S_o - \frac{f}{8R}u^2 = 0 \tag{5.7}$$

With g' the reduced gravity:

$$g^{'}(\phi) = g\frac{\rho_m(\phi) - \rho_w}{\rho_w} \tag{5.8}$$

After rewriting this provides the velocity of the steady state solution of the turbid density current:

$$u_c = \sqrt{\frac{8}{f}Rg'S_o} \tag{5.9}$$

With u_c the flow velocity of the turbid density current, the hydraulic radius R of the channel, the reduced gravity g'(ϕ), Darcy Weisbach friction factor f (= 0.025) and the slope S_o of the channel. Equation 5.9 is also proposed by Morris and Fan (1998)[46].

In chapter 4 section 4.1 it is described that a turbid density currents is gravity-driven flow, it is focused into the deepest part of the cross-section. It follows the thalweg or dredged channel. The river and current enter the reservoir it imposes a flow downstream that has to be compensated by a return flow to account for the balance of mass. The scenarios in subsection 5.2.2, subsection 5.2.3 and subsection 5.2.4 are based on the mass balance, Equation 5.10 within the river and the reservoir:

$$Q_r - Q_c - Q_{rw} = 0 \tag{5.10}$$

In which Q_r is the river discharge, Q_c the channel discharge and Q_{rw} the reservoir return flow. The above equation relies on the assumption that the inflowing sediment-water mixture from upstream flowing into the reservoir is in balance with the channel discharge and the resulting reservoir return flow.

In the first scenario "With Reservoir Return Flow" the entering turbid density current is compensated by return flow of the reservoir water.

The second scenario "Without Reservoir Return Flow" the reservoir return flow is assumed to be negligible ($Q_{rw} = 0$).

The third and last situation is a simplified situation in which there is no return flow, and the characteristics of velocity, surface area and density are equal in both the river and the channel.

5.2.2. Reservoir With Return Flow

In the first scenario it is assumed that the turbid density current is in balance with return flow and the channel flow in the reservoir. The mass balance for discharge of the currents:

$$Q_r - Q_c - Q_{rw} = 0 \tag{5.11}$$

With total river discharge Q_r, turbid density current discharge Q_c and the return discharge of the reservoir Q_{rw}. Since $Q = uA$, with flow velocity u and surface area A, the following holds:

$$u_r A_r - u_c A_c - u_{rw} A_{rw} = 0 \tag{5.12}$$

with flow velocity for the river u_r, channel u_c and reservoir u_{rw}. The area for the riverA_r, channel A_c and reservoir A_{rq}. The balance depends on density differences it is incorporated in the equation as follows:

$$\rho_r u_r A_r - \rho_c u_c A_c - \rho_{rw} u_{rw} A_{rw} = 0 \tag{5.13}$$

With density for the riverρ_r, channel ρ_c and reservoir ρ_{rw}. The turbid density velocity in the channel is assumed to be the same as Equation 5.9 and as proposed by Morris and Fan(1998)[46].

$$u_c = \sqrt{\frac{8}{f}g'RS_o} \tag{5.14}$$

With friction coefficient f(0.025), the hydraulic radius R(as proposed in subsection 5.1.3), reduced gravity g'(Equation 5.8) and an assumed slope slope S_o (0.001 - 0.5 [-]).
The velocity and area of the reservoir are unknown, Equation 5.13 is combined with Equation 5.15:

$$u_r A_r - u_c A_c = u_{rw} A_{rw} \tag{5.15}$$

The equation is solved in the following form:

$$(1-\frac{u_r A_r}{u_c A_c})\rho_{rw}+\rho_r\frac{u_r A_r}{u_c A_c}-\rho_c=0 \tag{5.16}$$

Using, Equation 5.1, Equation 5.2 and Equation 5.3, to determine the hydraulic radius, channel area and wetted perimeter. The area and velocity for the river, the densities for the river, channel and reservoir are constant. The only part were the Equation 5.16 depends on are the Width(W), Height(h) and Slope (S). The form for a turbid density current flowing into a reservoir with return flow is:

$$\rho_r\frac{u_r A_r}{\sqrt{\frac{8}{f}\frac{\rho_c-\rho_w}{\rho_w}g\frac{A}{P}}(A)}+(1-\frac{u_r A_r}{\sqrt{\frac{8}{f}\frac{\rho_c-\rho_w}{\rho_w}g\frac{A_{c,i}}{P_{c,i}}}(A_{c,i})})\rho_{rw}-\rho_c=0 \tag{5.17}$$

Equation 5.17 depends on the slope and hydraulic radius, which depend on width W and height h.

The physical parameters for the model can be found in Table 5.1. The results can are provided in section 6.1.

Table 5.1: Physical variables: Steady state turbid density current in a channelled reservoir. With return flow.

Turbidity Current in Reservoir With Return Flow			
Variable	Value	Unit	Notes
u_c	variable	[m/s]	Depends on the given slope(S) and Hydraulic radius(R)
A P R	Variable Variable Variable	[m/s] [m/s] [m/s]	The values depend on the Height(H) and Width (H) of the channel and are influenced by the slope and channel shape, either trapezoidal or Rectangular. The variation is provided in the graphs
S	Variable	[kg/m^3]	The slope varies between 0.001 and 0.05 and influences the channel velocity
ρ_c	1040	[kg/m^3]	The density of the channel is the same as that from the river, all sediment is transported by the turbidity current
u_r	2.0	[m/s]	Is a chosen value based upon average river discharge
A_r	500	[m^2]	Based on an average height of 5 m and a width of 100 m
ρ_r	1040	[kg/m^3]	The river density is the same as the channel density, it is assumed all sediment is transported by the turbidity current
ρ_{rw}	1000	[kg/m^3]	The ambient water of the reservoir is the water density
g	9.81	[m/s^2]	gravitational acceleration
ρ_w	1000	[kg/m^3]	assumed water density
f	0.025	[-]	darcy weisbach friction coefficient

5.2.3. Without Reservoir Return flow

In the previous section, assumes a return flow. The contribution of the return flow seems to be minimal; eliminating the return flow from the equation. In the below the derivation of the equations without reservoir return flow is given. The table with the variables is Table 5.2. Results are presented in section 6.1.

When the return flow is omitted, the mass balance is reduced to Equation 5.18 rewriting it with velocity and cross sectional area yields:

$$Q_r - Q_c = 0 \tag{5.18}$$

$$u_r A_r - u_c A_c = 0 \tag{5.19}$$

By adding the density and applying the previously derived channel velocity this yields:

$$\text{Mass Balance: } \rho_r u_r A_r - \rho_c u_c A_c = 0 \tag{5.20}$$

$$\text{Channel velocity: } u_c = \sqrt{\frac{8}{f} g' R S_o} \tag{5.21}$$

$$\text{Densities: } \rho_r = \rho_c (= 1040 kg/m3) \tag{5.22}$$

With the hydraulic radius for a rectangular or trapezoidal channel:

$$\text{Rectangular channel: } R_{rect} = \frac{A_c}{P} = \frac{\sqrt{A_c}}{3\sqrt{(A_c)}} \tag{5.23}$$

$$\text{Trapezoidal channel: } R_{trap} = \frac{A_c}{P} = \frac{WbH + 2H^2}{W_b + 2H\sqrt{5}} \tag{5.24}$$

Rewriting the equation and substituting the Hydraulic radius R and channel velocity u_c yield:

$$\frac{u_r^2 A_r^2 f \rho_c}{8g(\rho_c - \rho_w)S} = R A_c^2 \tag{5.25}$$

$$\frac{u_r^2 A_r^2 f \rho_c}{8g(\rho_c - \rho_w)S} = \frac{A_c^3}{P} \tag{5.26}$$

Equation 5.17 is solved assuming a channel height H resulting in a channel surface A_c and a wet perimeter P. the equation is solved for specific slopes that results in steady velocity u_c, by implementing the hydraulic radius in Equation 5.21. Results of the simulation are provided in section 6.1.

Table 5.2: Physical variables: Steady state turbid density current in a channelled reservoir. With return flow.

Turbidity Current in Reservoir With Return Flow			
Variable	Value	Unit	Notes
u_c	variable	[m/s]	Depends on the given slope(S) and Hydraulic radius(R)
A P R	Variable Variable Variable	[m/s] [m/s] [m/s]	The values depend on the Height(H) and Width (H) of the channel and are influenced by the slope and channel shape, either trapezoidal or Rectangular. The variation is provided in the graphs
S	Variable	[kg/m^3]	The slope varies between 0.001 and 0.05 and influences the channel velocity
ρ_c	1040	[kg/m^3]	The density of the channel is the same as that from the river, all sediment is transported by the turbidity current
u_r	2.0	[m/s]	Is a chosen value based upon average river discharge
A_r	500	[m^2]	Based on an average height of 5 m and a width of 100 m
ρ_r	1040	[kg/m^3]	The river density is the same as the channel density, it is assumed all sediment is transported by the turbidity current
g	9.81	[m/s^2]	gravitational acceleration
ρ_w	1000	[kg/m^3]	assumed water density
f	0.025	[-]	darcy weisbach friction coefficient

5.2.4. Without Return Flow: Simplified

Since particles stay in suspension at a specific flow velocity and turbulence, these particles should be kept in suspension if the velocity is not decreasing. So, in other words, if the velocity is constant or increases, particles will not settle. Reaching higher flow velocities when increasing slope or hydraulic radius in the reservoir. In this case, assuming that the channel surface, channel velocity and channel density of the current are the same upstream and within the channel:

$$u_r = u_c \tag{5.27}$$
$$A_r = A_C \tag{5.28}$$
$$\rho_r = \rho_c \tag{5.29}$$
$$\tag{5.30}$$

This results in the equation derived in first section namely the steady state solution:

$$\text{Channel velocity: } u_c = \sqrt{\frac{8}{f} g' R S_o} \tag{5.31}$$

The slope is between 0.001 and 0.05 and the hydraulic radius by a change in width and height. The only aspects that changes are u and R in this scenario the equation in the model appears in the following form:

$$S_o = \frac{u_c^2 f \rho_c}{8(\rho_c - \rho_w) R g} \tag{5.32}$$

Results are provided in section 6.1.

5.3. The Numerical Model

5.3.1. Dam Break

To verify convergence and consistency of the proposed numerical model, it is compared with an analytical solution. A standardised test for 1D Shallow Water Equations(Saint Venant Equations) is the dam break experiment, first proposed by Saint Venant (1871)[58] and Ritter 1892[56]. Later, Stoker (1957) [62] provides a solution to the dam break problem with a non-wet front in which a shock wave travels forward and a rare fraction wave backwards with a constant depth connecting the shock wave and the beginning of the rare fraction wave [32]. Since the dam break problem has an analytical solution, it is compared with the proposed numerical model proposed in subsection 4.3.3. To solve for the dam break experiment a prismatic channel with a horizontal bed, infinite length, and no bed friction is assumed, and removing the dam instantaneously [42]. Both wet and dry dam-break problem exists. A wet dam-break problem is performed and compared to the analytical solution to test how the scheme handles the shock.

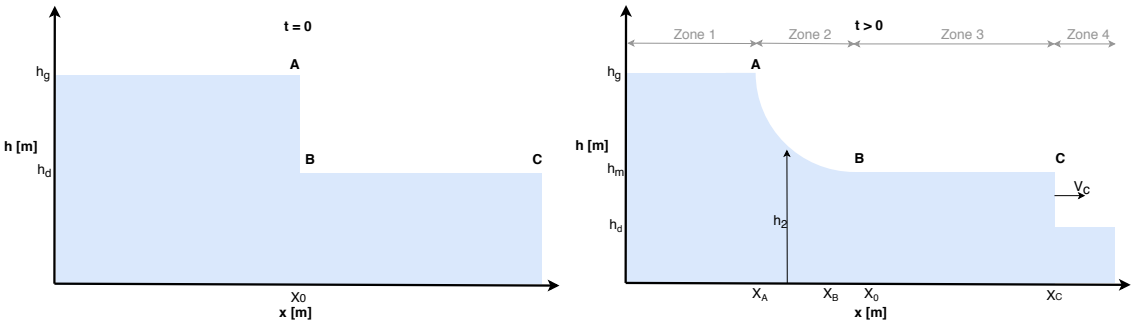

(a) Initial situation

(b) After time t

Figure 5.3: Schematised dam break problem with a wet downstream for t=0 and t>0

The problem has been schematised for the initial situation($t = 0$) before the dam break in Figure 5.3a and for the situation after the dam break($t > 0$) in Figure 5.3b. The problem can be approached as a Riemann problem, that is used to find the characteristics of a set of hyperbolic equations [38]. With constant initial

conditions and a discontinuity at X_0, Figure 5.3a. In which $X_0 \in \mathbb{R}$ with X_0 the point of the discontinuity. Defining the initial conditions of the water height, see Figure 5.3a:

$$h(0,x) = \begin{cases} h_g & x \leq x_0 \\ h_d & x \geq x_0 \end{cases} \quad \text{with } 0 \leq h_d \leq h_g \tag{5.33}$$

Initial conditions for the velocity:

$$u(0,x) = 0 \qquad \forall x \in \mathbb{R} \tag{5.34}$$

The source terms $E, D, f_g and f_f$ are zero and gravity $g'(\phi)$ is equal to the constant gravitational acceleration g.
The solution for the dam break for the set of hyperbolic non linear equations as proposed in subsection 4.2.2 and reformulated without source terms($E, D, f_g and f_f$) and with constant gravitational acceleration in this section in Equation 5.35a, Equation 5.35b and Equation 5.35c are obtained through the Method of Characteristics:

$$\text{Continuity equation:} \quad \frac{\partial h}{\partial t} + \frac{\partial uh}{\partial x} = 0 \tag{5.35a}$$

$$\text{Momentum equation:} \quad \frac{\partial uh}{\partial t} + \frac{\partial u^2 h}{\partial x} + g\frac{1}{2}\frac{\partial h^2}{\partial x} = 0 \tag{5.35b}$$

$$\text{Particle equation:} \quad \frac{\partial \phi h}{\partial t} + \frac{\partial u\phi h}{\partial x} = 0 \tag{5.35c}$$

In which the the characteristics of the Riemann Invariants are calculated(1) and the depth and velocity for the domain is determined(2). The derivation of the characteristics are provided in Martins (2016) [42]. The equations Equation 5.35a, Equation 5.35b and Equation 5.35c are discretised according to the Generalised Lax Friederich Method as proposed in subsection 4.3.1, with A = 0.1, B = 1.0 and C = 0.1.

The analytical description of the dam break problem, can be described by assuming $X_0 = 0$, and evaluate the results after $t > 0$. The initial condition($t = 0$) before the dam break occurs are provided in Equation 5.33, Equation 5.34 and can bee seen in Figure 5.3a. After the dam break, see Figure 5.3b, the problem is divided into four zones:

- Zone 1: is the upstream condition with height h_g and velocity $u_1 = 0$
- Zone 2: has a parabolic shape with decreasing height h_2 and increasing velocity u_2, it connects Zone 1 at height h_g with Zone 2 at height h_m
- Zone 3: has a constant velocity u_m and constant height h_m between point B and the shock C between h_m and h_d
- Zone 4: Starts with the shock C that is between h_m and h_d and it is the downstream condition with depth h_d and velocity $u_4 = 0$

In Table 5.3 the expression for the analytical solution of the 1D shallow water equations for a dam break are given as derived by Martins 2016[42] and Gunawan 2016[32]. Within Table 5.3 the heights, celerity's and different velocities are provided, according to the Riemann invariants and the characteristics in each of the four zones. In Table 5.4 the initial conditions for the model are provided. In Table 5.5 the analytical solutions are given as for the equations provided in Table 5.3 together with the numerical solutions obtained from the three grid sizes modelled($1.0, 0.5, 0.1$). The height and velocity gradients after $t = 50s$ are provided in Figure 5.4.

To conclude, by comparing the analytical solution and numerical solution(Figure 5.4), it can be seen that the numerical solution provides reasonable estimates. When decreasing the grid size, the solution converges towards the analytical solution. The numerical solution under-predicts the height, travel distance and velocity with approximately 10 %. Further studies are needed to identify where this under-prediction is originated.

Table 5.3: Dam Break expressions, for each zone, the Analytical Solution of the 1D Shallow Water Equations is given

Variable	Zone 1	Zone 2	Zone 3	Zone 4
h*	h_g	$h_2 = \frac{4}{9g}(c_g - \frac{x}{2t})$	h_m	h_d
u*	0	$u_2 = \frac{2}{3}(\frac{x}{t} + c_g)$	$u_m = 2(c_g - c_m)$	0
* = if	$x \leq X_A(t)$	$X_A(t) \leq x \leq X_B(t)$	$X_B(t) \leq x \leq X_C(t)$	$x \leq X_c(t)$
c	$c_g = \sqrt{gh_g}$	$c_2 = \sqrt{gh_2} = \frac{2}{3}(c_g - \frac{x}{2t})$	$c_m = \sqrt{gh_m}$	$c_d = \sqrt{gh_d}$
v_c	-	-	$v_c = \frac{h_m u_m}{h_m - h_d}$	-
Position(t>0)	$X_A(t) = c_g t$	$X_B(t) = (u_m - c_m)t = (2c_g - 3c - m)$	$X_C(t) = v_c t$	-

Table 5.4: Dam Break initial conditions for numerical simulation of 1D Shallow Water Equation

Grid size	X_0 [m]	h_g[m]	h_d [m]	Number of cells	Number time steps	t [s]
0.1	500	1.0 for $0 \leq x \leq X_0$	0.25 for $x \geq X_0$	10001	7500	50
0.5	500	1.0 for $0 \leq x \leq X_0$	0.25 for $x \geq X_0$	2001	1500	50
1.0	500	1.0 for $0 \leq x \leq X_0$	0.25 for $x \geq X_0$	1001	750	50

Table 5.5: Results for the Analytical solution and Numerical solution for t = 50 s

	Analytical Solution		Numerical Solution		
Parameter	Δ x	unit	Grid size	Grid size	Grid Size
-	-	-	1.0	0.5	0.1
h_g	1.0	m	1.0	1.0	1.0
c_g	3.13	m/s	-	-	-
X_A	157	m	327	333	336
X_B	27	m	482	474	476
X_C	161	m	147 (641-651)	147 (645-651)	147 (647-648)
h_d	0.25	m	0.245	0.245	0.25
h_m	0.55	m	0.55	0.54	0.55
c_m	2.28	m/s	-	-	-
u_m	1.69	m/s	1.61	1.61	1.61
h_2	0.51	m	1.0 - 0.55	1.0 - 0.54	1.0 - 0.55
u_2	0-1.69	m/s	0-1.61	0 - 1.61	0 - 161
v_c	3.22	m/s	-	-	-

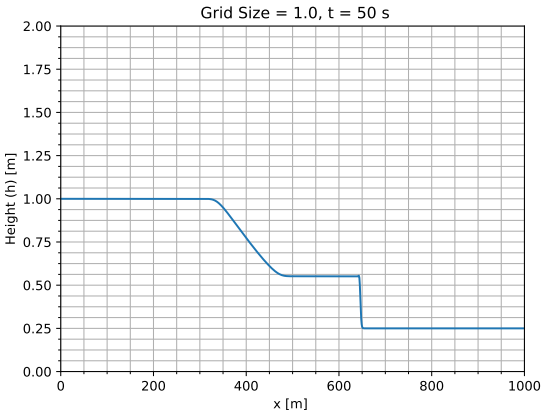

(a) Dam Break for grid size 1.0: Height

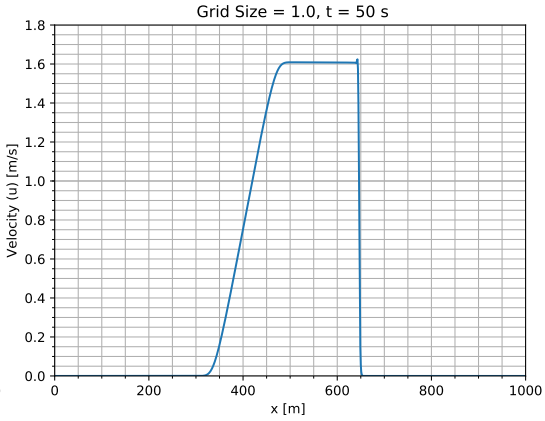

(b) Dam Break for grid size 1.0: Velocity

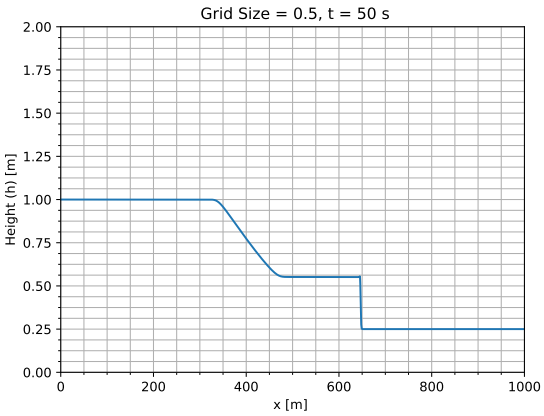

(c) Dam Break for grid size 0.5: Height

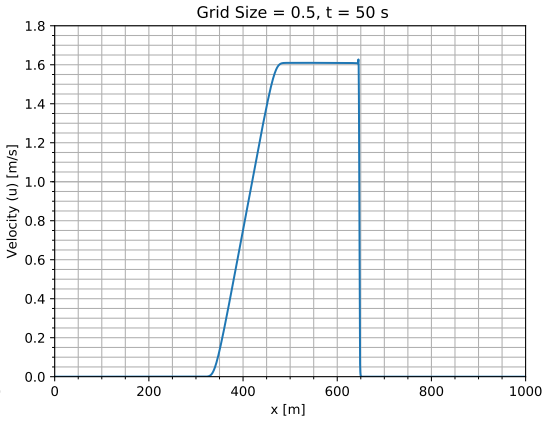

(d) Dam Break for grid size 0.5: Velocity

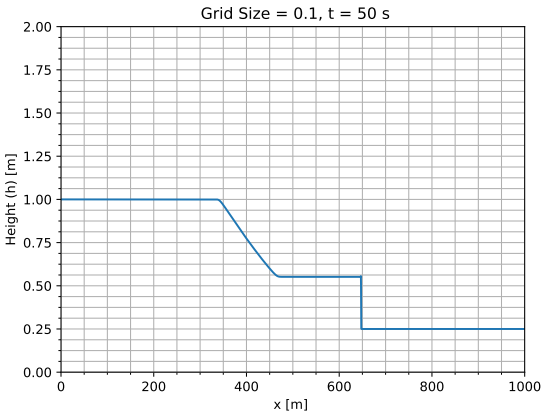

(e) Dam Break for grid size 0.1: Height

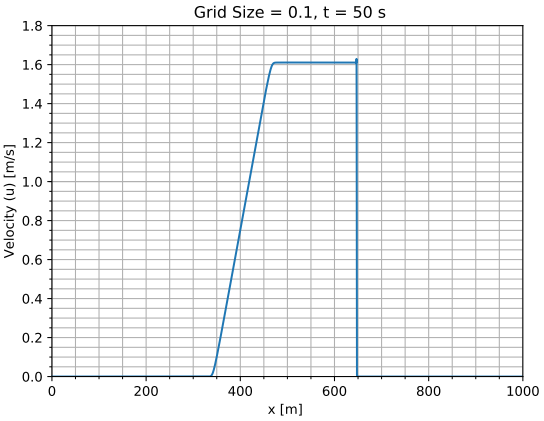

(f) Dam Break for grid size 0.1: Velocity

Figure 5.4: Dam Break: Numerical solutions($t = 50s$) of the dam break problem for the Generalised Lax Friederichs scheme for three different grid sizes(1.0, 0.5, 0.1) and initial height of $h_g = 1.0$ and $h_d = 0.5$

5.3.2. Choosing a Settling Model

Within the numerical simulations, a trade-off between time, diffusion and detail are essential; this can be studied further by a convergence study. Comparing the results, one can use the velocity, height or concentration profile. Since both the velocity and height profile change too quickly and the concentration profile is used. Concentration is the main subject of this study; it not allowed to give negative solutions.

Increasing the numerical detail yields a good solution but increases the computational time significantly. When applying the diffusion terms A = 0.1, B = 1 and C = 0.1 seems to give good solution compared to the results with [45]. To understand the results presented in Figure 5.5, one needs to understand the difference between the slow and fast mixing model explained below.

First, the derivation of the slow mixing model: When considering a rectangular system with horizontal area A and depth h and no velocity. The initial concentration of C_o, in the system, is distributed uniformly. If diffusion is slow in comparison to settling the diffusion, the mixing can be neglected[45]. Assuming the concentration within the particle cloud does not change as settling progresses. Particle distribution is uniform, have same particle size and density, the particles settle at the same velocity, v_s. The particle flux at the bed is due to vertical advection, $m = -v_s C_o A$. This flux continues until the entire water depth free of particles. The loss of particle mass M is constant and independent of the concentration or mass[45]. The depth-averaged concentration is defined as $C = M/hA$:

$$\frac{\partial M}{\partial t} = -v_s C_o \tag{5.36}$$

$$\frac{\partial C}{\partial t} = -\frac{v_s}{h} C_o C(t) = C_o(1 - \frac{v_s}{h} t), for t < \frac{h}{v_s} \tag{5.37}$$

To conclude, in the slow mixing model the particles settle in $T_{settle} = h/v_s$

Secondly, deriving the fast mixing model; In this case, mixing is rapid enough to maintain uniform concentration C throughout the system, even if particles settle. The flux at the bed is assumed to be:

$$m(z = 0) = -v_s C \tag{5.38}$$

Although mixing by diffusion mixing cannot be neglected, it assuming that C is uniformly distributed, neglecting diffusion terms because:

$$\frac{\partial C}{\partial z} = \frac{\partial C}{\partial y} = \frac{\partial C}{\partial x} = 0 \tag{5.39}$$

The conservation equation of mass is:

$$\frac{\partial M}{\partial t} = AH\frac{\partial C}{\partial t} = -v_s C A \tag{5.40}$$

$$\frac{\partial C}{\partial t} = -\frac{v_s}{h} C \tag{5.41}$$

The loss of particles depends on concentration with a constant speed of v_s/h. Partial concentration decreases exponentially with 95% of the initial mass lost in time according to:

$$t = \frac{3h}{v_s} \tag{5.42}$$

As the slow and fast mixing model are now clear, one can choose a settling model. Choosing a settling model is important to obtain the right settling velocity. The two models that described above differ in the importance of mixing and settling. The time-scale can compare the two processes for settling over the depth of the water body. As described above $T_{settle} \approx h/v_s$ and the time scale for mixing over the depth $T_D \approx h^2/D$ if $T_D >> T_{settle}$ the slow mixing model applies. When $T_D << T_{settle}$ the fast mixing model applies.

Using the scale $D \approx u_* h_*$ for turbulent channel flow, it is found that the ratio of time-scales:

$$\frac{\text{time-scale for settling over h}}{\text{time-scale for mixing over h}} = \frac{h/v_s}{h^2/D} = \frac{v_s}{u_*} \tag{5.43}$$

For turbulent channel flow if $v_p << u_*$ the turbulence in the water column is strong enough to keep the particles mixed, in this case, the fast model applies, and the suspended sediment load decays exponentially. If

$v_s >> u_*$ the turbulence is too weak to mix sediment vertically, the slow mixing model applies and suspended sediment load decays linearly.

The model is tested for settling of both 50 μm and for 100 μm, other modelling parameters provided in Table 5.6. All source terms are zero except for the settling term described as $\delta t v_s \phi$. For a volume concentration of 2%, height 1m and the velocity 0.3 m/s, $v_p << u_*$ holds, 95% should be settled after 3h/wp. For 50 μm at a velocity of 0.3 m/s at 1 m height 95% of the sediment should settle at 542m and for 100 um this is approximately 145m. The model shows to have a good approximation for the settling in a system with turbulent flow and rapid mixing, see the result in Figure 5.5. The results validate the model for settling.

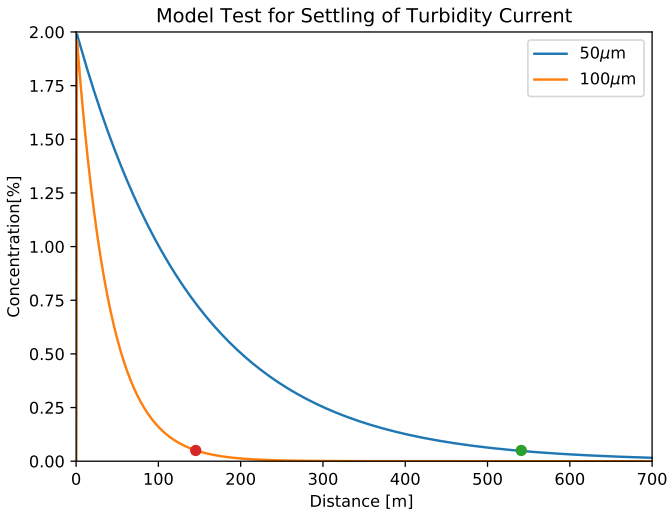

Figure 5.5: 1D Turbid Density current in a channel with settling only. The graph shows that 95% of the particles have settled after $3h/v_s$ proving to make a right approximation of settling in turbulent flow. With height 1m, flow velocity 0.3 m/s, $v_p << u_*$

Table 5.6: Parameters for choosing a settling model

Data for Figure 5.5		
Data type	Value	unit
Time	2000	[s]
Length	700	[m]
Cell size	0.1	[-]
Concentration	2.0	[%]
Height	1.0	[m]
Flow velocity	0.3	[m/s]
$v_{s,50\mu m}$	0.00166	[m/s]
$v_{s,100\mu m}$	0.00619	[m/s]
ρ_w	1000	[kg/m^3]
ρ_s	2650	[kg/m^3]
g	9.81	[m/s^2]

5.3.3. Influence of Grid Size

Due to the limitation of computers, computational modelling is a constant consideration between computational time and accuracy. Grid size influences both accuracy and computational time. A smaller cell induces more points in the grid; more detail is obtained. If the solution is consistent and stable, the numerical solution will approach the analytical solution more accurately. The Courant-Friedrich-Lewy(CFL) condition is a necessary condition for convergences. It states that variables are not able to exceed the boundaries of a cell within a time-step in order to maintain stability. Smaller grid cells imply a decrease of the time step size to satisfy the CFL condition. However, higher accuracy yields longer computational time, which increases non-linearly. A trade-off between detail, accuracy and computational time.

The concentration profile (ϕ) is compared for different numerical detail. Since the solution of the numerical scheme is convergent, it is expected it will approach the analytical solution. Based on the results of the computational time and detail, a grid size is chosen for further simulations.

The CFL condition states that variables can not go beyond a cell within a time step in order to maintain stability. Decreasing in the grid-cell size results in a decrease of the time step. The CFL condition is stated as:

$$u\frac{\Delta t}{\Delta x} \leq 1 \tag{5.44}$$

When decreasing Δx it implies a decrease of Δt. The CFL-condition is a necessary condition for convergence, but it is not a sufficient one. In the case of the used Forward in Time Central in Space (FTCS) scheme, the CFL provides an unstable solution. To solve this problem, the diffusion terms were introduced.

The Physical parameters are given in Table 5.7 and numerical parameters are given in Table 5.8. The results of the model simulations are given in Figure 5.6. These results are compared with the computational time, given in Table 5.7. F

It is concluded that a computational grid of 0.1 does give good results for a computational time of approximately 70 seconds. This is the runtime for just a part of the model. Since more arrays will be included,

computational time increases to approximately 1-3 hours. If one wants to obtain a rough estimate, a computational grid of approximately 1.0 or 2.0 will suffice(if the model stays within stability regions).

Table 5.7: Physical parameters to test the influence of grid size on the numerical model

Physical parameters															
d_{50} [μm]	h [m]	u [m/s]	ϕ [-]	L [m] ϕ [-]	W_b [m]	t[s]	S [-]	ν_s [m/s]	Δ	D_*	R [m]	ν	θ	θ_{cr}	g
50	1	0.3	0.02	700	0	2000	0	9	$1.66 \cdot 10^{-3}$	1.65	1.061	0	$1.3{\cdot}10^{-6}$	15	9.81

Table 5.8: Numerical parameters to test the influence of grid size on the numerical model

Numerical Parameters					
Δx [m]	Δt [s]	nx [-]	t [s]	nt [-]	Computation time[s]
2.0	0.133	351	2000	15000	2.1
1.0	0.067	701	2000	30000	3.5
0.5	0.033	1401	2000	60000	7.0
0.25	0.017	2801	2000	120000	18.0
0.1	$6.7{\cdot}\ 10^{-3}$	7001	2000	300000	69.5
0.05	$3.3{\cdot}\ 10^{-4}$	14001	2000	600000	220.9
0.01	$6.7{\cdot}\ 10^{-4}$	70001	2000	3000000	19862

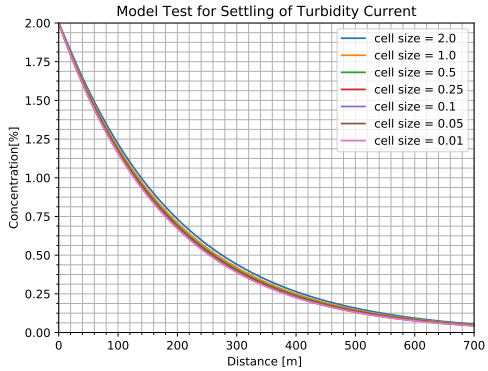

(a) Overview

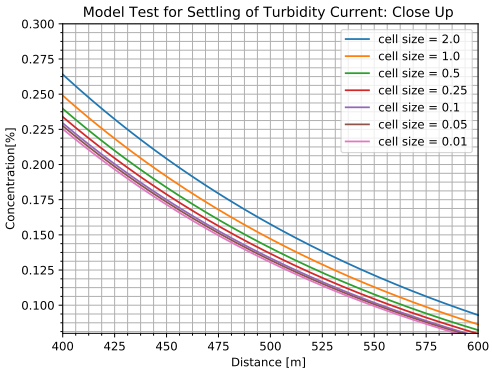

(b) Zoomed

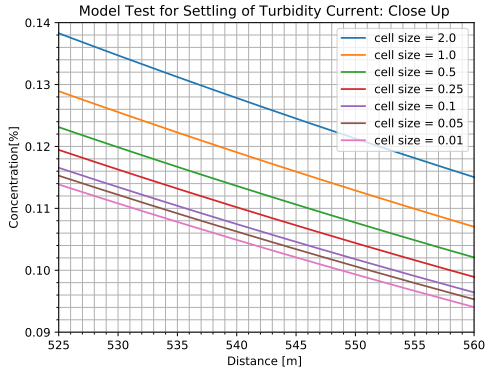

(c) Close-up

Figure 5.6: Comparison of the concentration development for different cell sizes for the model with settling only

5.3.4. Evolution

A shock has two solutions in one point on the left and right side of the point of interest. The Rankine-Hugoniot conditions that describe the relationship between the states on both sides of the shock wave. Investigating the numerical model to see how it handles shock, the solution of the numerical model is solved for eight time steps in Figure 5.7. For the numerical model without source terms results are provided in Figure 5.7a, Figure 5.7c and Figure 5.7e the evolution of the concentration, velocity and height are plotted respectively. For the numerical model with source terms results are provided in Figure 5.7b, Figure 5.7d and Figure 5.7f the evolution of the concentration, velocity and height are provided respectively. The height of the shock is solved according to the expected Navier-Stokes (low) front.

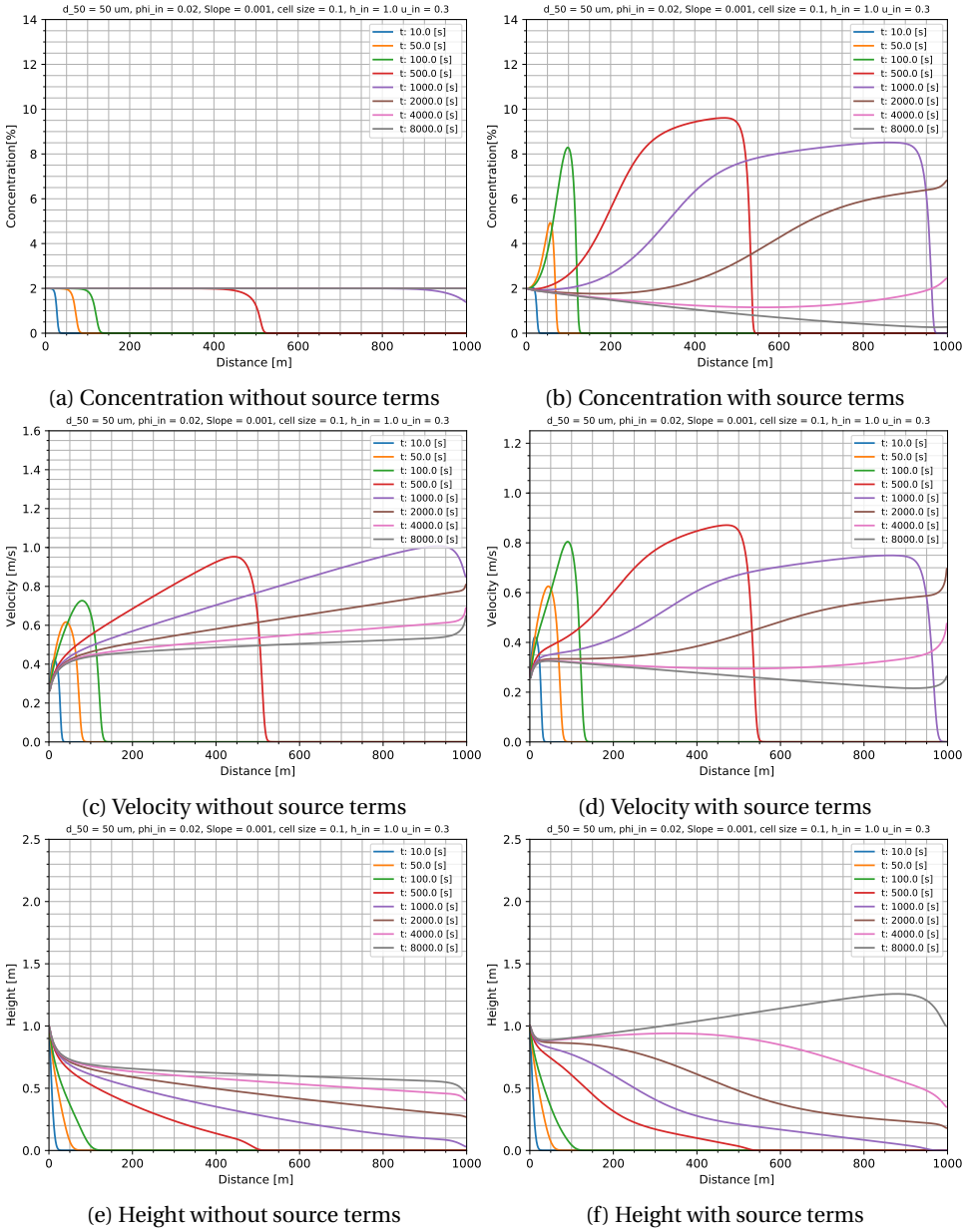

(a) Concentration without source terms

(b) Concentration with source terms

(c) Velocity without source terms

(d) Velocity with source terms

(e) Height without source terms

(f) Height with source terms

Figure 5.7: Evolution of the shock wave in the numerical model with and without sourceterms

5.3.5. Scenarios

The numerical one-dimensional shallow water equations with gravity, friction, deposition and erosion studied for several situations. First, the numerical model studied for 1. No Source Terms, 2. Deposition only, 3. Erosion Only and 4. Gravity and friction, see Table 5.9 providing the scenario and expected results. Second, the model evaluates four scenarios(5. full numerical model). It is used to see the effects of changing the parameters of 5.1 sediment sizes, 5.2 concentrations, 5.3 slopes and the hydraulic radius for 5.4 widths and 5.5 heights. The parameters that are used for the different scenarios are listed in Table 5.10, Table 5.11, Table 5.12 and Table 5.13. The results of the scenarios given in section 6.2.

Table 5.9: Scenarios for dynamic(numerical) model and the expected results of the simulations

Scenarios for modelling of the different source terms and the full model scenarios		
#	Scenario	Expected result
1.	**No Source Terms**	Shallow Water Equations and Particle conservation equation; No changes of the concentration over time
1.1	Concentration (1 - 8 %)	Changes velocity profile and height profile
2.	**Deposition(Settling) only**	Particle concentration settles with L = 3h/ v_s
2.1	Sediment size (d_{50} = 50, 100, 150, 200 μm)	Larger particles settle faster as v_s increases and according to particle settling relation L = 3h/ v_s
2.2	Concentration (1-8 %)	
3.	**Erosion only**	Maximum concentration is 60%
3.1	Non-hindered erosion	particles erode, concentration increases according to van Rijn 1984a
3.2	Hindered erosion	particles erode, and interact with each other according to [55] [72]. Erosion is less compared to non-hindered erosion
4.	**Gravity and Friction**	Produces velocity according to the steady state solution (d_{50} = 50 μ, u = 0.3 m/s, h = 1 m, ϕ = 0.02, w_b = 10)
4.1	Slope	Increased slope, increases flow velocity
4.2	hydraulic radius (height: 1.0, 2.0, 3.0, 4.0)	Increase hydraulic radius, increases flow velocity. Effect of Height is largest.
5.	**Full Equation: Deposition, Erosion, Gravity and Friction**	Concentration will become constant at a certain point
5.1	Sediment size d_{50} (50, 100, 150, 200 μm)	Larger sediment particles settle faster
5.2	Concentration ϕ (1-8 %)	increased concentration yields increased velocity, driving force of the current
5.3	Slope (0.001, 0.002, 0.004, 0.01, 0.05)	Increased velocity due to increased slope, erosion capacity increases
5.4	Hydraulic Radius: Water depth(height h) (1, 2, 4, 8, 16, 32)	Increased height, reduced friction and greater distance, settling time increases
5.5	Hydraulic Radius: Width (10, 20, 40, 80, 160)	Greater width, longer settling time
6.	**Case Study: Water Injection Dredging Case Study**	For details subsection 5.3.6

Table 5.10: Physical constant parameters

Physical parameters constants)	
Variable	Range
L [m]	1000
t[s]	8000
Δ	1.65
ν	$1.3 \cdot 10^{-6}$
g $[m/s^2]$	9.81
f	0.025
C_1	18
C_2	1
ρ_w [kg/m^3]	1000
ρ_s [kg/m^3]	2650

Table 5.11: Physical variable parameters

Physical parameters (Variables)	
Variable	Range
ϕ [-]	0.01-0.08
d_{50} [μm]	50-200
h [m]	1-32
u [m/s]	0.3
W_b [m]	10-160
t[s]	8000
S [-]	0.001-0.05
θ	loc.vel.dep
R [m]	0.83- 43.6
v_s [m/s]	Table 5.13
D_*	Table 5.13
θ_{cr}	Table 5.13

Table 5.12: Numerical parameters

Numerical parameters	
Variable	Value
Cell size	0.1
Time step	$6.7 \cdot 10^{-3}$
L	1000
nx	10001
nt	1200000
A	0.1
B	1
C	0.1

Table 5.13: Parameters depending on Particle Size d_{50}

Particle size and corresponding values			
d_{50} [μm]	D_*	θ_{cr}	v_s
50	1.062	0.133	0.00166
100	2.124	0.089	0.0062
150	3.186	0.066	0.0128
200	4.24	0.054	0.021

5.3.6. Case Study: Water Injection Dredging

Water Injection Dredging(WID) is a technique in which high-velocity water flow erodes sediment and brings it into suspension. Through nozzles and under low-pressure water is injected into the sediment. The beam with nozzles moves along the bottom as can be seen in Figure 5.8. Due to the high flow velocities, water penetrates the bottom, and the sediment is fluidised overcoming cohesive(fine sediment) and internal(coarse sediment) friction forces[77]. WID is a technique more suitable for very fine sand, silt and clay, mainly due to coarse sediment settling too quickly. The fine sediments are dispersed over the water column(1-3m high) forming a water-sediment mixture. The mixture results in a turbid density current that is forced by density/pressure differences and gravity. Since WID is a technique that only requires natural current to transport sediment, in comparison to other conventional dredging techniques, it does not require hoppers, barges or discharge pipelines. As an effect, WID is a cost-effective method to apply in areas where natural currents are available such as the channel.

The concept of channelling dam reservoir can provide the necessary natural current for sediment eroded by WID. Next, to this, the turbid density transport might be improved by WID as transport and concentration of sediment increases. Evaluating the concept of WID within channelled dam reservoirs, a case study is performed. This case study is done with the one-dimensional shallow water equation model modified in this section. Two source terms are provided: first, for the continuity equation a formula is proposed, based upon estimations and available equations given by van Rijn (2015) [74], Schrieck (2011)[68] and Swart (2015)[64]. Second, for the particle conservation equation, the erosion term is based upon Bisschop et al. (2010)[9] that considers high-velocity sediment erosion. The local impulse effects of the WID are assumed to be negligible in this case study. Further, WID along a length of 5m in the middle of the channel.

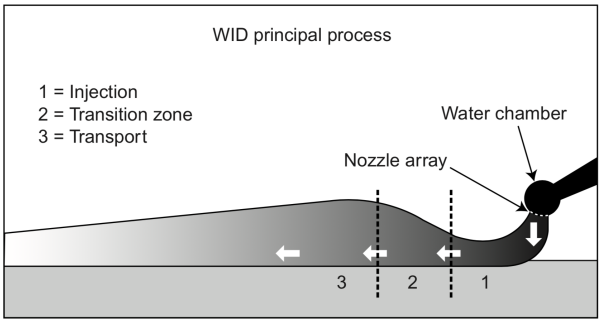

Figure 5.8: Sketch of Water Injection Dredging[77]

First, the source term for the continuity equation is derived. The WID injects water into the system, increasing the water height. To account for this a source term, denoted as V_{WID}, is added to the continuity equation. The source term is formulated by the use of equations and estimates provided by van Rijn (2015) [74], Schrieck (2011)[68] and Swart (2015)[64]. In Table 5.14 the estimates of WID related aspects are given.

Table 5.14: Caption

Water Injection Dredging Parts	Approximate values	Unit
Beam widths[74]	5 - 10	[m]
Nozzle spacing[64]	0.25 - 0.30	[m]
Nozzle diameter [64]	0.05 - 0.08	[m]
Nozzle velocity[74]	5 - 15	[m/s]
Number of Nozzles	16 - 33	[-]
Pressure drop over nozzle[64]	100 - 150	kPa
Current concentration [74]	20 - 100	kg/m3
Horizontal Jet pip [74]	0.6-0.8	m
Injected flow rate	1-2	m^3/s
Regular water injeciton device	0.3	$m^3/s/$

The following formula's are used for the derivation of the source term relation[74][64][12]:

$$\text{Nozzle velocity:} \quad u_{nozzle} = \sqrt{\frac{2\Delta p}{\rho_w}} \tag{5.45a}$$

$$\text{Nozzle area:} \quad A_{nozzle} = \frac{1}{4}\pi D^2 \tag{5.45b}$$

$$\text{Number of nozzles:} \quad N_{nozzle} = \frac{L_{beam}}{S_{nozzle}} \tag{5.45c}$$

$$\text{Total nozzle area:} \quad A_{tot} = N_{nozzle} A_{nozzle} \tag{5.45d}$$

$$\text{Total discharge:} \quad Q_{wid} = u A_{tot} C_{wid} \tag{5.45e}$$

$$\text{Specific discharge:} \quad q_{wid} = Q_{wid} / L_{beam} \tag{5.45f}$$

$$\text{Source term:} \quad V_{wid} = \frac{q_{wid}}{L_{wid}} \tag{5.45g}$$

As can be seen from Figure 5.8, the WID has a certain length over which super-critical flow changes into a hydraulic jump, between 2 and 3. There is no data available about the super-critical effective flow length from a jet. When the effective length of the super-critical flow is estimated, the added water height calculated. Flow velocities reach high values, 5 - 15 m/s; the length is in the order of 1 - 10m. Within this case study, an effective influence length of if the WID L_{wid} estimated at 5 m. Equation 5.45a up until Equation 5.45g requires an iterative process, to solve for this an equation is derived. The equation provides increased height due to increased water inflow. For the equation pressure drop, nozzle diameter and the jet influence length are the input parameters:

$$V_{wid} = \frac{\sqrt{2\Delta p}\pi D_n^2}{4\sqrt{\rho_w} L_{wid} S_{nozzle}} \tag{5.46a}$$

$$with: S_{nozzle} = \frac{L_{beam}}{N_{nozzle}} \tag{5.46b}$$

Further, the flow from the WID intrudes into the sediment layer, causing the flow height to increase. This study does not account for bottom changes. Although not used, for convenience, the intrusion depth can be calculated with[54]:

$$S_{intr} = \sqrt{\frac{3\rho_w u_{nozzle}^2 D_n^2}{C_u}} \tag{5.47}$$

(Note: The intrusion depth has higher influence on the flow height compared to the water input from the water injection dredging.)

Second, the concentration of sediment in the water column increases due to erosion caused by the WID; this is accounted for by a source term added to the particle conservation equation. Although an erosion term is formulated in Equation 4.10a, this equation will not suffice. The equation holds for low-velocity erosion only, in which sediment particles erode grain by grain. For high flow velocities, this assumption no longer holds. WID is a form of high velocity($u > 4m/s$) sediment erosion. The conventional erosion models, such as the one used in this study from van Rijn 1984[72] in Equation 3.17, overestimate the erosion induced by high flow velocities. High flow velocity erosion is influenced by properties of the soil mass(non-cohesive soils)[70]. The parameters that govern the erosion are dilatancy, permeability(particle size and porosity) and the (un)drained shear strength of the soil(particle size, porosity, composition/mineralogy, hydraulic gradient pushes the top layer)[8]. Further, the concentration in the water influences the flow by hindered erosion, influenced by the principles of dilatancy and permeability. For high-velocity erosion properties of the complete layer should be considered, instead of grains only.

Bisschop et al. (2010)[9] derived a simplified form of the high-velocity sediment erosion formula; it added as a source term to the model. The formula provides good approximations for jetting(u>4m/s) in dredging practice, for lower flow velocities(u>4m/s) the error is less than 10%. The formula by Bisschop et al. (2010)

for the source term of the particle conservation equation is provided in the following form:

$$\text{Source term: } v_e^5 = \alpha^2 D_*^{0.6} \left(\frac{\theta - \theta_{cr}}{\theta_{cr}} \right)^3 (\frac{k}{\delta})^3 \tag{5.48a}$$

$$\text{with: } \alpha = 0.00033 \frac{\sqrt{\Delta g d_{50}}}{1 - n_0} \tag{5.48b}$$

$$\text{Critical shields: } \theta_{cr} = \frac{\tau_{b,cr}}{(\rho_s - \rho_w) g d_{50})} \tag{5.48c}$$

$$\text{Dilatancy: } \delta = \frac{n_i - n_0}{1 - n_i} \frac{1}{\Delta(1 - n_0)} \tag{5.48d}$$

$$\text{Permeability: } k = C_k \frac{g}{\nu} D_{10}^2 \frac{n_0^3}{(1 - n_0)^2} \tag{5.48e}$$

With the sediment erosion term v_e, dimensionless particle size D_*, dimensionless density Δ, fall velocity g, median diameter of particles d_{50}, in situ porosity n_0, critical shields parameter θ_{cr}, critical bed shear stress $\tau_{b,cr}$, sediment density ρ_s, water density ρ_w, porosity of the sheared layer n_i, diameter 10% smaller d_{10}, kinematic viscosity fluid ν, coefficient depending on particle size distribution and angularity of the grainsC_k.

An increase of porosity is related to an increase of permeability; the permeability of a rather loosely packed granular material is approximately three times higher than of a densely packed granular material.

At last, the two terms that have been derived can be implemented into the model. This results in the continuity, momentum and particle conservation equation for the WID case study:

$$\text{Continuity equation: } \quad \frac{\partial h}{\partial t} + \frac{\partial uh}{\partial x} = V_{wid} \tag{5.49a}$$

$$\text{Momentum equation: } \quad \frac{\partial uh}{\partial t} + \frac{\partial u^2 h}{\partial x} + g'(\phi) \frac{1}{2} \frac{\partial h^2}{\partial x} = f_g - f_f \tag{5.49b}$$

$$\text{Particle equation: } \quad \frac{\partial \phi h}{\partial t} + \frac{\partial u \phi h}{\partial x} = E - D + v_e \tag{5.49c}$$

$$\text{with: } \quad V_{wid} = \frac{\sqrt{2\Delta p} \pi D_n^2}{4\sqrt{\rho_w} L_{wid}} \tag{5.49d}$$

$$\text{and: } \quad v_e = \sqrt[5]{(0.00033 \frac{\sqrt{\Delta g d_{50}}}{1 - n_0})^2 D_*^{0.6} \left(\frac{\theta - \theta_{cr}}{\theta_{cr}} \right)^3 (\frac{k}{\delta})^3} \tag{5.49e}$$

WID Case study assumptions

The effects of the WID evaluated by making assumptions on the aspects of the dredging technique. The case study assumptions and calculated values, based on equations in this section, are listed in Table 5.15. As no d_{10} value is available a d_{50} value is used. The results of the case study are provided in section 6.3. In which first, the evolution of concentration, velocity and height over time are given followed by a steady-state solution.

Table 5.15: Water Injection Dredging Case Study Assumption for Modelling

WID Model Aspects	Parameter	Value	Unit
Beam width	L_{beam}	10	[m]
Nozzle spacing	S_{nozzle}	0.30	[m]
Nozzle diameter	D_n	0.05	[m]
Nozzle velocity	u_{nozzle}	14.14	[m/s]
Number of Nozzles	N_n	33	[-]
Pressure drop over nozzle	Δp	100	[kPa]
Injected flow rate	Q	0.9	$[m^3/s]$
Sediment size	d_{10}	10	$[\mu m]$
Water density	ρ_w	1000	$[kg/m3]$
Dredge length	L_{wid}	5	[m]
Slope	S	0.001	[-]
In situ porosity	n_0	0.4	[-]
Porosotiy sheared layer	n_i	0.6	[-]
Cell size	Δx	0.1	[-]
WID location	-	500-505	[m]
WID location (Cells)		5000-5050	[-]
Height in	h_{in}	1.0	[m]

IV

Results and Discussion

6

Results

This part of the thesis provides the modelling results for both the steady-state solution and the numerical approach. The modelling approach was proposed in for the steady-state solution is provided in section 5.2, and the results in section 6.1. The numerical approach is provided in section 5.3 and the results for the numerical model of the turbid density current in the channel are provided in section 6.2.

6.1. Steady-State

6.1.1. With Reservoir Return flow

In Figure 6.1 velocity profile for the rectangular and trapezoidal channel is provided. Five different channel dimensions were evaluated. For both the rectangular channel as the trapezoidal channel: The velocity increases as the slope increases. As the channel area increases the maximum velocity decreases. In Figure 6.1a it obtained that the average channel dimensions are smaller than that of the trapezoidal channel. Velocities are slightly higher for the same channel cross-sectional area. In Figure 6.1b average channel dimensions are higher than that of the rectangular channel. The average velocity in the trapezoidal channel is slightly lower compared to the rectangular channel.

In Figure 6.2 channel velocity, hydraulic radius, depth and channel surface area for different channel widths in the trapezoidal channel are provided. As the width of the channel increase, as a result, velocity and hydraulic radius decrease and the depth decrease and the surface area decreases towards an asymptotic point. The width influences the solutions much less than the change in depth.

In Figure 6.2a channel velocity increases as the slope increases from 0 towards 0.05. The effect of width change is larger for the widths from 5 to 30 m than for 30 - 90 m. For 50 - 90 m, the solutions are approximately the same, no clear difference in answers is seen.

In Figure 6.2b hydraulic radius decreases rapidly for slopes between 0 and 0.01. The effect of the width change is significant for widths between 5-30m. For widths 40-90m the solutions similar for a hydraulic radius of 1.5m.

In Figure 6.2c depth decreases as the slope increases. For a width of 5m, the channel depths are largest. For a channel width of 90m, the depth is smallest. The solutions decrease with the highest gradient between 0 and 0.01.

In Figure 6.2d cross-sectional area decreases as the channel slope increases. There is a negative non-linear relationship for the results. For the width of 5m, the cross-sectional areas are smallest, for 90m, the cross-sectional areas are largest. Between the lines of the 5-40m width, the spacing is even and clear, for the 50-90m widths the spacing is small and some lines for area overlap.

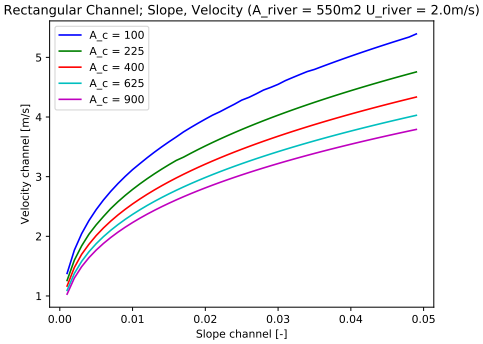

(a) Rectangular channel with reservoir return flow changing velocity as an effect of changing slope

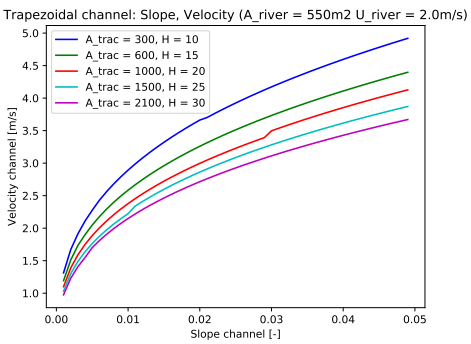

(b) Trapezoidal channel with reservoir return flow changing velocity as an effect of changing slope

Figure 6.1: With reservoir return flow, flow velocities for rectangular channel and slope for changing cross sectional area of the channel

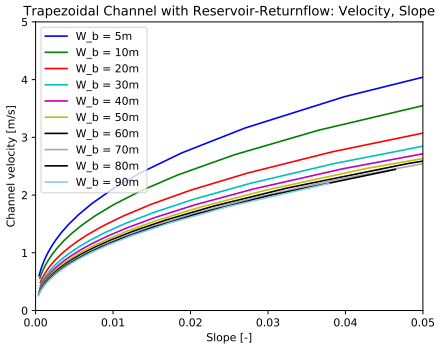

(a) Velocity

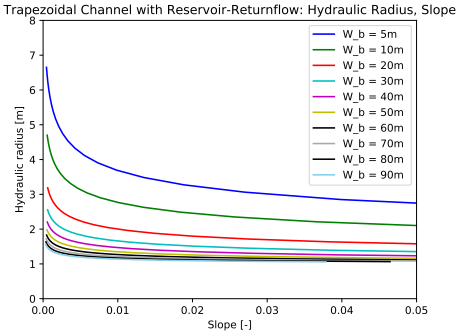

(b) Hydraulic radius

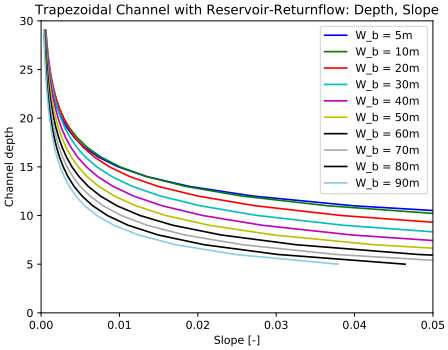

(c) Channel Depth

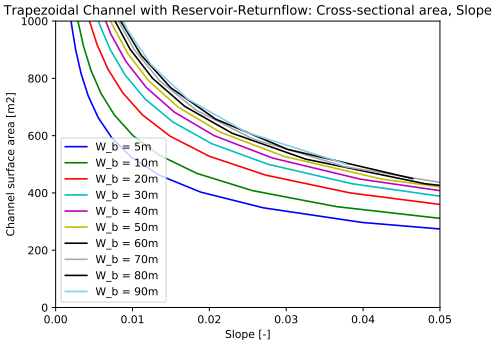

(d) Cross-sectional area

Figure 6.2: Trapezoidal Channel with Reservoir Return Flow the influence of slope and width on velocity, hydraulic radius, depth and cross-sectional area

6.1.2. Without Reservoir Return Flow

n Figure 6.3 the rectangular channel without reservoir return flow is provided. Channel densities are constant in the cross-section of the channel. As slope increases, flow velocity increases, hydraulic radius decreases and area decreases. In Figure 6.3a velocity increases non linearly with increasing slope. In Figure 6.3b cross-sectional area of the channel decreases non linearly as the channel slope increases. In Figure 6.3c hydraulic radius decreases non linear but less than in Figure 6.2b. From the graphs, it can be obtained what the minimum quantities of velocity, area and hydraulic radius need to be. For example, at a slope of 0.01, minimum velocity is 2.0 m/s, hydraulic radius 400 m2 and the hydraulic radius is 5.0.

In Figure 6.4 the trapezoidal channel without reservoir return flow with changing widths is provided. As the channel slope increases, flow velocity increase. On the other hand, water depth, hydraulic radius and cross-sectional area of the channel decrease. Within Figure 6.4a flow velocity increases non-linearly with the slope. As the width increases the flow velocity decreases. In Figure 6.4b the channel depth decreases non-linearly with increasing slope. The effect of the change in width is unclear. Between 0 and 0.01 solutions decrease rapidly, and in 0.01 towards 0.05, the solutions are more stable. In Figure 6.4c hydraulic radius decreases as slope increases non linearly and is constant from 0.01-0.05. The effect of width is less compared to change in-depth as can be obtained from Figure 6.4b.In Figure 6.4d the cross-sectional area decreases non-linearly with the channel width.

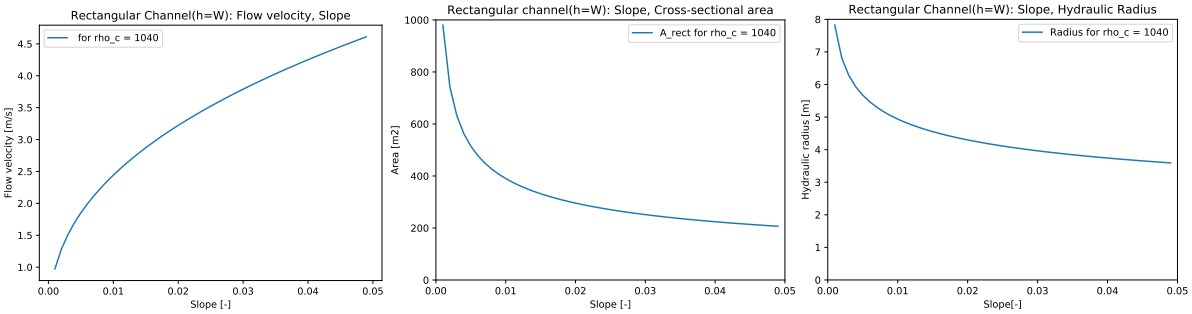

(a) Velocity (b) Cross-sectional area (c) Hydraulic radius

Figure 6.3: Rectangular Channel: Influence of slope on the flow velocity, hydraulic radius and cross sectional area

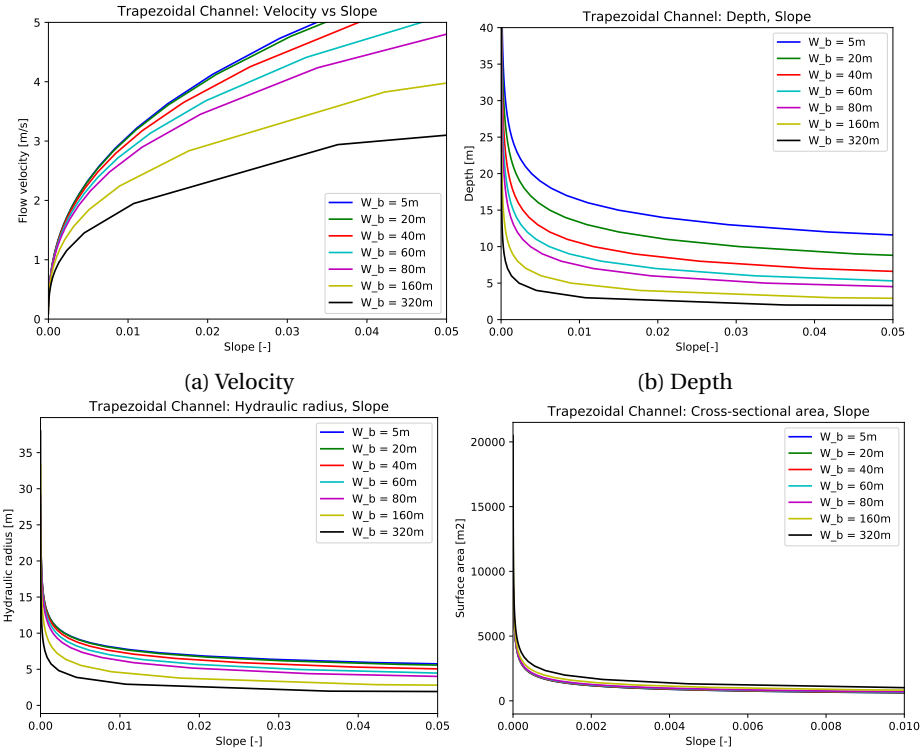

(a) Velocity

(b) Depth

(c) Hydraulic Radius

(d) Cross-sectional area

Figure 6.4: Trapezoidal Channel without return flow: Influence of slope and width on velocity, depth, hydraulic radius and cross sectional area

6.1.3. Without Reservoir Return Flow: Simplified

In Figure 6.5 without reservoir return-flow and equal area, density and velocity up and downstream. The solution is plotted for channel velocities of 1 - 5 m/s. The cross sectional area Hydraulic radius and Discharge are plotted for changing slope. Each solution decreases non-linearly width increased slope. From the graphs the minimum flow velocity at a certain hydraulic radius and slope can be obtained.In Figure 6.5a increased velocity yields increased slope to solve for the equation . In Figure 6.5b increasing velocity yields increasing slope and larger hydraulic radius at larger slope. In Figure 6.5c increasing velocity yields increasing slope and larger discharge.

From the figures it can be obtained what a minimum slope should be to maintain a certain velocity combined with either surface area, hydraulic radius or discharge within the channelled reservoir.

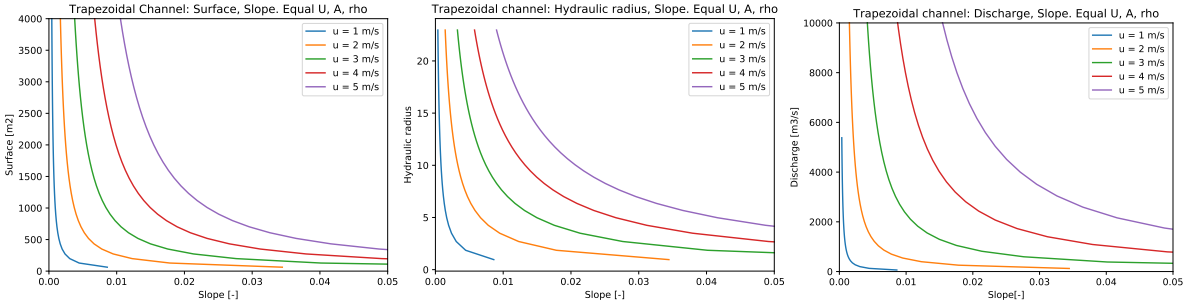

(a) Cross sectional area (b) Hydraulic radius (c) Discharge

Figure 6.5: Trapezoidal Channel without reservoir return flow and equal up-and downstream velocity and radius, influence of slope on surface area, hydraulic radius and discharge for different flow velocities

6.2. Numerical

6.2.1. Without Source Terms

In Figure 6.6 no source terms are included in the model. The concentration profiles are constant along the length, see Figure 6.6a. However, changes are observed as velocity is increased (Figure 6.6b and height is decreased (Figure 6.6c) velocity(increased) and height(decreased). For Figure 6.6b, velocities are higher for increased concentration and from left to the right boundary velocity increases by 0.1 m/s for each concentration. Velocity increases suddenly at the left boundary(x=0) and right boundary(x=L). For Figure 6.6c, height of the current decreases as concentration and velocity are higher. The effects of concentration change is less for concentration larger than 5 %. At both the left boundary(x=0) and right boundary(x=L) concentration decreases with a steep gradient.

The effects on the boundary and velocity and height change can be an effect of the boundary conditions or the change of super-critical to sub-critical flow. The densimetric Froude number is around unity and becomes smaller at the right boundary, this causes both the upstream and downstream to be effected, sub-critical flow occurs. The rapid changes on the boundary can be an effect of the boundary conditions.

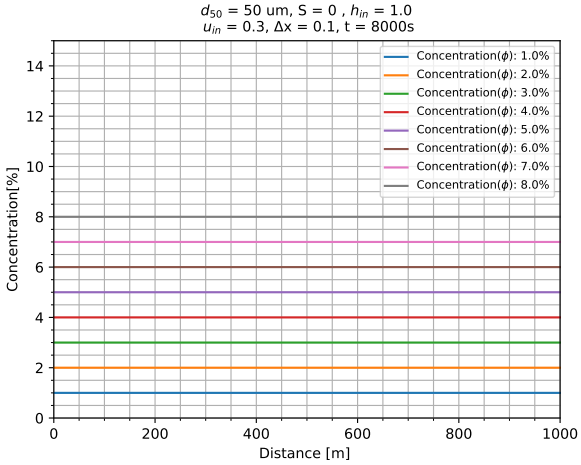

(a) Concentration

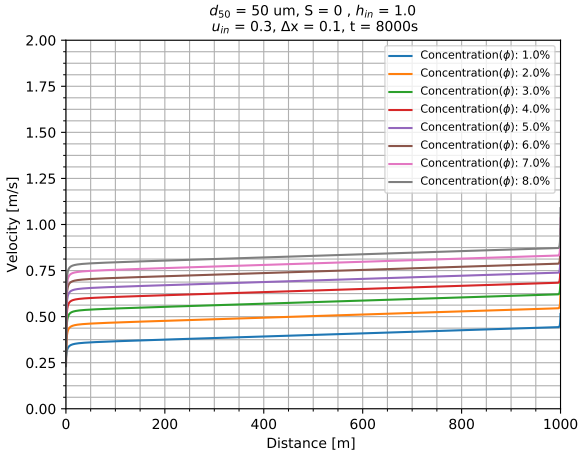

(b) Velocity

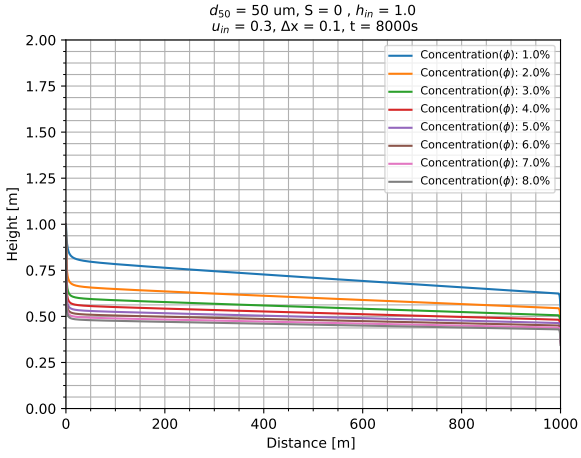

(c) Height

Figure 6.6: Numerical model without source terms concentration, velocity and height profile for concentrations between 1-8%

6.2.2. Deposition

2.1 Sediment Size

In Figure 6.7(a,c,e) deposition term for different particle sizes d_{50} with incoming concentration 2%, height 1m and velocity 0.3 are provided. In Figure 6.7a concentration decreases non-linearly along the length of the channel. Larger particle sizes settle faster due to higher settling velocity according to Equation 3.24. The particles concentrations settle according to subsection 5.3.2 $(3h/v_s) * u_{in}$ and 95% settled: for d_{50}= 50, 100, 150, 200 μm this is 45, 70, 150, 550m respectively. In Figure 6.7c velocity increases rapidly and non linearly on the left boundary(x=0) towards 0.7 m/s, the velocity of d_{50} = 50 μ increases with smaller gradient. In Figure 6.7e height decreases with a steep gradient and non linearly from the left boundary(x=0) towards $h = 0.5m$. Height for d_{50} = 50 μ decreases slowest which is a combined effect of the model evaluating concentration, velocity and d_{50}.

2.2 Concentration

In Figure 6.7(b,d,f) deposition term for different incoming concentrations(1-8 %), velocity 0.3 m/s, height 1.0 m and d_{50} 50 μm. Figure 6.7b concentration decreases non linearly for each particle size according to $(3h/v_s) * u_{in}$ 95% is settled, as mentioned in previous paragraph 2.1 Sediment Size. The concentrations are settled at L > 800 m. Figure 6.7d The velocity at the left boundary increase with large gradient. The velocities become constant at L > 400m. Highest velocities are found for concentration of 8.0 %. In Figure 6.7f height decreases for each concentration and is constant at L>250m. At the left boundary height decreases rapidly and at the right boundary height is constant. The results provide similar results to sediment size changes, increased concentration results in decreased height and increased velocity.

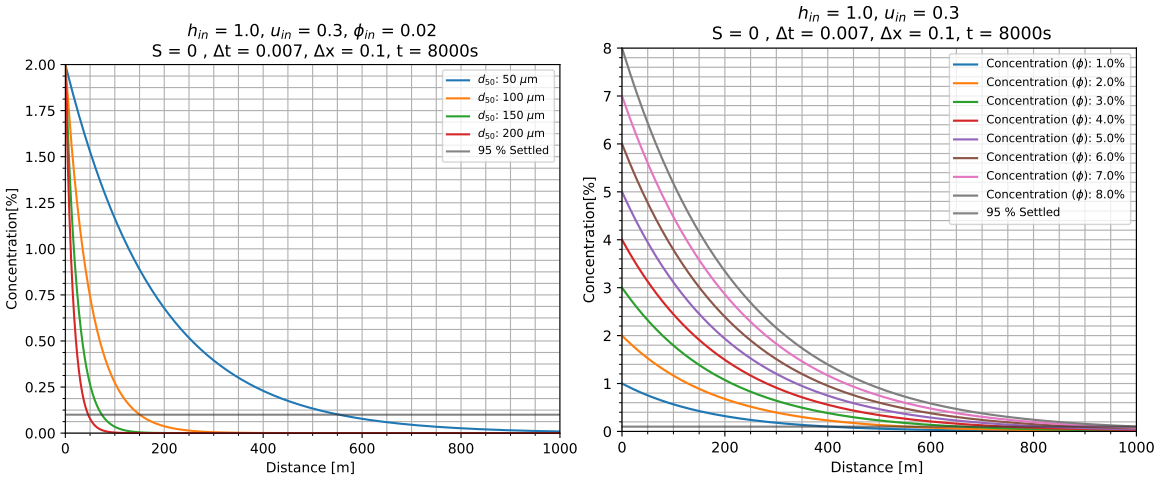

(a) Concentration: Different d_{50}

(b) Concentration: Different ϕ

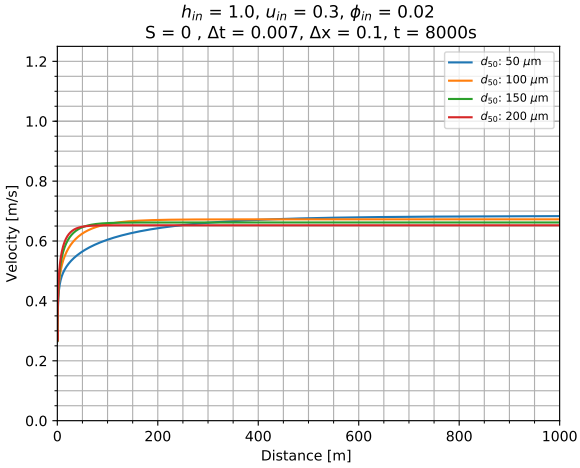

(c) Velocity: Different d_{50}

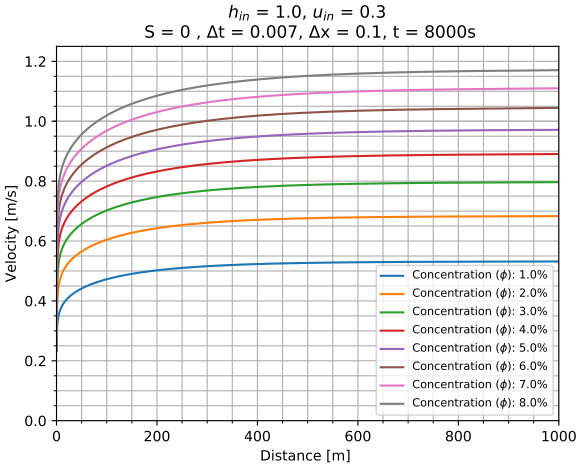

(d) Velocity: Different ϕ

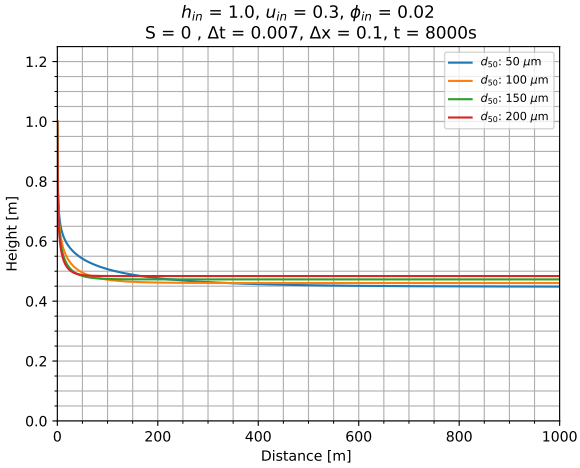

(e) Height: Different d_{50}

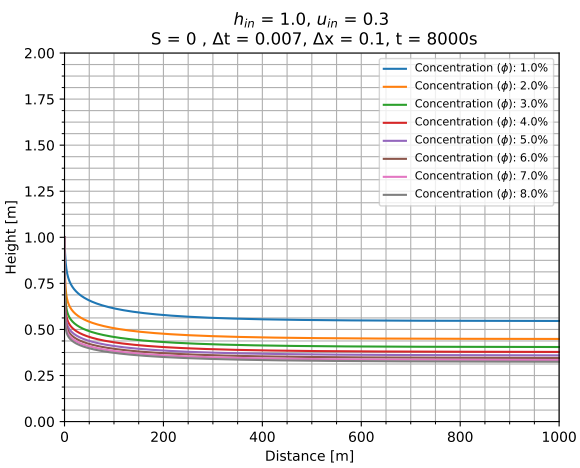

(f) Height: Different ϕ

Figure 6.7: Numerical model for deposition only, concentration, velocity and height for both different sediment sizes d_{50} (a, c, e) and different concentrations ϕ (b, d, f).

6.2.3. Erosion

3.1 Non-Hindered Erosion

Figure 6.8(a,c,e) non-hindered erosion term for different particle sizes. With an incoming concentration 2%, height 1.0 m and velocity 0.3 m. Particles erode from the bottom, increasing the concentration from the initial 2 %. In Figure 6.8a concentration is increasing with a small gradient up until L = 400 m. Compared to L > 400m, the concentration starts increasing with large gradient and non-linearly along the length of the channel. It is caused by a positive feedback mechanism that is not damped by settling and friction. In Figure 6.8c velocity, responds by similar behaviour and is constant up until L = 400m, from L > 400m the velocity increases non-linearly. At the left boundary, a decrease of the velocity is noticeable, from 0.3 m/s towards 0.2-0.25m/s. In Figure 6.8e height, decreases non linearly from the left boundary (x=0) towards the right boundary (x=L). Particles erode rapidly compared to the hindered erosion.

3.2 Hindered Erosion

Figure 6.8(b,d,f) the hindered erosion term for different particle sizes. With an incoming concentration 2 %, height 1.0 m and velocity 0.3 m/s. Particles erode from the bottom increasing the concentration with a starting concentration of 2 %, the incoming velocity of 0.3 m/s and height of 1.0 m. The particles are eroding slower than in the non-hindered settling situation. In Figure 6.8b The concentration is constant until L = 150m and increases non-linearly until the end of the system(x=L). Figure 6.8d The velocity is constant up to L = 200 m and increases non-linearly towards the end of the system. At the left boundary(x=0) the velocity decreases towards 0.25 m/s and at the right boundary(x=L) the velocity increases suddenly. Figure 6.8f The height decreases non-linearly and somewhat linearly from the left towards the right boundary. For 850 < L < 100 the velocity change is reduced. At the right boundary, a sudden decrease of velocity is noticed; it is an effect of the hindered erosion term that limits erosion.

By comparing height, velocity and concentration for hindered and non-hindered erosion. It clearly shows that hindered erosion is increases slower than non-hindered erosion. It is an effect of hindered erosion. It is affected by particles and reduced turbulence that affects the concentration in the flow reducing its erosive capacity.

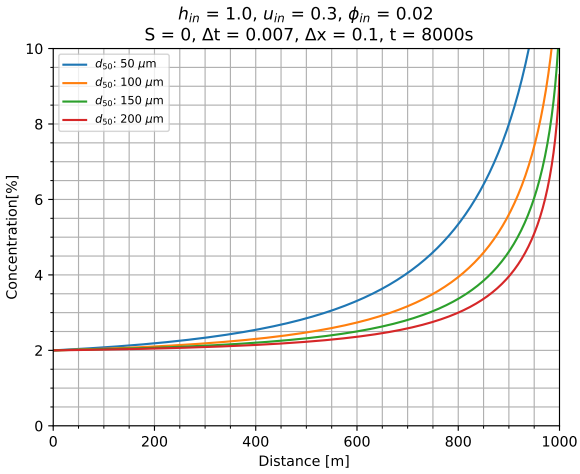

(a) Concentration: Non-Hindered Erosion

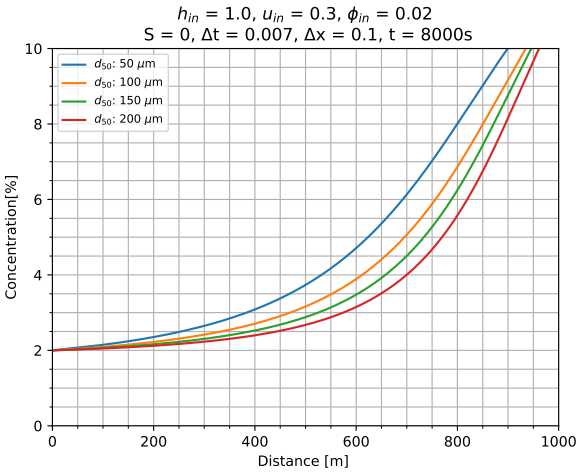

(b) Concentration: Hindered Erosion

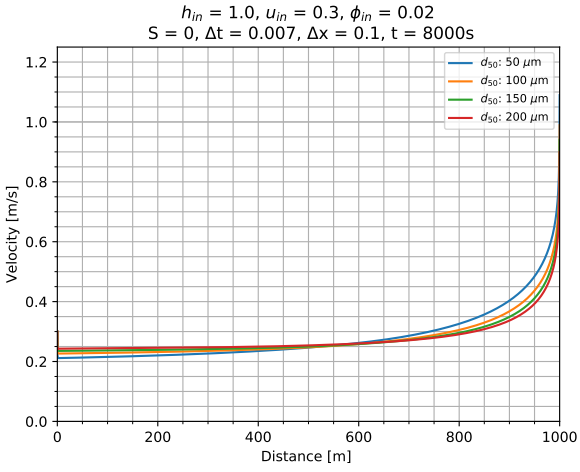

(c) Velocity: Non-Hindered Erosion

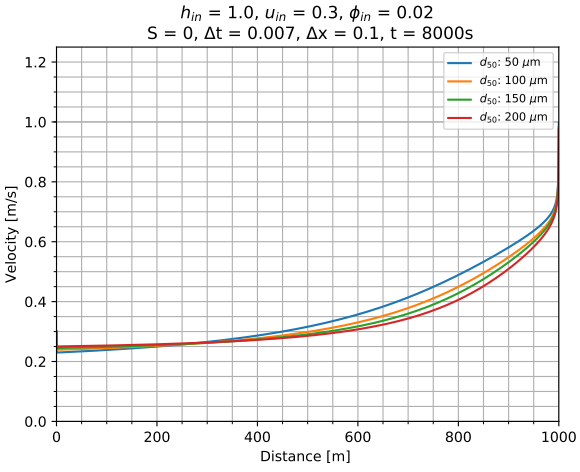

(d) Velocity: Hindered Erosion

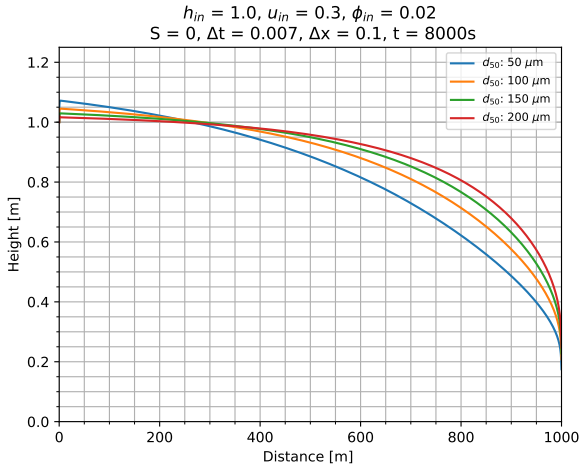

(e) Height: Non-Hindered Erosion

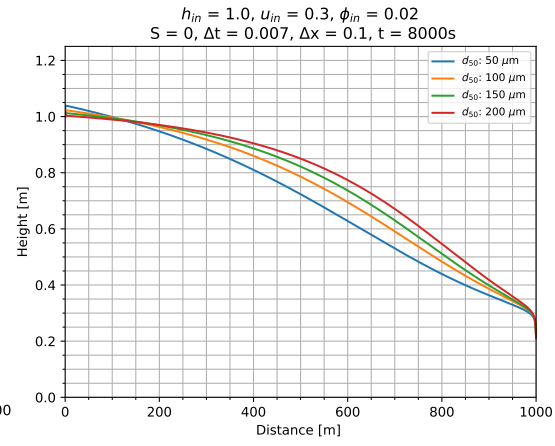

(f) Height: Hindered Erosion

Figure 6.8: Non-hindered(a,c,e) and Hindered(b,d,f) erosion for different sediment sizes: Concentration, velocity and height profile

6.2.4. Gravity and Friction

4.1 Gravity

In Figure 6.9(a,c,e) the gravity and friction term for different slopes are provided. Incoming concentration 0.02 %, velocity 0.3 m/s and height 1.0 m. There are no source terms in the system that govern the erosion and settling of sediment. In Figure 6.9a it is obtained that changing the slope is not effecting the concentration, it stays constant at 2.0% for different slopes 0.001-0.050. In Figure 6.9c velocity increases as the slope increases. At the left boundary (x=0) the velocity increases towards the steady-state solution. The steady-state velocities give solutions as would be expected from the given slopes and are equal to $u_c = \sqrt{\frac{8}{f} g' R s}$. In Figure 6.9e height decreases as slope increases. At the left boundary(x=0) a steep gradient in the velocity is observed for the slopes 0.004, 0.010 and 0.050. The model is approaching its steady-state solution. The right boundary shows a rapid decrease of height for 0.001, 0.002 and 0.004. The smaller slopes affect the velocity of the flow, causing it to be either super or sub-critical flow. The densimetric Froude number is lower than unity causing sub-critical flow in which effects downstream are transported upstream. The sudden at the boundaries are effect the solution if the super-critical flow becomes sub-critical. Another effect could be due to the boundary condition imposed on the right boundary of the model.

4.2 Hydraulic Radius

In Figure 6.9(b,d,f) gravity and friction terms for different hydraulic radii are. Incoming concentration is 0.02 %, velocity is 0.3 m/s and height 1.0 m. There are no source terms in the system that govern the erosion and settling of sediment. A result of this is that concentrations are constant for changing hydraulic radius in Figure 6.9(b,d,f). In Figure 6.9d velocity increases on the left boundary towards the steady-state solution equal to $u_c = \sqrt{\frac{8}{f} g' R s}$. Due to the low slope, the velocity increases towards the right boundary. It could be an effect of either a low densimetric Froude number(Fr < 1) or the imposed boundary condition. In Figure 6.9f height (almost) instantly decreases on the left boundary towards the steady-state solution yet decreasing non-linearly at the right boundary.

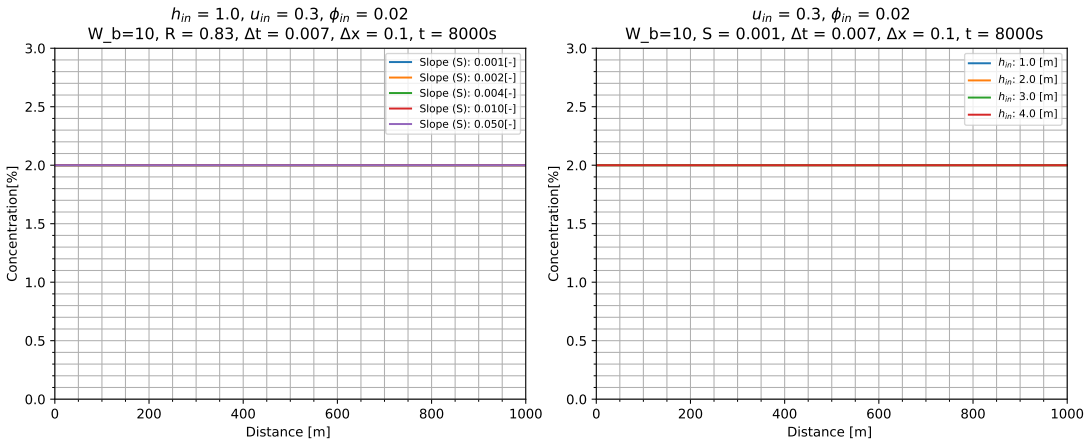

(a) Concentration: Gravity

(b) Concentration: Hydraulic Radius

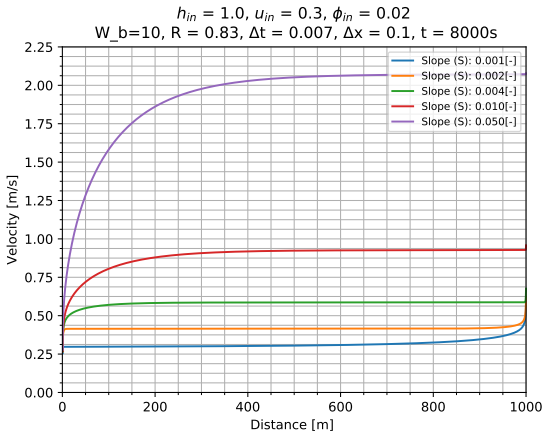

(c) Velocity: Gravity

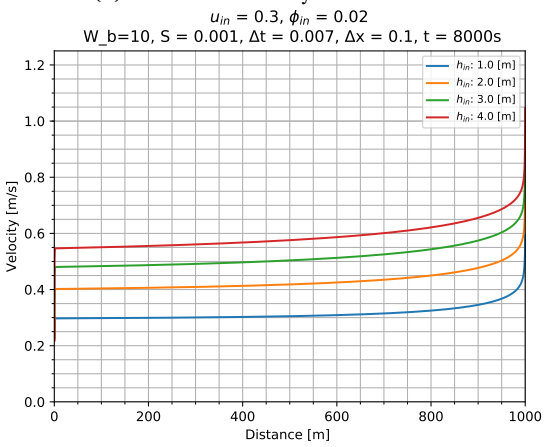

(d) Velocity: Hydraulic Radius

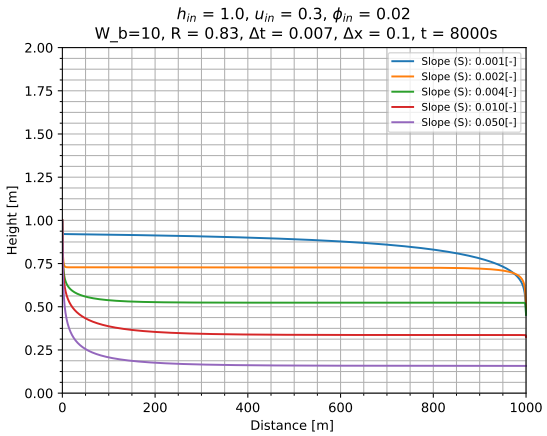

(e) Height: Gravity

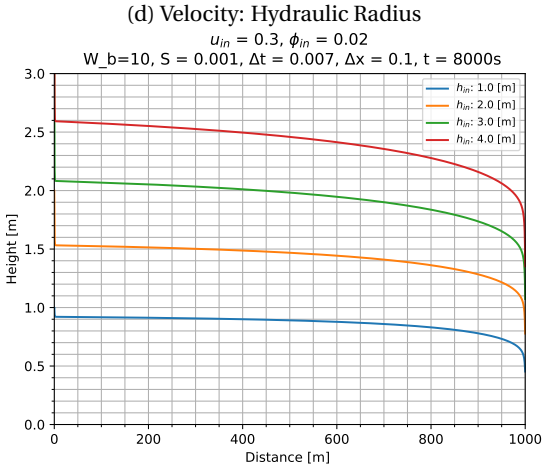

(f) Height: Hydraulic Radius

Figure 6.9: Changing slopes(a,c,e) and changing hydraulic radii(b,d,f) for numerical model with the gravity and friction source term only.

6.2.5. Complete Numerical Model Scenarios

5.1 Sediment Size

In Figure 6.10(a,c,e) the complete numerical model for changing sediment size in that includes the source terms for deposition, erosion, gravity and friction is provided. With incoming concentration of 2.0 %, velocity 0.3 m/s and height 1.0 m.

In Figure 6.10a concentration decreases non-linearly along the length of the domain. Sediment settles significantly slower compared to the deposition only situation. For d_{50} = 50 μm the minimum particle concentration is 0.2 %. About 95 % of the particles are settled out from suspension at 400, 300 and 250m for 100, 150, 200 μm respectively.

In Figure 6.10c velocity decreased along the length of the channel as an effect of decreased concentration and increased height. The velocity gradient for particle sizes of 50 μm is significantly smaller compared to 100, 150, 200 μm. At the left boundary(x=0) velocity increases and after that decreases along the length. Between 50<L<400 velocity decreases linearly. Between 400<L<800 velocity decreases non-linearly, from L>800 velocity is approximately constant. At the right boundary, an increase of velocity is recognised for 50 μ, which might be an effect of sub-critical densimetric Froude number(Fr <1) or the boundary condition.

In Figure 6.10e height increases and decreases along the length of the channel. At the left boundary(x=0) height decreases with a steep gradient, yet staying around the 0.3 m/s incoming velocity. The height for 50μm is approximately constant along the length. For d_{50} 100, 150, 200 μm the height is constant between 0<x<200, increases for 200< L < 800 and 200< L<900. Decreases from L >800 and L> 900, first linear and then non-linearly.

5.2 Concentration

In Figure 6.10(b,d,f) the complete numerical model including the source terms deposition, erosion, gravity and friction with changing concentration, is provided. The incoming concentrations changes between 1-8%, velocity 0.3 m/s and height of 1.0 m.

In Figure 6.10b concentrations decrease for concentrations from 1-3%. While concentrations ≥ 4% increase along the length of the channel. For the provided parameters, the turbid density currents start to have a positive feedback mechanism from concentrations higher than 4 %. At the right boundary, the concentration increases with a steep gradient between 950 < L < 1000, this might be an effect of the boundary condition. A low slope is causing a low velocity and thus lower Froude number(Fr<1) causing subcritical flow.

In Figure 6.10d velocities decrease along the channel length. At the right boundary, a sudden increase in velocity is recognised, probably due to lower Froude number. The concentration of 1 % has Froude number larger than unity, which results in super-critical flow.

In Figure 6.10f height is somewhat constant for concentrations 2, 3 and 4%, in which a rapid decrease on the right boundary is seen due to the Froude number being lower than 1. The concentration of 1.0% shows, an increase in velocity along the length of the reservoir, a sudden decrease at the right boundary that is not seen in the velocity graph. The 5-8% decrease in velocity with rapid decreasing height at the right boundary due to either boundary conditions or Froude number.

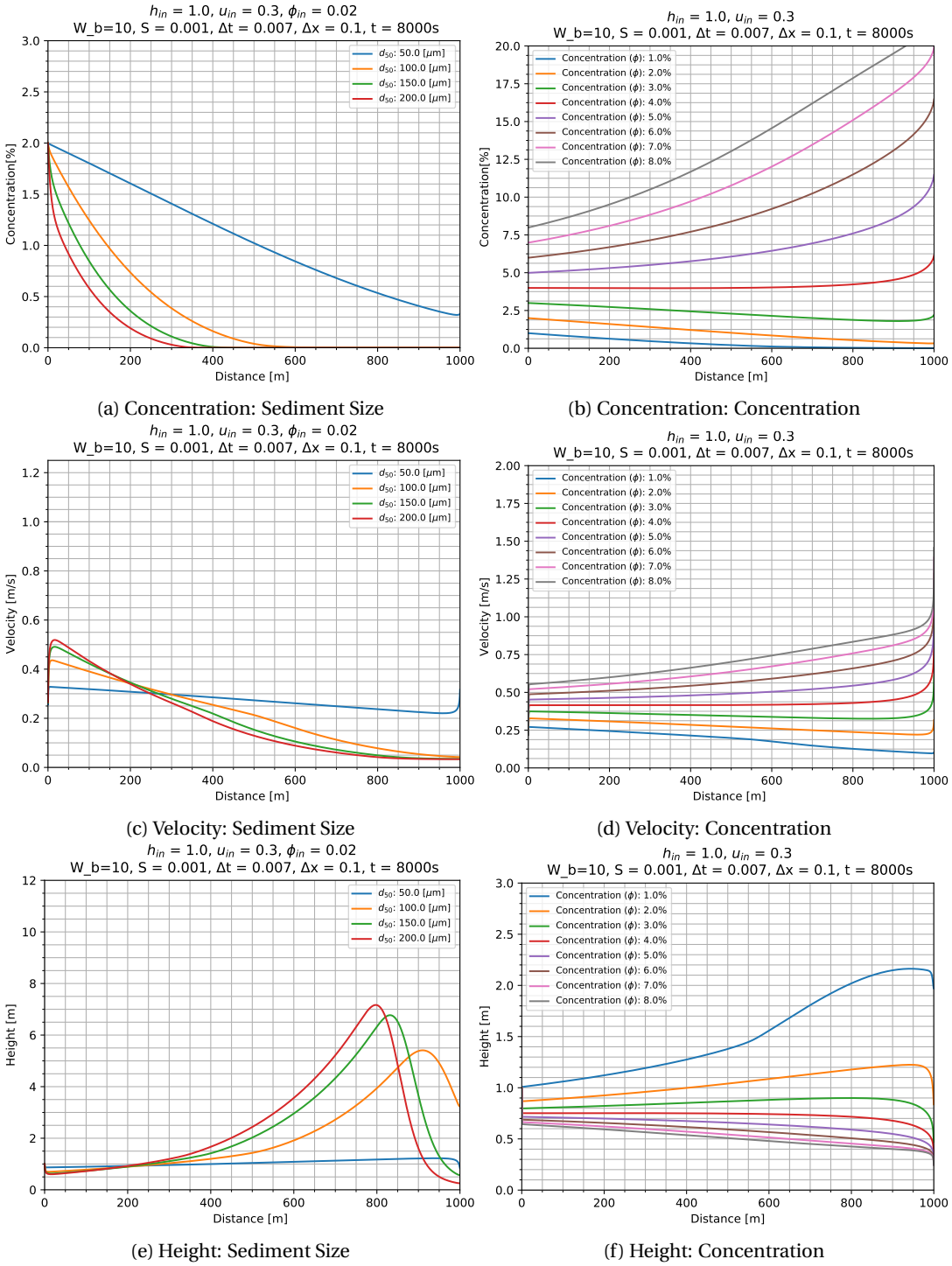

(a) Concentration: Sediment Size

(b) Concentration: Concentration

(c) Velocity: Sediment Size

(d) Velocity: Concentration

(e) Height: Sediment Size

(f) Height: Concentration

Figure 6.10: Results of concentration, velocity and height for different sediment sizes(a,c,e) and different concentrations(b,d,f) for the complete numerical model

5.3 Slope

In Figure 6.11(a,c,e) the complete numerical model including the source terms deposition, erosion, gravity and friction with changing slopes(0.001-0.05[-]) is provided. With incoming concentration of 2.0 %, velocity of 0.3 m/s and height of 1.0 m.

In Figure 6.11a the concentration decreases for a slope of 0.001 the current could is not self-accelerating and friction forces are higher than driving forces for the slopes ranging from 0.002-0.05 the concentrations increases. The concentration for the slope of 0.002 increases linearly and becomes stable at the end of the domain at 9.5%. The slope of 0.004 increases linearly up to 300m and is constant for >300m at 12 %. The concentration for the slope of 0.05 is stable from approximately 50m at 13 %. Compared to the gravity and friction where the concentration was stable, the concentration increases in this case.

In Figure 6.11c velocity decreases for a slope of 0.001 and increases for slopes larger and equal than 0.002. For different parts in the first section, a linear increase is noticed. After the increase, the velocities become constant along the channel. For the slopes of 0.001 and 0.002 increase at the boundary is noticed that, yet the effects are much smaller than in the gravity and friction only situation, which could be the effect of boundary conditions or Froude number smaller than unity. The velocities are higher compared to the gravity and friction only situation in subsection 6.2.4.

In Figure 6.11e height for 0.001 increases along the length and at the boundary, the Froude number or boundary conditions decreases its solution. The heights for slopes 0.002 and larger decrease linearly and than become constant.

5.4 Hydraulic Radius: Depth

In Figure 6.11 provides the complete numerical model including the source terms deposition, erosion, gravity and friction with changing hydraulic radius as an effect of depth change. With incoming concentration of 2.0 %, velocity of 0.3 m/s, height of 1.0 m and slope 0.001[-].

In Figure 6.11b concentration in the channel increases non linearly as the depth of the channel increases except for the height of 1.0 m. It can be an effect of low velocity which related to the hydraulic radius. When the height of the channel is too small, the velocity and the resulting turbulence is too small to keep the sediment in suspension.

In Figure 6.11d velocities increase along the channel length as the depth increases. At the right boundary(x=L) the velocity increases with a steep gradient that could be an effect of boundary conditions rather than Froude number as Fr > 1, and thus super-critical flow occurs.

Figure 6.11f The height decrease along the length of the channel. At the left boundary, a rapid decrease in height is seen. For example, the depth of 16.0 m decreases towards 10m. It could be either due to low initial velocity or a boundary condition. At the right boundary, heigh decreases suddenly as an effect of boundary condition or low Froude number; it was stable before the boundary.

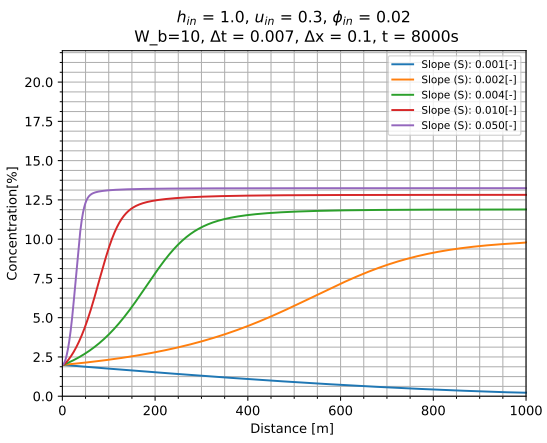

(a) Concentration: Slope

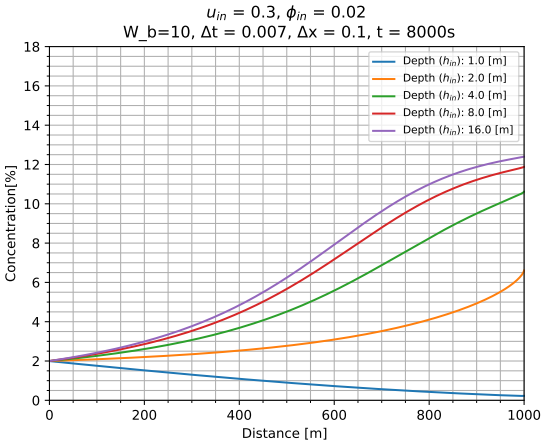

(b) Concentration: Hydraulic Radius (Depth)

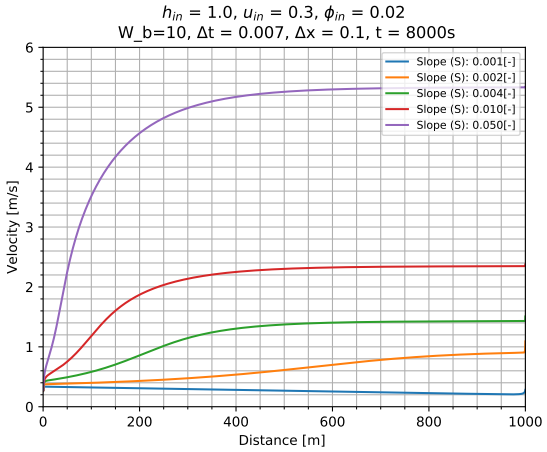

(c) Velocity: Slope

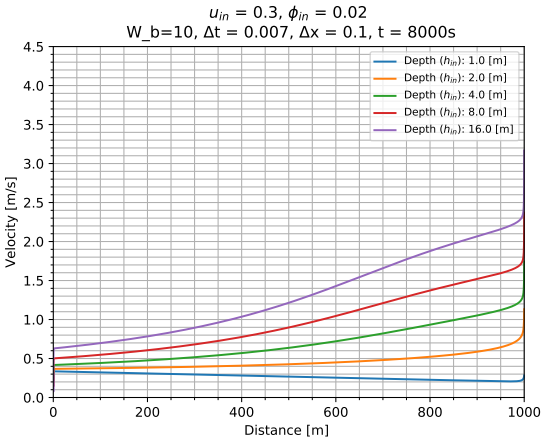

(d) Velocity: Hydraulic Radius (Depth)

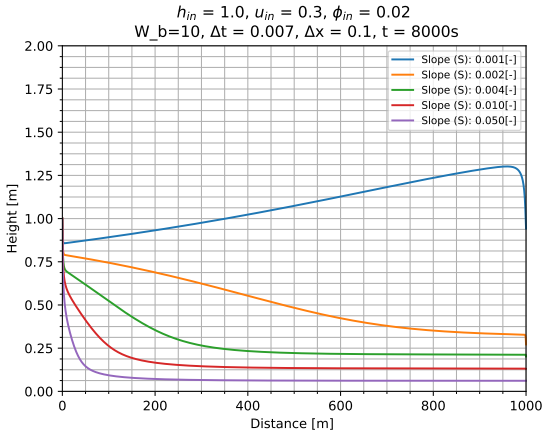

(e) Height: Slope

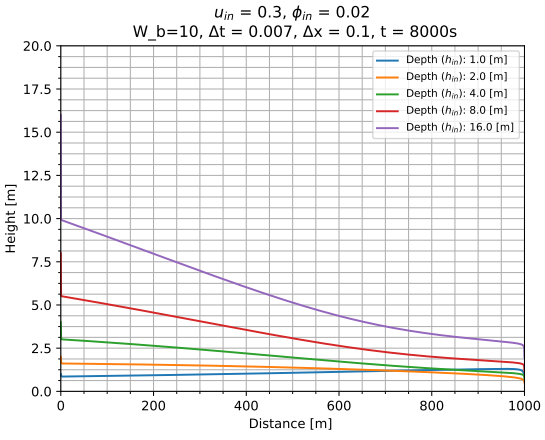

(f) Height: Hydraulic Radius (Depth)

Figure 6.11: different slopes(a,c,e) and depths(b,d,f) for the complete numerical model.

5.5 Hydraulic Radius: Width

In Figure 6.12 provides the complete numerical model including the source terms deposition, erosion, gravity and friction with changing hydraulic radius as an effect of width change. With incoming concentration of 2.0 %, velocity of 0.3 m/s, height of 1.0 m and slope 0.001[-].

In Figure 6.12a, the concentration of the flow decreases along the channel length. The average concentration is higher as the width of the channel is increased. The effect is less significant than the height change — the concentration increases at the right boundary, which again is an effect of the low Froude number.

In Figure 6.12b velocity decreases linearly over the length of the channel. At the left boundary, the velocity increases with a steep gradient towards approximately 0.32 m/s. At the right boundary concentration with steep gradient occurs due to low Froude number or boundary condition.

In Figure 6.12c height decreases at the left boundary towards approximately 0.85 m. From the left boundary, the heights increase towards a point of 950m. Between 950 < L < 1000 the height suddenly decreases as an effect of Froude number or boundary conditions.

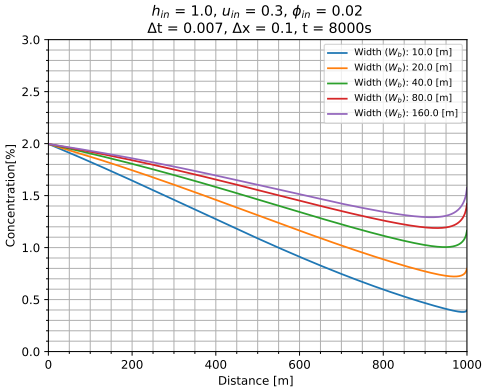

(a) Concentration

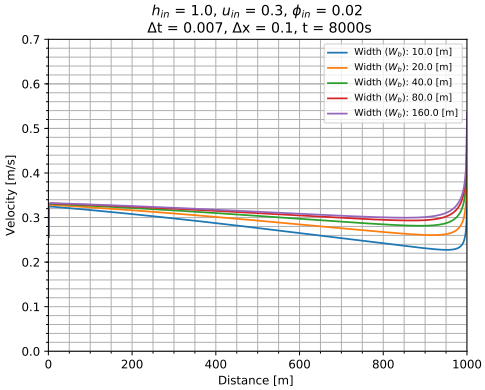

(b) Velocity

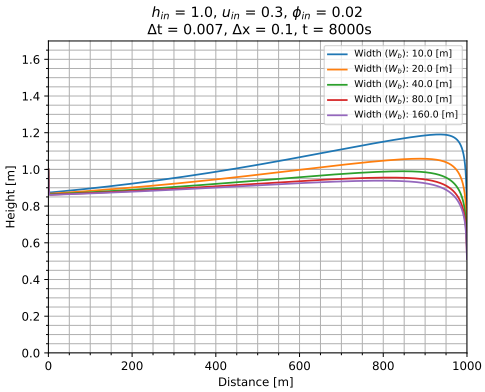

(c) Height

Figure 6.12: Complete Model: different widths

6.3. Case Study: Water Injection Dredging

The WID case study results and explanation of these are provided in this section. The derivation for the equations and the list of input parameters are provided in subsection 5.3.6. First the evolution of the WID is modelled in Figure 6.13(a,c,e). It can be seen that the concentration over the height instantly increases towards 30%. This increase in concentration is added over a small height as can be obtained from Figure 6.13(e). A small front is formed that moves in the positive x-direction. After t = 500 seconds, the turbid density current starts to interact with the input of the WID and the front has moved further into the domain. The concentration, velocity and height to the left of the water injection dredge are significantly higher compared to previous modelling situations. As time increases the situation for the water injection dredging starts to move towards a stable situation.

The solution for t = 100 000 s is provided in section 6.3(b,d,f). The height on the left of the water injection dredge is approximately 3.6m, while the concentration and velocity in the current are almost zero. It could be an effect of the water injection dredging, causing flow in two directions. In the downstream direction of the water injection dredge the velocity, concentration is significantly higher. The height is 0.5m, velocity 0.55 m/s and concentration is around 8%. The total amount of sediment moved by the current in the channel is higher compared to the situation before dredging.

In both Figure 6.13(a,c,e) and Figure 6.13(b,d,f) boundaries seem to suffer from either boundary conditions or the densimetric froude number.

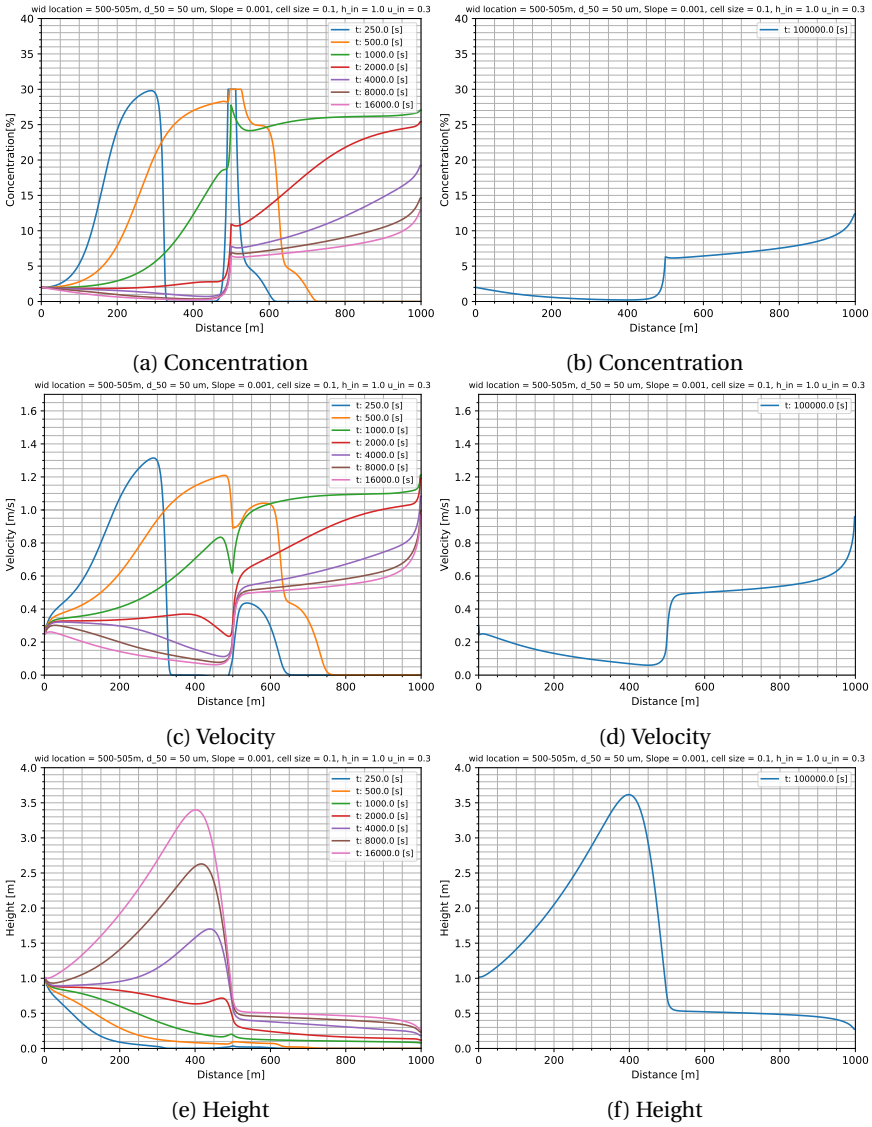

(a) Concentration

(b) Concentration

(c) Velocity

(d) Velocity

(e) Height

(f) Height

Figure 6.13: Case Study: Water Injection Dredging

7

Discussion

This thesis starts with a literature study(Part II), followed by a conceptualisation and modelling approach (chapter 5) on channelling turbid density currents in dam reservoirs. Channelling aims to inhibit the settling of sediment particles in dam reservoirs. In the literature review, an overview of sedimentation in, and management of, dam reservoirs is given. Followed by a study on sediment transport mechanisms, that are involved in sedimentation in reservoirs. Empirical relations describe the transport mechanisms. The concept proposes the channelling of turbid density currents in dam reservoirs. This form of sediment transport is mainly responsible for the transport of fine sediments into dam reservoirs. The concept of channelling turbid density current is that channel dimensions can be controlled and positively influence the transport of sediment within the current. Both a new steady-state model and a new numerical model are developed to investigate the concept. The incorporation of WID in the channel improves the concept. The model provides a straightforward, easy to use tool to make first estimations for the applicability of channelling turbid density currents and the support by water injection dredging.

Sedimentation of dam reservoirs and management techniques is a new research field, mainly because sustainability has gained public interest in recent years. In the meantime, studies on sediment transport have been performed already for many decades. Nevertheless, sediment transport estimations deal with significant uncertainties, leading to a large number of empirical relations to make estimations. Only some apply to the proposed concept. More studies have to be done on the subject of sediment transport in the coming decades to improve the reliability and precision of these relations. Furthermore, within the field of sediment transport, turbid density currents are examined. Both numerical and scaled experiments have been developed to make approximations on their behaviour. Likewise, numerical models or schemes and scaled experiments are research subjects on their own. Whereas these aspects are investigated separately, they are not integrated into a format that is proposed and utilised within this thesis. To provide an answer to the main research questions: "Is channelling turbid density currents an effective measure to transport sediment through dam reservoirs?" The proposed conceptual solution is an integrated approach of studies on dam reservoir management, (fine) sediment transport, turbid density currents, Water Injection Dredging and an analytical and numerical scheme to evaluate and estimate the effectiveness of channelling turbid density currents in dam reservoirs. Two research methods are proposed to investigate the channelling concept. Firstly, a steady-state solution is used in which the effects of hydraulic radii and slope are investigated. Secondly, a dynamic numerical approach is used in which gravity, friction, deposition and erosion are incorporated. The influence of concentration, sediment size, slope and hydraulic radii are investigated. The results of these studies are provided in chapter 6.

As outlined in the previous paragraph, this study uses assumptions to provide an integrated approach to counteract the problem of sedimentation in dam reservoirs and to study its effectiveness. This is the first study to do so in this format. The assumptions on sediment transport and channelling are provided in chapter 3 and chapter 5. Within this section, the discussion results of the steady-state solution and numerical model are interpreted, and their meaning is explained and evaluated. Second, within the results, general patterns and findings are seen, it is discussed if these aspects confirm or reject the findings within this study and what there limitations and implications are. This is followed by critical evaluation and analysis of strong and weak aspects within this study, the models precision, validity and any unexpected behaviour are discussed, the available literature is listed, and suggestions are made to contribute future research. Final conclusions

are provided in chapter 9.

7.1. Interpretation of the Results

An interpretation and explanation of the meaning of the results for the steady-state solution, numerical validation, numerical source terms and full numerical model are provided.

7.1.1. Steady state

First, the steady-state approach is used to describe the kinematic behaviour of the turbid density current through a channel. The solutions provide the maximum possible velocities in the channel as friction and omitting entrainment of water and the bed. Three situations have been investigated using a mass balance for the channel, river and reservoir for both rectangular and trapezoidal channels transporting turbid density currents with reservoir return flow, without reservoir return flow and a simplified form with similar up and downstream parameters.

No significant differences between rectangular and trapezoidal channels can be obtained. If one wants to estimate channel dimensions, first estimates can be made for the dimensions of the rectangular channel using the simple relation of the hydraulic radius to estimate width and height; $w = h = 3R$. Further, the slope and hydraulic radius do significantly influence the velocity of a turbid density current, increasing these parameters yields an increase in velocity. Within the hydraulic radius, changing the depth has a more significant effect than changing the width. This is because in the formula for the hydraulic radii of the trapezoidal channel ($R_{trap} = \frac{W_b H + 2H^2}{W_b + 2H\sqrt{5}}$) height is quadratic and thus its influence is stronger than the width. It is also the reason why a small change in depth has more influence than a small change in slope. From this, it can be concluded that height and slope provide the opportunity to control the velocity of the current.

The channel flow with reservoir return flow yields flow velocities slightly less than that of the channel flow without return flow, but these differences are minimal. Change in slope or hydraulic yields a non-linear change in flow velocity according to $x^{\frac{1}{2}}$, which is a logical result of the formula by Morris and Fan (1992) due to the square root; [46] ($u_c = \sqrt{\frac{8}{f} g' R S_o}$).

Within the third scenario, parameters of concentration, velocity and area are kept the same in the upstream and downstream direction. The results of this third scenario can be used as a nomogram to make estimations on flow velocity, which will maintain specific sediment transport, surface area, hydraulic radius and discharge. A factor not investigated is the change in concentration of the current. The effect of concentration should be studied as a higher concentration can cause an increase in flow velocity, providing a better capability of sediment transport.

If the particle size is known, it can be determined if the particles stay in suspension from the rouse profiles as a first estimate using rouse profiles in section A.3. (E.g. d_50 =63 μm, velocity of 2 m/s, volume concentration $\approx$ 12 %) The approach could be used the other way around as-well. When one knows a certain particle diameter, minimum velocity can be determined. With the minimum velocity, one can then approximate if a turbid density current can travel through available channel dimensions.

Finally, the slopes in each of the three scenarios are at the higher range compared to conventional dam reservoirs and channels($S = 0.001$). The slopes should be provided in more detail between 0-0.1 to improve the steady-state study. These slopes are closer to the working range for the available slopes for the channel in the reservoir.

In short, hydraulic radius and slope influence the velocity of the turbid density current most significantly and the results of the third scenario in the steady-state solution can be used as nomogram to estimate the density current velocity, hydraulic radius(depth and width) and cross-sectional area. Slopes smaller than 0.01 have to be simulated in more detail to provide graphs that provide better workability.

7.1.2. Numerical Model

Secondly, the numerical model is a dynamic solution incorporating time, concentration, velocity, length, width, height, slope, friction, gravity, deposition, erosion and sediment size of the turbid density current within the channel. This form of the dynamic model is not yet available in the literature, and a more substantial part of this research is performed to incorporate the source terms of friction, gravity, erosion and deposition. The numerical model uses one-dimensional one-layer shallow water equations with Boussinesq approximation for the continuity and momentum equation in combination with a particle conservation equations. Assuming the turbidity current is influenced by the four source terms. The effects bed deformation, top

friction and water entrainment are omitted in this study; this might result in overprediction of concentration, velocity and height of the current.

The system of equations does not have an analytical solution; a numerical solution is proposed. The goal was to find a numerical scheme that was easy to implement. The scheme that provided an easy discretisation method is the Generalised Lax Friederichs scheme that includes three diffusion terms. The scheme is easy to use compared to some other conventional numerical models and provides the opportunity to make quick numerical estimations. A numerical dam break experiment has validated the numerical model. The numerical solution of the dam break model showed to underestimate the analytical solution by approximately 10 %. It is not clear what the reason for this underestimation is, it might be an effect of the diffusion terms in which the upstream has a higher effect than downstream. Next, to this, smaller grid size approximations showed convergence towards the analytical solution. Next, to this, the settling model experiments were in agreement with the settling model[45]. The numerical solution provides reasonable first estimates and looks promising, although performing experimental tests are required to validate this numerical model.

7.1.3. Source Terms for the Numerical Model

Four source terms studied for the numerical model, namely, gravity and friction, erosion and deposition. The validity of the source terms is based on the assumption that each source term describes its process correctly.

First, without source terms, the concentration is constant; it was expected that velocity and height were constant too. Velocity increases and height decreases, it is assumed that this is an effect densimetric Froude number that becomes lower than unity at the boundaries, combined with the boundary conditions imposed on the right boundary.

Secondly, the deposition term is decreasing nonlinearly with increasing length. Tested and showed to provide good results according to $t = \frac{3h}{v_s}$ [45]. The velocity(0.65 m/s) and height(0.47 m) become constant when all particles are settled out of the current. Increasing the concentration yields the same settling pattern, while velocity increases and height decreases.

Thirdly, the erosion term that is used gives similar solutions as proposed by [72], [69]. The non-hindered erosion provides modelling problems as the velocity is to the power 3 (u^3) and solutions become infinite. Hindered erosion solution gives better results as the term limits the growth of the solution. The erosion term does give good results, yet it has not proven to be valid, further research on the erosion term is recommended.

Fourthly, the friction and gravity term are evaluated and show that the constant velocities agree with $u_c = \sqrt{\frac{8}{f} g' RS}$ as proposed by Morris and Fan 1998 [46] and classical fluid mechanics. Concentration is constant as no settling or eroding term is provided. Increasing slope yields increased velocity according and becomes constant at a certain as is according to Morris Fan (1998)[46], Tonina (2012) [67] and MIT (2008)[45] solution and becomes constant. Increasing the hydraulic radius yields higher flow velocities per the steady-state solutions. On the right boundary sudden increase of the velocity is seen, the boundary conditions probably cause it. The friction, gravity and deposition term provide excellent results, compared to results presented in and respectively.

Testing the source terms separate does not necessarily prove that the combination of source terms provide an ultimate solution. The erosion term needs validation, and the full model needs to be validated with another numerical experiment or a scaled experiment to verify the source terms.

7.1.4. Full Numerical Model

For the full numerical model, five scenarios have been evaluated. Firstly, sediment size for a constant incoming velocity of 0.3 m/s, sediment concentration decreases, velocity decreases and height increases. The exception is 50 μm due to a constant decrease in concentration, and velocity decreases linearly with constant height. It shows that particles larger than 50 μm are almost unable to be transported by the current velocities. Secondly, the influence of concentration is minimal. Velocity is higher for higher concentration, height increases and more significantly for 1.0% which is contradicting. Thirdly, increasing slope yields increased concentration and velocity. Velocity is much higher than for gravity friction only. Next to this concentration increases, increasing the velocity significantly. Fourthly, the depth(hydraulic radius) is increased increasing concentration, velocity increases. Fifthly, the width(hydraulic radius) slightly decreasing concentration, decreasing velocity, increasing height, effects are much smaller than height change.

To summarise, the full numerical model showed that slope and depth change(hydraulic radius) have the most substantial influence on velocity, concentration and height of the solution. The change in width and concentration have far less influence. Turbid density currents hardly transport sediment sizes largen than 50

μm.

7.1.5. Case Study: Water Injection Dredging

A case study is simulating Water Injection Dredging(WID) by two source term equations, namely a formula for the height increase caused by the WID that is derived within this thesis and the erosion of sediment simulated by high-velocity sediment erosion as proposed by Bisschop et al. (2010) [27]. The location of the WID is in the middle of the domain. The concentration in the flow immediately increases, and height only slightly increase. It means that concerning the available flow height, only a small amount of sediment is added to the system. As time increases, the height with high sediment concentration increases. The increased concentration moves in two directions, in which the movement in the downstream direction is faster, which is an effect of the slope. Results show that the WID increase sediment transport in the downstream direction. It suggests that WID is an appropriate solution to increase turbid density transport. Although this may be true, the case study is a purely experimental approach to determine if it can positively influence the channelled turbid density current. The results are not validated as no other data or experiments are available. To conclude from this experiment, one needs to perform WID experiments to validate results. Further, the WID is applied continuously while in reality, the WID will only work during certain periods and over certain distances, this will change the results too.

7.2. Patterns

Within the results, general patterns are seen. These are highlighted in this section, discussing the implications and limitations.

Within the numerical model, at the right boundary, a sudden decrease or increase of the solution is seen. These are either an effect of boundary conditions or the densimetric Froude number that determines sub- or super-critical flow, the influence is more significant for small slopes and (resulting) low flow velocities. It is found that in some cases, the densimetric Froude number on the boundaries is lower than unity, which yields a sub-critical flow. In the centre of the domain, the Froude numbers are above unity. In some cases, the densimetric Froude number is above unity and solution still increases. An example can be found in the evaluation of the source term for friction and gravity. The Froude numbers are above unity, and still, a sudden increase is seen on the boundary. The effect might be related to the imposed Dirichlet boundary conditions or initial condition that imposes a minimum height in the system, but this can not be excluded based upon available information. The implication is that there is either an over- or under-prediction of velocity that prevents the solution to divide by zero, concentration and height. A limitation is that the solution on the boundaries is unreliable. A solution might be to change and test different boundary conditions and initial conditions. In literature, some examples are found that solve hyperbolic equations and subcritical flow that use different numerical schemes effectively. Next, to this velocity and height are directly related as, when velocity decreases, height increases and vice versa.

By comparing the results of the steady-state and numerical solution, it is found that the slope and depth have the most substantial influence on the solution. Concentration affects the numerical solution only slightly. Besides this, the solutions for gravity, friction and change in slope show a certain distance over which velocity enlarges towards a particular steady solution. The same occurs for the depth, concentration and width but is less noticeable. It implies that incoming concentrations, heights and velocities of the system are either to low or too high and will change the initial height and concentration of the flow. It takes the system a particular time to move towards a steady solution, implying that on the first part of the solution, the system needs time to 'spin-up'. It is limiting the area to make good predictions towards the middle of the domain. Solved by making estimations in advance using the balance of Erosion(E) and Sedimentation(D) one can determine if the current starts to erode or deposit depending on a positive or negative value. This depends on the channel velocity(u_c), which can be determined by the channel dimensions.

7.3. Evaluation

A critical evaluation of strengths, weaknesses, precision and validity of this study approach and results. These are supplemented by literature suggestions to improve future research on the subject of channelling turbid density currents in dam reservoirs. (3)

The strengths of this study are: that a numerical model for turbid density currents in a channel with a straightforward discretion method is used. It is easy to implement and most importantly, the model is easy to use. The results can be obtained within 10-30 seconds, depending on the number of parameters

incorporated. The model provides an excellent tool to make first estimates. Several studies have been done on turbid density currents. However, this is the first model to explicitly model a turbid density current in a channelled dam reservoir and, to include a form of Water Injection Dredging to measure the effects on turbid density currents.

The weaknesses and opportunities for improvement in this study are that: (1)as the numerical model is not validated by experiment, results have to be interpreted with caution. (2) As the model is only doing experiments with an incoming height of 1.0 m, a velocity of 0.3 m/s and a concentration of 2.0%. (3) For the hydraulic radius, the wetted perimeter for open channel flow is assumed, which might over-predict the hydraulic radius. (4) The right boundary of the numerical approach significantly influences the solution. (5) The erosion term used is for open channel flow; it should be validated if this term can be used for turbid density currents without change. (6)Within the deposition, term settling velocity of particles is strongly influenced by the increase in fluid concentration mainly because the fall of the particles induces an upward movement of water; the buoyancy of the particle increases due to high-density fluid, and by the interaction between particles (effect of concentration - hindered settling). The transport capacity of the flow tends to increase with high sediment concentration. However, these changes also depend on the composition of sediment present in suspension, which is not taken into account[41]. Not accounting for (7)Coriolis and centrifugal forces in the dam reservoirs, (8)water entrainment, (9) bottom change. (10) friction along the top and front of the current. (11) Simulations are one dimensional(1D) while turbid density currents are a three dimensional(3D) process. (12) To plot the results in the form of concentration, height a velocity makes them less applicable to other situations, by non-dimensionalising the equation with the Froude number they can be used in more situations.

The precision within sediment studies is a complicated subject, over- or under-prediction for sediment transport by currents is in the range of 2-5 times the natural range[61]. The model is based upon many empirical relations and combined with a numerical solution. It will lead to deviation from reality; to quantify, this is impossible without a data set of experiments.

With respect to validity, the steady-state solution is a valid solution to predict the velocity of a turbid density current[46]. Sedimentation term is valid for turbulent flow[45]. No clear evidence is provided for the validity of the erosion term. The dam break model shows that the numerical scheme under estimates height and velocity with 10% compared to the analytical solution for a dam break.

To continue research on this subject, several literature suggestions: The steady-state solution and information on turbid density currents in dam reservoirs are provided by Morris and Fan (1998) [46]. Huppert (1993)[34] provides a paper on Particle driven gravity currents with a different numerical method. Bonnecaze (1999)[10] improves this by providing a solution for Particle driven density currents on a slope. Parker (1987) provides experiments on turbid density currents over erodible beds. Cao (2004)[18] provide a numerical solution for a dam break over an erodible bed, which could provide a bed change source term. Oehy(2007)[48] provides a study on the control of turbid density currents in reservoirs over solid and permeable obstacles. Hu(2009) provides a fully coupled(from the river to reservoir) mathematical modelling of turbidity current over erodible bed [33]. Wang (2017)[75] provides a one-dimensional morphodynamic model coupling open-channel flow and turbid density currents in dam reservoirs. It includes the 1D equation of turbidity currents and gravity closure relationships by Pantin(1979), Cao (2009)[17] and Parker (1986) [52].

V

Conclusion and Recommendations

8

Conclusion

To conclude, from both the steady-state solution and the numerical solution, channelling a turbid density current can be an effective measure in order to transport fine sediment through dam reservoirs. Both the slope and depth of the channel have the most significant influence on the effectiveness of this measure.

This conclusion is based on several sub-questions as shown in the next paragraphs

- The main mechanisms causing sedimentation of dam reservoirs are the reduction of velocity and turbulence that transport sediment in the form of bed-, suspended-and wash-load transport. The change in width mainly causes the reduction of velocity and turbulence. (SQ1)
- To successfully manage dam reservoirs an integral approach of several techniques, such as reduction of sediment yield, route sediment, focus, remove sediment and several adaptive strategies are necessary. The effectiveness of the technique is mainly dependent on dam reservoir type(fine sediment, widening, sufficient depth available) and the efficiency of these management techniques are unclear and require more research. (SQ2)
- A turbid density current containing suspended sediment is denser than the ambient fluid in the reservoir, supported by turbulence and, driven by density differences and gravity. The characteristics of the turbid density current can be described by the head, body and tail of the current each having their own internal and external mechanisms. Turbid density currents settle due to increased friction along the bottom and top of the current as of the width of the reservoir increases. (SQ3)
- Both the steady-state and the numerical model show that slope and depth(hydraulic radius) have the most substantial influence on the velocity in increasing sediment transport. Changes in-depth have a more significant influence compared to the change of width, as depth appears quadratic in the equation of the hydraulic radius. (SQ4)
- The turbid density current is mathematically described by the one-dimensional shallow water equations, with a Boussinesq approximation, supplemented by the particle conservation equation. The Generalised Lax Friedrichs scheme, with diffusion terms A = 0.1, B = 1.0 and C = 0.1, provided a valid and straightforward numerical solution for the dynamic one-dimensional shallow water equations. The dam break experiment validates the numerical scheme, that provides an analytical solution. The results of the numerical solution underestimate the velocity and height of the analytical solution by approximately 10%. (SQ5)
- The effect of the Water Injection Dredge is described by two source terms. The erosion term for WID term added to the particle conservation equation and, the source term for the added water causing an increase in height. The model results show that Water Injection Dredging successfully enhances sediment transport in a channelled dam reservoir. Further research, computational or experimental, is required to validate the assumptions made for the integration of the Water Injection Dredge in the model. (SQ6)
- The developed model provides a very simple, quick and easy to use estimation tool. The modelling tool can assess the applicability of channelling turbid density currents in dam reservoirs. The model provides the opportunity to change concentration, depth, width and the slope and also to asses the effects of water injection dredging.

- Median particle diameters(d_{50}) of 50, 100, 150 and 200 have been modelled. Particles larger than 50 μm are hardly kept in suspension by turbid density transport. The model shows that turbid density transport is only suitable for (very) fine sediment only.
- Increasing the slope of the channel in the dam reservoir, fine sediment transport(d_{50} =50 μm) increases.
- The four source terms, gravity, friction, erosion and deposition are successfully incorporated in the 1D single-layer shallow water equation and particle conservation equation.
- The graphs from the steady-state solution can be used as a graphical tool, nomogram, to estimate first dimensions for a channel in a reservoir. It provides the first estimates for the slope, velocity and hydraulic radius for a trapezoidal reservoir channel.

The numerical solution provides good first estimates and looks promising, although performing experimental tests are required to validate this numerical model.
Sedimentation is causing sustainability problems for dam reservoirs around the world. Several types of sediment transport are responsible for the sedimentation of reservoirs; one of these is the turbid density current. Several management techniques have been developed to counteract sedimentation and increase the sustainability of reservoirs. This report examines a concept in which turbid density currents are channelled within dam reservoirs to enhance sediment transport, thereby reducing sedimentation of dam reservoirs. Two computational models are introduced to investigate the concept, a steady-state model describing the velocity of the current and a numerical model that describes the dynamic behaviour. Many assumptions are made in modelling of the turbid density current in a channel, the model has limitations, with implications for the application of the results. chapter 7. However, this concept provides a viable new solution that can be developed for application in reservoirs with fine sediment in order to increase the sustainability of dam reservoirs.

Further studies, both computational and experimental, are needed. These need to provide considerably more evidence, that channelling turbid density currents is both theoretically and practically feasible within dam reservoirs. The recommendations for future research are provided in chapter 9.

9

Recommendations

For future research on channelling turbid density currents in dam reservoirs, this chapter provides recommendations for theoretical and practical applications.

- Use the model to make first estimations for the channelling of turbid density currents and the application of Water Injection Dredging in dam reservoirs.
- Model related recommendations:
  - Experimental research to validate findings of computational model.
  - Do research on the boundaries of the proposed numerical model, assessing both the boundary conditions and Froude number to ascertain what affects the solution of the model. The model results can be non-dimensionalised by assessing the Froude number along the channel instead.
  - The model can be expanded by incorporating other source terms such as bottom deformation[18], water entrainment, bed entrainment and friction along the top, to make a complete description of the processes within and along with the turbid density current [75] [18].
  - The model can be improved by coupling upstream river transport with turbid density current in a dam reservoir[33][75].
  - Expand the one-dimensional model into a two-layer equation[63] or even expand to two or three-dimensional models although, two and three-dimensional models significantly increase computational time.
  - Asses the effect of slope and depth on different particle sizes.
  - Use different numerical schemes to discriminate/discern the system of equations and compare it with the results provided by the Generalised Lax Friedrich Schemes and assess the reasons for underprediction of velocity and height. A possible solution could be found with the use of the method of characteristics.
- Scaled experiments to validated the source terms for the channelled turbid density currents and to measure the effects of Water Injection Dredging within it.
- This concept is applicable to a certain amount of dam reservoirs. Do a feasibility study for large dam reservoirs, to asses which dam reservoirs are suitable for the proposed solution of channelling, including a list of criteria to asses the applicability of the concept. Characteristics such as; fine sediment, no delta (implies course sediment), enough space (width/height) to make a channel and for dredging equipment(if the channel is supported by Water Injection Dredging).
- When much sediment is eroded and released from a dam reservoir the river downstream has to cope with an increased amount of sediment, the capability of the river to on the one hand transport the sediment and the effects on the downstream environment and community should be assessed.
- Water Injection Dredging:
  - Improve the description and assumptions of Water Injection Dredging as little is known about the process.
  - Assess the applicability of a Water Injection Dredge, is it able to access the reservoir. It might be possible to apply WID alike applications locally increasing the flow velocities. Such as jets on several locations in the channel. Further study of water injection dredging as most of the information on dredging is kept within companies.

Bibliography

[1] Alavian, B. V., Jirka, G. H., Denton, R. A., Johnson, M. C., and Stefan, H. G. Density Currents Entering Lakes and Reservoirs. *Hydraulic Engineering*, 118(11):1464–1489, 1992.

[2] Alavian, V. Behavior of Density Currents on an Incline. *Journal of Hydraulic Engineering*, 112(1):27–42, 1986. ISSN 0733-9429. doi: 10.1061/(ASCE)0733-9429(1986)112:1(27). URL http://ascelibrary.org/doi/10.1061/%28ASCE%290733-9429%281986%29112%3A1%2827%29.

[3] Anderson, J. D., Degroote, J., Degrez, G., Dick, E., Grundmann, R., and Vierendeels, J. *Dynamics, Computational Fluid*. 1992. ISBN 9783540850557.

[4] Annandale, G. W. RESCON 2 : Rapid identification of optimal strategies to mitigate reservoir sedimentation and climate change impacts on water supply reliability. 2, 2017.

[5] Annandale, G. W., Morris, G. L., and Karki, P. *Extending the Life of Reservoirs*. The World Bank, 2016. ISBN 9781464808388.

[6] Bagnold, R. A. Auto-suspension of transported sediment; turbidity currents. *Proceedings of the Royal Society of London. Series A. Mathematical and Physical Sciences*, 265(1322):315–319, 1962. ISSN 2053-9169. doi: 10.1098/rspa.1962.0012.

[7] Bagnold, R. A., Udall, S. L., and Pecora, W. T. An Approach to the Sediment Transport Problem From General Physics. *Geological Survey PRofessional Paper*, 422(1):137, 1966. URL https://pubs.usgs.gov/pp/0422i/report.pdf.

[8] Bisschop, F. *Erosion of sand at high flow velocities*. PhD thesis, Delft University of Technology, 2018.

[9] Bisschop F., Visser, P., Rhee, C. v., and Verhagen, H. Erosion Due to high flow velocities: A decription of relevant processes. pages 1–10, 2010.

[10] Bonnecaze, R. T. and Lister, J. R. Particle-driven gravity currents down planar slopes. *J. Fluid Mech. (1999)*, 390:75–91, 1999.

[11] Borland, W. M. and Miller, C. R. Distribution of Sediment in Large Reservoirs. *Transactions of the American Society of Civil Engineers 125*, 160–80, 1960.

[12] Bronsvoort, K. Sedimentation in reservoirs: Investigating reservoir preservation options and the possibility of implementing Water Injection Dredging in reservoirs, 2013. URL https://repository.tudelft.nl/islandora/object/uuid%3A191323c1-b2ec-4d3e-9e28-2958c1ee287c.

[13] Brownlie, W. R. Prediction of Flow Depth and Sediment Discharge in Open Channels. Report No. KH-R-43A. *Report No. KH-R-43A*, (November):232, 1981. ISSN 02725002. doi: 10.7907/Z9KP803R.

[14] Brune, G. Trap Efficiency of Reservoirs. *Transactions, American Geophyiscal Union*, 34(3):12, 1953. doi: https://doi.org/10.1029/TR034i003p00407.

[15] Bulu, A. *Open Channel Flow*. Virginia Tech, 2010. URL http://www.undergradcatalog.registrar.vt.edu/0910/eng/cee.html#Anchor-Civil-47383.

[16] Cao, Z. Equilibrium Near-Bed Concentration of Suspended Sediment. *Journal of Hydraulic Engineering*, 125(December):1270–1278, 1999. doi: https://doi.org/10.1061/(ASCE)0733-9429(1999)125:12(1270).

[17] Cao, Z. and Carling, P. A. Mathematical modelling of alluvial rivers: reality and myth. Part 2: Special issues. *Proceedings of the Institution of Civil Engineers - Water and Maritime Engineering*, 154(4):297–307, 2009. ISSN 1472-4561. doi: 10.1680/wame.2002.154.4.297.

[18] Cao, Z., Pender, G., Wallis, S., and Carling, P. Computational Dam-Break Hydraulics over Erodible Sediment Bed. *Journal of Hydraulic Engineering*, 130(July):689–703, 2004. doi: 10.1061/(ASCE)0733-9429(2004)130:7(689).

[19] Cao, Z. Turbulent Bursting-Based Sediment Entrainment Function. *Journal of Hydraulic Engineering*, 123(3):233–236, 1997. ISSN 0733-9429. doi: 10.1061/(asce)0733-9429(1997)123:3(233).

[20] Celik, I. and Rodi, W. Modeling Suspended Sediment Transport in nonequilibrium situations. *Hydraulic Engineering*, 114(10):1157–1191, 1988.

[21] Chamoun, S., De Cesare, G., and Schleiss, A. J. Managing reservoir sedimentation by venting turbidity currents: A review. *International Journal of Sediment Research*, 31(3):195–204, 2016. ISSN 10016279. doi: 10.1016/j.ijsrc.2016.06.001. URL http://dx.doi.org/10.1016/j.ijsrc.2016.06.001.

[22] Edwards, D. E. Turbidity Currents: Dynamics, Deposits and Reversals, 1993.

[23] Efthymiou, N. P., Palt, S., Annandale, G. W., and Karki, P. Reservoir Conservation Model Rescon 2 Beta. Technical report, International Bank for Reconstruction and Development / The World Bank, Washington, 2017.

[24] Einstein. The Bed-Load Function for Sediment Transportation in Open Channel Flows. 1950.

[25] Elzinga, L. Dredging of Reservoirs, 2017. URL https://repository.tudelft.nl/islandora/object/uuid%3Aa4f54843-399e-4d03-abcd-4944bb685e9c.

[26] ESSP and ICOLD. Global Reservoir and Dam database. URL gwsp.org.

[27] F. Bisschop, C. R., P.J Visser and Verhagen, H. Erosion Due to High Flow Velocities. pages 1–10, 2010.

[28] Ferguson, R. and Church, M. A simple universal equation for grain settling velocity. *JOURNAL OF SEDIMENTARY RESEARCH*, 74(6):933–947, 2004. URL http://jsedres.sepmonline.org.offcampus.lib.washington.edu/content/74/6/933.full.pdf+html%5Cnpapers2://publication/uuid/A254A180-2E5C-424D-8A35-6E1F5A33364C.

[29] Fruchard, F., Camenen, B., and Fruchart, F. Reservoir sedimentation : different type of flushing - friendly flushing example of genissiat dam flushing To cite this version : Reservoir Sedimentation Different Type of Flushing - Friendly Flushing Example of Genissiat Dam Flushing. 2012.

[30] Gerbeau, J.-f., Perthame, B., Gerbeau, J.-f., Perthame, B., and System, V. S.-v. Derivation of Viscous Saint-Venant System for Laminar Shallow Water ; Numerical Validation To cite this version : HAL Id : inria-00072549 Derivation of viscous Saint-Venant system for laminar shallow water ; numerical validation. 2006.

[31] Gibiansky, A. Fluid Dynamics: The Navier-Stokes Equations, 2011. URL http://andrew.gibiansky.com/blog/physics/fluid-dynamics-the-navier-stokes-equations/.

[32] Gunawan, H. P. *Numerical simulation of shallow water equations and related models*. PhD thesis, Universite Parist-est, 2016.

[33] Hu, P. and Cao, Z. Fully coupled mathematical modeling of turbidity currents over erodible bed. *Advances in Water Resources*, 32(1):1–15, 2009. ISSN 03091708. doi: 10.1016/j.advwatres.2008.07.018. URL http://dx.doi.org/10.1016/j.advwatres.2008.07.018.

[34] Huppert, H. E. and Lister, J. R. Particle-driven gravity currents. *Journal of Fluid Mechanics*, 250:339–369, 1993. ISSN 14697645. doi: 10.1017/S002211209300148X.

[35] Knoblauch, H. Overview of density flows and turbidity currents. *Water Resources Research Laboratory*, page 27, 1999.

[36] Kondolf, G. M., Gao, Y., Annandale, G. W., and Morris, G. L. Sustainable sediment management in reservoirs and regulated rivers: Experiences from five continents. *Earth's Future*, 2(5):256–280, 5 2014. ISSN 23284277. doi: 10.1002/2013EF000184. URL http://doi.wiley.com/10.1002/2013EF000184.

[37] Lai, J. S. and Shen, H. W. Flushing sediment through reservoirs. *Journal of Hydraulic Research*, 37(6): 237–255, 1999. ISSN 00221686. doi: 10.1080/00221689609498499.

[38] Leveque, R. Finite-Volume Methods for Hyperbolic Problems. 2002.

[39] Litrico, X. and Fromion, V. Modeling of Open Channel Flow. *Modeling and Control of Hydrosystems*, pages 17–41, 2009. doi: 10.1007/978-1-84882-624-3{_}2.

[40] Mahmood, K. Reservoir Sedimentation. *Washington, D.C; World Bank; 1987 [?]. 128 p. (Technical Paper, 71)*, -(71):134, 1987.

[41] Manica, R. Sediment Gravity Flows: Study Based on Experimental Simulations. *Hydrodynamics - Natural Water Bodies*, 2012. doi: 10.5772/28794.

[42] Martins, R., Leandro, J., and Djordjević, S. Analytical Solution of the Classical Dam-Break Problem for the Gravity Wave–Model Equations. *Journal of Hydraulic Engineering*, 142(5):06016003, 2016. ISSN 0733-9429. doi: 10.1061/(asce)hy.1943-7900.0001121.

[43] Middleton, G. V. Experiments on Density and Turbidity II uniform flow of density currents. *Canadian Journal of Earth Sciences*, 3(4):523–546, 1966. ISSN 0008-4077. doi: 10.1139/e66-038. URL `http://www.nrcresearchpress.com/doi/10.1139/e66-038`.

[44] Miedema, S. A. Constructing the Shields Curve part A: Fundamentals of the sliding, rolling and lifting mechanisms for the entrainment of particles. *Journal of Dredging Engineering*, 12(1):1–49, 0. doi: 10.1115/omae2011-49232.

[45] MIT. *Transport of particles*. MIT, 2008.

[46] Morris, G. and Fan, J. *Reservoir Sedimentation Handbook*. McGraw-Hill Book Co., 1998. ISBN 0-07-043302-X.

[47] Morris, G. L. Management alternatives to combat reservoir sedimentation. *First International Workshop on Sediment Bypass Tunnels*, pages 181–193, 2015.

[48] Oehy, C. D. and Schleiss, A. J. Control of turbidity currents in reservoirs by solid and permeable obstacles. *Journal of Hydraulic Engineering*, 133(6):637–648, 2007. ISSN 0733-9429. doi: 10.1061/(ASCE)0733-9429(2007)133:6(637). URL –.

[49] Ortiz, J. D. and Klompmaker, A. A. Turbidity Currents. Technical report, The Oceanography Society, 2015.

[50] Palmieri, A., Shah, F., Annandale, G. W., and Dinar, A. Reservoir Conservation Volume I: The RESCON Approach Economic and engineering evaluation of alternative strategies for managing sedimentation in storage reservoirs. Technical report, The International Bank for Resconstruction and Development / The World Bank, Washington, 2003.

[51] Pantin, H. M. Self-accelerating turbidity currents. *Journal of Fluid Mechanics*, 171:145–181, 1986. ISSN 14697645. doi: 10.1017/S0022112086001404.

[52] Parker, G., Garcia, M., Fukushima, Y., and Yu, W. Experiments on turbidity currents over an erodible bed Experiments on turbidity currents over an erodible bed Etude experimental de courants de turbidité sur un lit affouillable. *Journal of Hydraulic Research*, 25(February):123–147, 1987. ISSN 0022-1686. doi: 10.1080/00221688709499292.

[53] Pietrzak, J. *Class Notes for CIE5302: An Introduction to Stratified Flows for Civil and Offshore Engineering*. TU Delft, 2015.

[54] Rajaratnam, N. *Turbulent jets*. Elsevier Scientific Publishing Company, 1976.

[55] Richardson, J. F. and Zaki, W. Sedimentation and Fluidisation. Part 1. *Trans. Inst. Chem. Eng*, 32:35–53, 1954. URL `http://garfield.library.upenn.edu/classics1979/A1979HZ20300001.pdf`.

[56] Ritter, A. Die fortpflanzung der wasserwellen. *Zeitschrift des Vereines Deutscher Ingenieure*, 33:947–954, 1892.

[57] Rowe, P. A convenient empirical equation for estimation of the Richardson-Zaki exponent. *Chem. Eng. Science*, 42(11):2795–2796, 1987.

[58] Saint-Venant, A. B. d. Théorie du mouvement non permanent des eaux, avec application aux crues des rivières et a l'introduction de marées dans leurs lits. *Comptes Rendus de l'Académie des Sciences*, 73: 147–154, 1871.

[59] Schiereck, G. J. and Verhagen, H. J. *Introduction to Bed, bak and shore protection*. Delft Academic Press / VSSD, 2nd editio edition, 2016. ISBN 97890-6562-4031.

[60] Schleiss, A. J., Franca, M. J., Juez, C., and De Cesare, G. Reservoir sedimentation. *Journal of Hydraulic Research*, 54(6):595–614, 11 2016. ISSN 0022-1686. doi: 10.1080/00221686.2016.1225320. URL `https://www.tandfonline.com/doi/full/10.1080/00221686.2016.1225320`.

[61] Soulsby, S. *Dynamics of marine sands*. Thomas Telford Publications, Thomas Telford Service Ltd, 1997. ISBN 978-0-7277-2584-X.

[62] Stoker, J. Water Waves. The MAthematical Theory with Applications. *Interscience Publ., Inc., New York*, 1957.

[63] Stovers, M. *Particle-driven gravity currents*. PhD thesis, Delft University of Technology, 2016.

[64] Swart, R., Swart, R., Van Rhee, C. m., Van der Schrieck, G. m., Miedema, S. m., and Kollen, J. m. Autonomous dredging of mud. (December), 2015.

[65] Talebbeydokhti, N. and Naghshineh, A. Flushing Sediments through reservoirs. *Iranian Journal of Science and Technology*, 28(B1):119–136, 2004.

[66] Tong, W. and Wu, Y. Generalized Lax-Friedrichs Scheme for Convective-Diffusion Equation. *Springer-Verlag Berlin Heidelberg*, 2(4):321–322, 2012.

[67] Tonina, D. Fluid Mechanics, 2012.

[68] van der Schrieck, G. *Dredging Technology, guest lecture notes CT5300*. Delft University of Technology, 2011.

[69] Van Rhee, C. Sediment entrainment at high flow velocity. *Journal of Hydraulic Engineering*, 136(9): 572–582, 2010. ISSN 0733-9429. doi: 10.1061/(asce)hy.1943-7900.0000214.

[70] Van Rhee, C. and Talmon, A. M. Sedimentation and erosion of sediment at high solids concentration. *18Th International Conference on Hydrotransport*, pages 211–222, 2010.

[71] van Rijn, L. C. Sedimentation of Sand and Mud in Reservoirs and Rivers. pages 1–15, 2013.

[72] van Rijn, L. Sediment Transport, Part II: Suspended Load Transport, 1984. ISSN 19437900.

[73] van Rijn, L. SIMPLE GENERAL FORMULAE FOR SAND TRANSPORT IN RIVERS, ESTUARIES AND COASTAL WATERS, 2000.

[74] van Rijn, L. Water injection dredging equipment. 2015.

[75] Wang, Z., Xia, J., Deng, S., Zhang, J., and Li, T. One-dimensional morphodynamic model coupling open-channel flow and turbidity current in reservoir. *Journal of Hydrology and Hydromechanics*, 65(1):68–79, 2017. ISSN 13384333. doi: 10.1515/johh-2016-0046.

[76] Winterwerp, B. J. C., Bakker, W. T., Mastbergen, D. R., and Rossunv, H. V. Hyperconcentrated Sand-Water Mixture Flows Over Erodible Bed. *Journal of Hydraulic Engineering*, 118(11):1508–1525, 1992.

[77] Winterwerp, J. C., Wang, Z. B., van Kester, J. A. T. M., and Verweij, J. F. Far-field impact of water injection dredging in the Crouch River. *Proceedings of the Institution of Civil Engineers - Water and Maritime Engineering*, 154(4):285–296, 2002. ISSN 1472-4561. doi: 10.1680/wame.2002.154.4.285.

[78] Zijlema, M. *Computational Modelling of Flow and Transport*. Delft University of Technology, 2015. ISBN 0691730008.

VI

Appendices

A

Sediment Transport Principles

A.1. Definitions on Sediment Transport

Several definitions of bed load transport have been have been provided. Two of those are given by Bagnold(1956) and by Einstein (1950) [73]:

1. Bagnold (1956): Bed-load transport is transport in which particles have successive contact with the bed and are limited by the effect of gravity.
2. Einstein (1950): Bed-load transport is the transport of sediment particles in a thin layer of two particle diameters thick just above the bed. The movement is by sliding, rolling and some jumps with a longitudinal distance of a few particle diameters. The bed layer is considered as a layer in which the mixing due to the turbulence is so small that it cannot influence the sediment particles, and therefore suspension of particles is impossible in the bed-load layer. Further, it is assumed that the average distance travelled by any bed-load particle in a series of successive movements is a constant distance of 100 particle diameters, independent of the flow condition, the transport rate and the bed composition. Saltating motion is referred to as suspended load transport, as the jump length is larger than a few grain diameters(Einstein 1950).

A definition given on suspended-load transport is given by bagnolds:

1. Bagnold 1956 defines suspended-load transport as that in which the excess weight of the particles is supported by random successions of upward impulses imported by turbulent eddies. The suspended sediment particle velocity is almost equal to the fluid velocity. Suspended sediment particles are described with sediment concentration, this is expressed in volume(m^3)/fluid volume(m^3) or solid mass (kg)/fluid volume(m^3)

A.2. Concentration profile

A.2.1. Derivation of Rouse Profile

In a stationary uniform flow, the time derivative $\frac{\delta c}{\delta t} = 0$ and the coordinate in $x = 0$ the equation simplifies to:

$$\frac{\delta}{\delta z}(wc) = \frac{\delta}{\delta z}(\epsilon \frac{\delta c}{\delta z}) \tag{A.1}$$

In this case vertical velocity of particles is equal to the settling velocity $w_s = -w$, substition of w_s and integration of Equation A.1 results in the following equation:

$$w_s c = -\epsilon \frac{\delta c}{\delta z} \tag{A.2}$$

In channel flow the eddy viscosity is assumed to be a parabolic function:

$$K_s = \kappa u_* (1 - \frac{z}{H}) \tag{A.3}$$

When an linear profile is assumed, referred to as the power law:

$$K_s = \kappa u_* z \tag{A.4}$$

Or a uniform distribution:

$$noginvullen \tag{A.5}$$

Where H(or z)= Waterdepth,κ = Von Karman constant = 0.4, u_* = friction velocity = $\sqrt{\frac{\tau_b}{\rho}}$, τ_b= bedshearstress. Substitution in equation Equation A.2 yields:

$$w_s c = -\frac{\kappa u_*}{\sigma} z(1-\frac{z}{H})\frac{\delta c}{\delta z} \tag{A.6}$$

Rearranging and integration:

$$\int_{c_a}^{c} \frac{\delta c}{c} = -\frac{w_s \sigma}{\kappa u_*} \int_{z_a}^{z} \frac{\delta z}{z(1-\frac{z}{H})} \tag{A.7}$$

Integral on the right of Equation A.7, can be seen as a standard integral:

$$\int \frac{dx}{x(ax+b)} = -\frac{1}{-b} ln \frac{ax+b}{x} \tag{A.8}$$

with $b = 1$ and $a = -\frac{1}{H}$ and x = z it follows that:

$$\ln c - \ln c_a = \frac{w_s \sigma}{\kappa u_*} [\ln \frac{1-\frac{z}{H}}{z}]_{z_a}^{z} \tag{A.9}$$

or

$$\ln c - \ln c_a = \frac{w_s \sigma}{\kappa u_*} (\ln \frac{1-\frac{z}{H}}{z} - \ln \frac{1-\frac{z_a}{H}}{z_a}) \tag{A.10}$$

Rewriting equation Equation A.10 results in equation Equation A.11. In which the exponent is referred to as the Rouse number, which is an important parameter to determine whether the transport mechanism is suspended transport or bed load transport.

$$\frac{c}{c_a} = (\frac{H-z}{z} \cdot \frac{z_a}{H-z_a})^{\frac{w_s \sigma}{\kappa u_*}} \tag{A.11}$$

$$B = \frac{w_s \sigma}{\kappa u_*} \tag{A.12}$$

Ratio of B determines slope of the profile

$$u_* = sqrt(\frac{\tau_o}{\rho_w}) \tag{A.13}$$

$$Powerlaw : C(z) = C_a (\frac{z}{z_a})^{-B} \tag{A.14}$$

A.2.2. Several concentration profiles

$$u_* = sqrt(ghi) \tag{A.15}$$

if i goes up, u_* goes up, b goes down, c(z) goes up.

The concentration distribution is plotted for different values as a function of depth z/H. When B increases, the settling velocity only has only a limited amount of sediment in suspension in the water-column.

Shear stress in fluids.The extent of a turbidity current depends on the shear stress at the bed and the turbulence intensity. The capacity to keep the sediments in suspension. Their life period depends directly on the discharge and indirectly on the sediment concentration.

A real fluid moving along a solid boundary will put a shear stress at the boundary.

In fluid dynamics, the **no-slip condition** for viscous fluids assumes that at a solid boundary, the fluid will have zero velocity relative to the boundary.

The fluid velocity at all fluid–solid boundaries is equal to that of the solid boundary.[1] Conceptually, one can think of the outermost molecules of fluid as stuck to the surfaces past which it flows.

Particles close to a surface do not move along with a flow when adhesion is stronger than cohesion. At the fluid-solid interface, the force of attraction between the fluid particles and solid particles (Adhesive forces; dissimilar particles or surfaces to cling to one another) is greater than that between the fluid particles (Cohesive forces; similar or identical particles/surfaces to cling to one another). This force imbalance brings down the fluid velocity to zero.

For all Newtonian fluids in laminar flow, the shear stress is proportional to the strain rate in the fluid, where the viscosity is the constant of proportionality. For non-Newtonian fluids, the viscosity is not constant. The shear stress is imparted onto the boundary as a result of this loss of velocity.

Given the flow characteristics, the manner in which sediment is transported by the (turbid)flow can be estimated using the Rouse number. This relates to the settling velocity of a grain to the shear boundary stress acting on it. The Rouse number(b) is defined as:

$$b = \frac{w_s}{\kappa u_*} \tag{A.16}$$

w_s = settling velocity of particles, κ = von Kármán constant, generaly taken as 0.41, u_* = shear velocity [m/s] The values of the Rouse numbber can differ between the following values:

- $0 < b < 0.8$ "wash load" transport of very fine sediment
- $0.8 < b < 1.2$ suspended sediment transport
- $1.2 < b < 2.5$ 50% suspended sediment transport
- $b > 2.5$ bed load transport

Sand in suspension is a result of diffusion of sand upwards due to turbulence of the water and a settling of the grains due to gravity. The equation governing this balance is(The rouse number given above is part of a solution of this equation):

$$w_s C = -K_s \frac{dC}{dz} \tag{A.17}$$

w_s = settling velocity of sediment grains, C = volume concentration of sediment at height z, K_s = eddy diffusivity, depends on the height above the bed, it could be solved as a uniform, linear or a parabolic distribution. When equation Equation A.17 is solved the vertical distribution of the concentration of the suspended sediment is given, ofcourse subjected to several assumptions. These different assumptions lead to different expressions for the concentration profile. The shape of this profile depends upon the Rouse number.
Entertainment of sediment from the bed is governed by skin friction:

$$\tau_{0s} = \rho u_{*s}^2 \tag{A.18}$$

As form drag of ripples does not act directly on grains lying on the surface of the bed, but it generates turbulence which governs the diffusion process. the distinction disappears for sheet flow conditions. Diffusion of sediment higher into the water column is governed by the total shear-stress:

$$\tau_s = \rho * u_*^2 \tag{A.19}$$

In turbulent flow the shear stress is equal to:

$$\tau = \mu \frac{dy}{dx} - u'v'\rho = \rho u_*^2 \tag{A.20}$$

If the eddy diffusivity($K_s = \kappa u_* z$) is assumed to increase linearly with height above the bed the corresponding concentration profile is the power-law profile:

$$C(z) = C_a (\frac{z}{z_a})^{-b} \tag{A.21}$$

If eddy diffusivity is assumed to vary parabolically with the height($K_s = \kappa u_* z[1-(z/h)]$) the rouse profile is obtained:

$$C(z) = C_a(\frac{z}{z_a}\frac{h-z_a}{h-z})^{-b} \tag{A.22}$$

van Rijn(1984) assumed a lower half that varies parabolically with the height and is constant with height in the upper half of the watter column. van Rijn also took account of the difference between diffusion of sediment and fluid momentum, and the density stratification by the sediment, by introducing a modified form of the exponent b. As provided in [61]Equation 3.17

$$C(z) = C_a(\frac{z}{z_a\frac{h-z_a}{h-z}})^{-b'} \text{ for } z_a < z < \frac{h}{2} \tag{A.23a}$$

$$C(z) = C_a(\frac{z_a}{h-z_a}^{b'})exp(-4b'(\frac{z}{h}-\frac{1}{2})) \text{ for } \frac{h}{2} < z < h \tag{A.23b}$$

with (A.23c)

$$b' = \frac{b}{B1} + B_2 \tag{A.23d}$$

$$B_1 = 1 + 2(\frac{w_s}{u_*}^2) for 0.1 < \frac{w_s}{u_*} < 1 \tag{A.23e}$$

$$B_1 = 2 for \frac{w_s}{u_*} >= 1 \tag{A.23f}$$

$$B_2 = 2.5(\frac{w_s}{u_*})^{0.8}(\frac{C_a}{0.65})^{0.4} for 0.01 \leq \frac{w_s}{u_*} \leq 1 \tag{A.23g}$$

$$B_2 = 0 for w_s > u_* or z_a > 0.1h \tag{A.23h}$$

z = waterdepth
z_a = reference height near the bottom
$C(z)$ = sediment concentration at height z
C_a = sediment reference concentration at height z_a
h = Water depth
b = Rouse number

The concentration can be expressed as volume/volume or mass/volume, when C(z) and C_a have the same units. To make a prediction of the concentration reference concentration C_a at reference height z_a should be known. Both the Rouse and van Rijn equations give reasonable predictions, the powerlaw is useful when there is a desire to simplicity of mathematical calculations.

To predict C_a and Z_a Garcia and Parker 1991 have tested several expressions of which the following two give the best predictions:
Smith and Mclean (1977):

$$C_a = \frac{0.00156T_s}{1+0.0024T_s} \text{ at height } z_a = \frac{26.3\tau_{cr}T_s}{\rho g(s-1)} + \frac{d_{50}}{12} \tag{A.24}$$

van Rijn (1984)Equation 3.17:

$$C_a = \frac{0.015dT_s^{3/2}}{z_a D_*^{0.3}} \text{at height} z_a = \frac{\Delta_s}{2} \text{with} \Delta_s \text{given by a minimum value of } z_a = 0.01h \tag{A.25}$$

Zyserman and Fredsoe (1994)[61]:

$$C_a \frac{0.331(\theta_s - 0.045)^{1.75}}{1+0.720(\theta_s - 0.045)^{1.75})} \tag{A.26}$$

In equation xxx to xxx the following parameters are used:

C_a = concentration (volume/volume) at height z_a
Z_a = reference height

τ_{0s} = skin-friction bed shear stress
τ_{cr} = threshold bed shear stress for motion of sediment
$T_s = (\tau_{0s} - \tau_{cr})/\tau_{cr}$
d_50 = median grain diameter
h = water depth
g = gravity acceleration
ρ_w = density of water
ρ_s = density of sediment
$s = \rho_s/\rho_w$
ν = kinematic viscosity of water
$D_* = (\frac{g(s-1)}{\nu^2})^{1/3} d_{50}$
$\theta_s \frac{\tau_0 s}{g\rho(s-1)d_{50}}$ = skin-friction
Δ_s = height of sandwaves

A.2.3. Description of Suspended Sediment Transport

Calculations performed by programme and order of calculations:

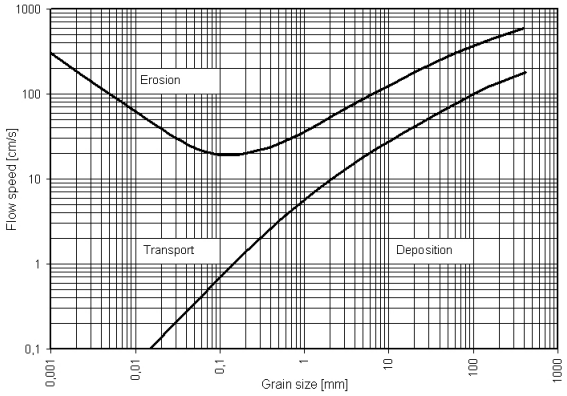

Figure A.1: Hjulstrom curve

$$D_{50} = isagivenvalue \tag{A.27}$$

Density ratio of sediment and water:

$$s = rho_s/rho_w \tag{A.28}$$

Roughness length for hydrodynamically rough flows [61]:

$$z_0 = \frac{d_{50}}{12} \tag{A.29}$$

Dimensionless grainsize diameter:

$$D_* = (\frac{g(s-1)}{\nu^3})^{1/3} d \tag{A.30}$$

Fall velocity(w_s) as derived by soulsby (1997)[61] formula for natural sands, based on optimising two coefficients in a combined viscous plus bluff body drag law against data for irregular grains:

$$w_s = \frac{\nu}{d_50}((10.36^2 + 1.049D_*^3)^{1/2} - 10.36) \text{ for all } D_* \tag{A.31}$$

The drag coefficient:

$$C_D = (\frac{\kappa}{1 + ln(z0/h)})^2 \text{with} \kappa = 0.40 \tag{A.32}$$

The bed shear stress is related to the depth-averaged current velocity u through the drag coefficient by the quadratic friction:

$$\tau_{0s} = \rho_w C_d u^2 \tag{A.33}$$

Threshold bed shear-stress formula as corrected by Soulsby and Whitehouse 1997 [61]:

$$\theta_{cr} = \frac{0.30}{1+1.2D_*} + 0.055(1 - exp(-0.020D_*)) \tag{A.34}$$

Threshold bed shear stress:

$$\tau_{cr} = \theta_{cr} g(rho_s - rho_w * d_{50}) \tag{A.35}$$

The transport parameter:

$$T_s = \frac{\tau_{0s} - \tau_{cr}}{\tau_{cr}} \tag{A.36}$$

Calculating the reference height and reference concentration using the relation provided by Smith and McLean (1977):

$$C_a = \frac{0.00156T_s}{1+0.0024T_s} \text{ at height } z_a = \frac{26.3\tau_{cr}T_s}{\rho g(s-1)} + \frac{d_{50}}{12} \tag{A.37}$$

Total skin friction:

$$u_* = C_D^{1/2} u \tag{A.38}$$

Calculating the rouse number:

$$b = \frac{w_s}{\kappa u_*} \tag{A.39}$$

Calculating the concentration at a certain height using the simple power law profile

$$C(z) = C_a(\frac{z}{z_a})^b \tag{A.40}$$

Calculating the concentration at a certain height using the Rouse profile:

$$C_z = C_a(\frac{z}{z_a}\frac{h-z_a}{h-z})^{-b} \tag{A.41}$$

Calculating the concentration in kg/m3:

$$C_m = C(z)\rho_s \tag{A.42}$$

A.2.4. Shear stress

Skin-friction contribution acts directly on the sediment grains, and it is therefore this contribution which is used to calculate the threshold of motion, bed load transport(with a few exceptions), and reference concentration or pick-up rate for grains in suspension. On the other hand, it is the total bed shear-stress that corresponds to the overall resistance of the flow, and determines the turbulence intensities which influence the diffusion of suspended sediment to higher levels in the water column(Chapter) 8. [61]

- Skin friction:(tau0s) produced by (and acting on) the sediment grains
- form drag (tau0f) produced by the pressure field associated with the flow over ripples and-or larger features on the bed
- sediment-transport contribution (Tau0t) caused by momentum transfer to mobilise grains

$$\tau_0 = \tau_{0s} + \tau_{0f} + \tau_{0t} \tag{A.43}$$

Thee contributions to Ustar, Theta and Z0 can be identified, using the subscripts s, f, t to produce relationships like equations (1), (2), (3 for each contribution.

If the bed is flat, and sediment transport is not intense, then equation Equation A.43 simplifies to tau0 = tau0s, and the distinction between total en skin-friction quantities is not necessary. This case is not uncommon for coars grains(d50>0.8mm), but finer sands are usually either ripppled(possibly with larger bedforms) or have intense sheet-flow transport. Calculate skin-friction bed shear-stress, tau0s, friction velocity, ustarS, and shields parameter, ShieldsS, using d=d50:

- if ThetaS < ThetaCR, then bed is immobile (assume rippled)
- ThetaCR < ThetaS < 0.8, then bed is mobile and rippled and or duned
- if thetaS > 0.8 then bed is mobile and flat with sheet-flow
- UstarS <= wS then no suspension
- if Ustar S > wS then sediment is suspended
- d50 > 0.8 ripples do not form w

for determining Tau0, a river based method can be used to determine the tau0. Ranging in value from (e.g. 0.384, 0.6, 0.965), resp, engelund, white et al, van rijn. Thesemethods predict dunes rather than ripples as the main roughness element.

A.3. Preliminary modelling: Concentration Profiles

Within this section the results of the Suspended sediment transport relations are provided.

- Suspended sediment transpot profiles for concentration and flow velocity(Rouse?)

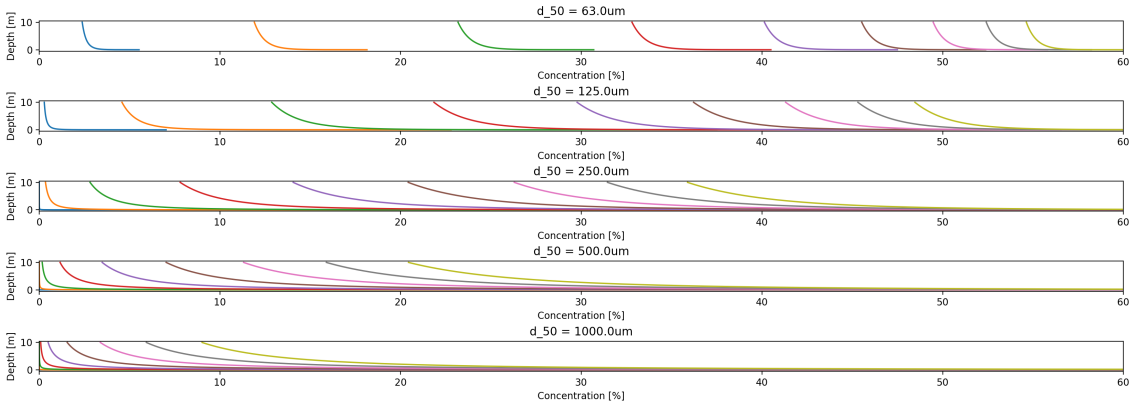

Figure A.2: Five graphs showing the concentration profiles for different d50 sedimetn sizes ranging from 63 um - 1 mm. The different lines in the graph show flow velocity ranging from 1 - 9 m/s.

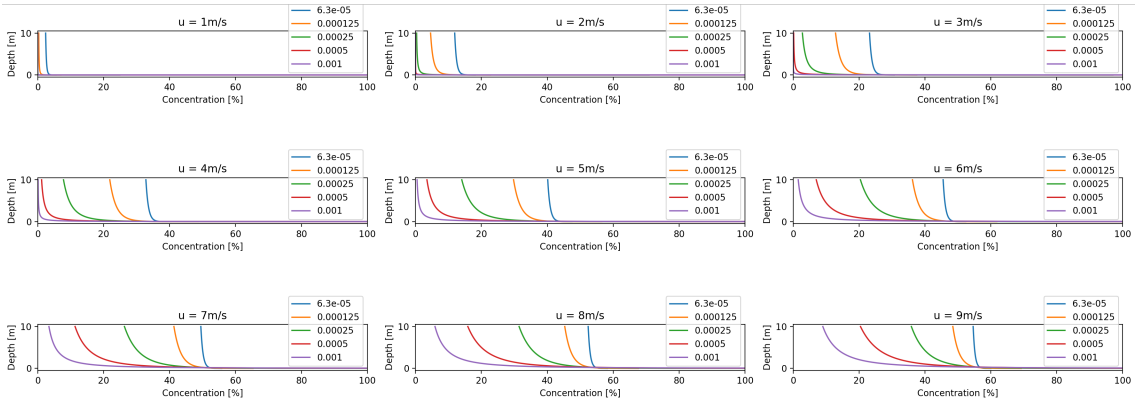

Figure A.3: 9 graphs showing different different flow velocities and the resulting concentration profiles due to different sediment sizes.

B

Derivation of 1D Shallow Water Equations for a Turbid Density Current

B.1. Navier-Stokes equations

B.1.1. Newton's Second Law

The Navier-Stokes equations describe the relation of velocity, pressure, temperature and density of a moving fluid. They can be derived with the basic conservation equation and continuity equations applied on the properties of fluids. To derive the fluid motion in equation form the continuity equation that dictates conditions of conservation apply the equation to the conservation of mass and momentum. These equations combined with a physical aspects [31].

The derivation of the momentum equation can be done in several ways. A quick derivation can be done by using Newton's laws combined with the application of the chain rule. Newtons second law:

$$\vec{F} = m\vec{a} \tag{B.1}$$

Body force is $\vec{F} = \vec{b}$ and substituting density for mass as a fixed control volume and infinitesimal fluid parcels are considered:

$$\vec{b} = \rho \frac{d}{dt}\vec{v}\,(x, y, z, t) \tag{B.2}$$

The body force acts throughout the fluid body. Applying the chain rule to derivative of the velocity:

$$\vec{b} = \rho\left(\frac{\partial \vec{v}}{dt} + \frac{\partial \vec{v}}{\partial x}\frac{\partial \vec{v}}{\partial t} + \frac{\partial \vec{v}}{\partial y}\frac{\partial \vec{y}}{\partial t} + \frac{\partial \vec{v}}{\partial z}\frac{\partial \vec{z}}{\partial t}\right) \tag{B.3}$$

Using the vector differential operator notation:

$$\vec{b} = \rho\left(\frac{\partial \vec{v}}{\partial t} + \vec{v}\cdot\nabla\vec{v}\right) \tag{B.4}$$

The conservation equations is complete. To derive the equations of motions for fluids assumptions about forces on the behaviour of fluids are needed. The force on the body force on the fluid is separated into two components, fluid stresses caused by viscosity assuming a Newtonian fluid and the external forces (later defined as slope and friction)[31]:

$$\vec{b} = \nabla\cdot\sigma + \vec{f} \tag{B.5}$$

In Equation B.5, σ is the stress tensor and $\vec{f}$ the external forces. The stress tensor σ consists of two terms, the hydrostatic pressure force and the stress deviator term. The stress deviator term accounts for shape change of the body. The $\vec{f}$ term can be composed of gravity and friction.

B.1.2. General Form of the Navier-Stokes Equation

The stress tensor σ can be denoted into two terms for the general form of the Navier-Stokes equation. First, the stress tensor[31]:

$$\sigma = \begin{pmatrix} \sigma'_{xx} & \tau_{xy} & \tau_{xy} \\ \tau_{yx} & \sigma'_{yy} & \tau_{yz} \\ \tau_{zx} & \tau_{zy} & \sigma'_{yy} \end{pmatrix} \tag{B.6}$$

From there the stress tensor can be split:

$$\begin{pmatrix} \sigma'_{xx} & \tau_{xy} & \tau_{xy} \\ \tau_{yx} & \sigma'_{yy} & \tau_{yz} \\ \tau_{zx} & \tau_{zy} & \sigma'_{yy} \end{pmatrix} = -\underbrace{\begin{pmatrix} p & 0 & 0 \\ 0 & p & 0 \\ 0 & 0 & p \end{pmatrix}}_{1} + \underbrace{\begin{pmatrix} \sigma_{xx} & \tau_{xy} & \tau_{xy} \\ \tau_{yx} & \sigma_{yy} & \tau_{yz} \\ \tau_{zx} & \tau_{zy} & \sigma_{yy} \end{pmatrix}}_{2} \tag{B.7}$$

1. The volumetric stress changing the volume of the body in the form of pressure force like the hydrostatic pressure. acting perpendicular on the the volume
2. The stress deviator tensor consists of normal-and shear-stresses determining the deformation and movement of the body.

Writing the stress deviator tensor in the form of T and substituting in Equation B.7 yields:

$$\sigma = -pI + T \tag{B.8}$$

With p the stress tensor, I the identity or unit matrix and T the stress deviator. Substituting equations Equation B.8 into Equation B.5 with $\vec{b}$ equal to Equation B.4 yields the most general form of the Navier-Stokes equation[31]:

$$\underbrace{\rho(\frac{\partial \vec{v}}{\partial t} + \vec{v} \cdot \nabla \vec{v}}_{1} = \underbrace{-\nabla p}_{2} + \underbrace{\nabla T}_{3} + \underbrace{\vec{f}}_{4} \tag{B.9}$$

with:

1. Inertial forces of the fluid.
2. The volumetric stress tensor: Pressure forces inhibits motion due to normal stresses and enlarging or reducing size of the body.
3. The stress deviator tensor: shear stress and horizontal friction. Shear stress induces viscous flow and turbulence.
4. The external force term: such as friction and gravity

The Navier-Stokes equations are is the balance of momentum and can not be applied until more aspects of the flow have been specified. **To fully describe fluid flow additional information is needed. The additional information includes boundary data, conservation of mass, balance of energy and/or an equation of state. It depends on the type of fluid. But a at least a stress tensor T must be determined and if the fluid is compressible an equation of state and energy are needed.** The continuity equation for 3D shallow water equations is described in the next section. The continuity equation for incompressible fluid is a statement for the conservation of mass:

$$\frac{\partial \rho}{\partial t} + \nabla(\rho u) = 0 \tag{B.10}$$

To apply the general form of the Navier-Stokes equation several elements have to be specified: The type of fluid needs an expression for the stress tensor and the fluid is assumed to be incompressible. An equation of state and an equation dictating conservation of energy are needed.

B.1.3. Newtonian Fluid

If an incompressible Newtonian fluid is assumed the assumption is concerned with the nature of the stress tensor. In this case the stress is proportional to the rate of deformation of the fluid, this means the change in velocity in the direction of the stress. The rate of deformation e.g. in the x-direction[31]:

$$\tau_{ij} = \mu(\frac{\partial u_i}{\partial x_j} + \frac{\partial u_j}{\partial x_i}) \tag{B.11}$$

The proportionality constant μ represents the viscosity of the fluid. The Navier-Stokes equation uses Stress divergence of $\nabla \cdot T$[31]:

$$\nabla \cdot T = \mu\nabla \begin{pmatrix} \sigma_{xx} & \tau_{xy} & \tau_{xy} \\ \tau_{yx} & \sigma_{yy} & \tau_{yz} \\ \tau_{zx} & \tau_{zy} & \sigma_{yy} \end{pmatrix} = \mu \begin{pmatrix} 2\frac{\partial u}{\partial x} & \frac{\partial u}{\partial y} + \frac{\partial v}{\partial x} & \frac{\partial u}{\partial z} + \frac{\partial w}{\partial x} \\ \frac{\partial u}{\partial y} + \frac{\partial v}{\partial x} & 2\frac{\partial v}{\partial x} & \frac{\partial v}{\partial z} + \frac{\partial w}{\partial y} \\ \frac{\partial u}{\partial z} + \frac{\partial w}{\partial x} & \frac{\partial v}{\partial z} + \frac{\partial w}{\partial y} & 2\frac{\partial w}{\partial z} \end{pmatrix} \tag{B.12}$$

This could be extended to the divergence terms in the same manner, the divergence can be replaced with a vector:

$$\nabla \cdot T = \mu\nabla^2 v \tag{B.13}$$

The Navier-Stokes equations for a incompressible Newtonian fluid with a conservative external field yield [31]:

$$\underbrace{\rho(\frac{\partial \vec{v}}{\partial t} + \vec{v} \cdot \nabla \vec{v})}_{1} = \underbrace{-\nabla p}_{2} + \underbrace{\mu\nabla^2 \vec{v}}_{3} + \underbrace{\vec{f}}_{4} \tag{B.14}$$

with:

1. Inertial force of the fluid consisting of the variation and convection term
2. The (hydrostatic) pressure forces by normal stresses and internal source term.
3. Stress term for horizontal friction an shear stress causing diffusion
4. External forces on the fluid such as gravitational forces and friction forces imposed by the bottom and wall. The terms are also referred to as source terms.

The equation Equation B.14 is the fundamental equation in the field of Hydraulic Engineering. It should be noted that many non-Newtonian approaches exist such as Bingham platics and Power-law fluids, this is beyond the scope of this thesis and are not discussed here.

The derivation provided in the above is a summary of [31].

B.2. Shallow Water Equations

B.2.1. Derivation of 1D Single Layer Shallow-Water Equations

Having derived the Navier stokes equations for an incompressible Newtonian fluid one can now derive the Shallow Water Equations(SWE's). To do so, several assumptions have to be made to arrive at the 1D Shallow Water equations.

First, rewriting the Navier stokes equations, Equation B.14 in the form of partial differential equations, this yields [63]:

$$\rho(\frac{\partial u}{\partial t} + u\frac{\partial u}{\partial x} + v\frac{\partial u}{\partial y} + w\frac{\partial u}{\partial z}) = -\frac{\partial p}{\partial x} + \mu\nabla^2 u + f_x \tag{B.15}$$

$$\rho(\frac{\partial v}{\partial t} + u\frac{\partial v}{\partial x} + v\frac{\partial v}{\partial y} + \frac{\partial u}{\partial z}) = -\frac{\partial p}{\partial y} + \mu\nabla^2 v + f_y \tag{B.16}$$

$$\rho(\frac{\partial w}{\partial t} + u\frac{\partial w}{\partial x} + v\frac{\partial w}{\partial y} + \frac{\partial w}{\partial z}) = -\frac{\partial p}{\partial z} + \mu\nabla^2 w + f_z \tag{B.17}$$

First assumption: the current depth/height and current width are much smaller than the length[34]. The flow is one dimensional and parallel to the bottom and walls of the channel and is varying slowly in time and horizontal direction. The terms in Equation B.16 become equal to zero. Also horizontal processes, x−direction, are most important for the dynamics of the current. The accelerations in the vertical direction are very small. One can assume hydrostatic pressure distribution. This is still reasonable when the current propagates on a very small incline. This yields to the hydrostatic balance for Equation B.17:

$$0 = -\frac{\partial p}{\partial z} - \rho g \tag{B.18}$$

Changes in y and z direction are very small compared to the x direction, y and z are neglected for Equation B.15 this yields:

$$\rho(\frac{\partial u}{\partial t} + u\frac{\partial u}{\partial x}) = -\frac{\partial p}{\partial x} + \mu\nabla^2 u + f_x \tag{B.19}$$

Secondly, either inertial or viscous forces dominate the current. The Reynolds number indicates the ratio of inertial resistance to viscous resistance for a flowing fluid:

$$Re = \frac{UL}{\nu} \tag{B.20}$$

In the Equation B.20; U is the velocity, L is the length(hydraulic radius or height) and v is the kinematic viscosity($1.3 \cdot 10^{-6}$) of the current. When the Reynolds number is larger than 1000 the current is inertial or inviscid, also referred to as turbulent flow. When the Reynolds number is smaller is more viscous or even laminar. Most currents within dam reservoirs will be in the turbulent regime, high Reynolds number, as the kinematic viscocity is very small compared to U and L. This results in the assumption that the current is inviscid. The viscous force term is small, second term on the right hand side of Equation B.19 is neglected:

$$\rho(\frac{\partial u}{\partial t} + u\frac{\partial u}{\partial x}) = -\frac{\partial p}{\partial x} + f_x \tag{B.21}$$

Thirdly, change of water depth over the length is very small, no (short-)waves nor a bottom topography is present influencing the water depth. Equation B.19 is integrated over the height h. This results in the pressure p with p_0 being the constant atmospheric pressure, this yields:

$$p(x,t) = p_0 + \rho g h(x,t) \tag{B.22}$$

Substituting B.22, the pressure equation, into B.21 and dividing by ρ yields:

$$\frac{\partial u}{\partial t} + u\frac{\partial u}{\partial x} = -g\frac{\partial h}{\partial x} + f_x \tag{B.23}$$

Integrating Equation B.23 over the height of the water column gives the 1D SWE for conservation of momentum:

$$\frac{\partial uh}{\partial t} + \frac{\partial u^2 h}{\partial x} + g\frac{1}{2}\frac{\partial h^2}{\partial x} = f_x \tag{B.24}$$

In which f_x is a source term, i.e. equal to friction and/or gravity if accounted for.
Fourthly, a turbid density current is driven by density difference. This assumption yields the following shallow water equation for the conservation of momentum:

$$\frac{\partial uh}{\partial t} + \frac{\partial u^2 h}{\partial x} + g'(\phi)\frac{1}{2}\frac{\partial h^2}{\partial x} = f_x \tag{B.25}$$

With $g'(\phi)$ being the reduced gravity. This equation can be solved with the continuity equation, Equation B.26, and the particle conservation equation Equation 4.11c which will be introduced in the section for the particle conservation equation. The continuity equation, for the conservation of mass, yields:

$$\frac{\partial h}{\partial t} + \frac{\partial uh}{\partial x} = 0 \tag{B.26}$$

Fifth, a homogeneous fluid is assumed, particles are distributed evenly across the height and length of the fluid. The density of the ambient fluid is constant and density of the current varies over length and time as particles will settle from the current. The density of the current is given by:

$$\rho_c(\phi) = \phi(x,t)\rho_s + (1-\phi(x,t))\rho_a \tag{B.27}$$

In which ρ_a is the density of the ambient fluid, ρ_s the sediment density and ϕ the volumetric concentration of the particles. The reduced gravity term yields:

$$g^{'}(\phi) = g\frac{\rho_c(\phi)-\rho_a}{\rho_a} \tag{B.28}$$

The reduced gravity is a function of the volume concentration of particles. It is assumed that ϕ is small and used as a Boussinesq approximation. Neglecting the O(ϕ) in the equation of mass and momentum except for teh gravitational term. The influence of the top fluid can be neglected due to the fact that the reservoir depth with ambient fluid is very large compared to the gravity current[34].

B.2.2. Summary: 1D Single Layer Shallow Water Equations

Continuity equation

$$\frac{\partial h}{\partial t} + \frac{\partial}{\partial x}(uh) = 0 \tag{B.29}$$

Momentum equation

$$\frac{\partial uh}{\partial t} + \frac{\partial u^2 h}{\partial x} + g'(\phi)\frac{1}{2}\frac{\partial h^2}{\partial x} = f_x \tag{B.30}$$

With $f_x = 0$ and the reduced gravity(g') in the form:

$$g^{'}(\phi) = g\frac{\rho_c(\phi)-\rho_a}{\rho_a} \tag{B.31}$$

B.3. Particle Conservation Equation

The concentration of particles in the current varies over depth and along the length of the turbidity current. Particles are kept in suspension and are move due to turbulence caused by advection. Particles leave the current by deposition and enter by erosion. Distribution of particles is assumed to be uniform along the depth of the current. Entrainment of water is neglected in this study, information on water entrainment is found in chapter 7. To account for the particles in the current one can now introduce the particle conservation equation[10][34]:

$$\frac{\partial \phi h}{\partial t} + \frac{\partial u\phi h}{\partial x} = E - D \tag{B.32}$$

The left side describes the conservation of particles. The right side contains, E the erosion of sediment and D the deposition of sediment explained in the next section which explains the source terms continuity, momentum and particle conservation equations.

B.4. 1D SWE with Particle Conservation, Friction, Gravity, Deposition and Erosion

Continuity equation

$$\frac{\partial h}{\partial t} + \frac{\partial uh}{\partial x} = 0 \tag{B.33}$$

Momentum equation with friction and gravity

$$\frac{\partial uh}{\partial t} + \frac{\partial u^2 h}{\partial x} + g'(\phi)\frac{1}{2}\frac{\partial h^2}{\partial x} = f_x \tag{B.34}$$

With reduced gravity(g'):

$$g^{'}(\phi) = g\frac{\rho_c(\phi)-\rho_a}{\rho_a} \tag{B.35}$$

And with f_x,:

$$f_x = g'(\phi)So - \frac{f}{8R}u^2 \tag{B.36}$$

The derivation of f_x including the slope and friction terms is provided in subsection B.5.1.
Particle conservation equation:

$$\frac{\partial \phi h}{\partial t} + \frac{\partial u \phi h}{\partial x} = D - E \tag{B.37}$$

With D and E equal to:

$$D = \tag{B.38}$$

$$E = \tag{B.39}$$

The derivation of D and E is provided in

B.5. Derivation of Source Terms

B.5.1. Friction and gravity

It was first assumed that $f_x = 0$. Within this section the $f_x \neq 0$. It is assumed that gravity and friciton within the channel are present. Conservation of momentum:

$$\frac{\partial uh}{\partial t} + \frac{\partial u^2 h}{\partial x} + g'(\phi)\frac{1}{2}\frac{\partial h^2}{\partial x} = f_x \tag{B.40}$$

There are two body forces acting on the channel fluid gravity and friction:

$$f_x = f_{x,g} + f_{x,f} \tag{B.41}$$

where $f_{x,g}$ is the body force due to gravity and $f_{x,f}$ is the body force due to friction.
The gravity component is calculated using trigonometry:

$$F_g = sin(\theta)gM \tag{B.42}$$

Where F_g is the force of gravity in the x-direction, g the gravitational acceleration force, θ the angle of the slope and M the mass.
The angle θ is described as:

$$sin\theta = \frac{Oppositeside}{adjacentside} \tag{B.43}$$

For small θ, which is the case for the slopes of rivers and channels and which is the case for the conceptual channels within the dam reservoirs, it can be assumed that:

$$\sin\theta = \tan\theta = \frac{Oppositeside}{adjacentside} = S \tag{B.44}$$

This yields:

$$f_{x,g} = gS \tag{B.45}$$

$f_{x,g}$ is the force per unit mass and S as the slope.

With the assumption that the energy grade line is not the same as the channel slope and for a reach of consistent slope there is consistent friction loss along the reach, this yields:

$$f_{x,f} = gS_f \tag{B.46}$$

To insert Equation B.46 and Equation B.45 into Equation B.40 it will become the 1D Saint-Venant equation in x direction:

$$\frac{\partial uh}{\partial t} + \frac{\partial u^2 h}{\partial x} + g'(\phi)\frac{1}{2}\frac{\partial h^2}{\partial x} = -g(S_f - S) \tag{B.47}$$

Assumptions for one dimensional unsteady open channel flow in the form of Saint-Venant equations:

1. The flow is one dimensional, the velocity is uniform in a cross-section and the transverse free-surface profile is horizontal
2. The streamline curvature is very small and the vertical fluid accelerations are are neglible; as a result, the pressure distrubtions are hydrostatic
3. Flow resistance and turbulent losses are the samea s for a steady unfirom equilitbirum flow for the same depth and velocity regardless of trends of the depth
4. the bed slope is small enough to satisfy: $cos\theta \approx 1$ and $sin\theta \approx tan\theta = \theta$
5. The water density is constant
6. The Saint Venant equations were developed for fixed boundary channels: That is, sediment motion is neglected....

Water flowing in a river is subject to two principal forces: gravity and friction. Gravity as driving force and friction resisting it. The balance between these forces determines the ability of flowing water to transport and erode sediment. The conservation of mass and momentum, given below, can be used to derive shear stress that acts on the channel bed, velocity profile and equations governing channel flow[67]:

$$\text{Conservation of Mass:} Q = Au \tag{B.48}$$

$$\text{Conservation of Momentum:} \rho_1 Q_1 u_1 = \rho_2 Q_2 u_2 \tag{B.49}$$

There are general types of flow:

- Steady: Velocity is constant with time
- unsteady: Velocity is variable with time
- Uniform: Velocity is constant with position
- non-uniform: Velocity is variable with position

To make a mathematical model the flow in a channel should be uniform and steady. Although in natural rivers the flow is non-uniform and unsteady, some models do incorporate this, but this will take a lot of computational effort.

Rivers or channel have irregularities in bed and bank topography that causes convergence and divergence of flow. These impose local gradients in flow velocity and shear stress. To make a solvable model, local differences are averaged by taking a reach average view of the river or channel.

A force balance of a volume of water in a reach with length l and slope θ is taken. It is assumed that accelerations are negligible and a non moving bed. A balance between gravitational force causing accelerating down stream and frictional resistance by the boundary slowing down the fluid to zero at the bed. This causes internal deformation of the fluid flow.

The gravitational force downstream:

$$F_g = 2AL\rho g sin\theta \tag{B.50}$$

The boundary/frictional resistance force:

$$F_f = \tau_b LP \tag{B.51}$$

τ_b is the average drag force per unit area on the boundary. Assuming no additional energy inputs or losses the gravitational force and the frictional resistance force have to be in balance:

$$F_f = F_f \tag{B.52}$$

$$\tau_b LP = AL\rho g sin\theta \tag{B.53}$$

The length L, wet perimeterP, surface area A, gravitational acceleration g, slope angle θ.
Assuming angles in the dam reservoir are small $sin\theta \approx tan\theta = S$, dividing by L and rearranging:

$$\tau_b = (\frac{A}{P})\rho g S \tag{B.54}$$

Defining the hydraulic radius as $R = A/P$, simplifying the equation to an expression for the reach average shear stress:

$$\tau_b = R\rho gS \tag{B.55}$$

(If channels are wide it could be assumed that $A/P \approx D$ thus resulting a in an equation approximately equal to the depth. Than it could be approximated by the depth slope product "The force exerted by flow on the channel bed is proportional to flow depth and slope":)

$$\tau_b = \rho gDS \tag{B.56}$$

This shear stress formula still does not provide any information on the flow velocity within the channel. This is done by Chezy in 1775 he applied a mathematical anayliss of the mechanics of uniform flow. For this two assumptions were made:

1. Force driving flow which is the down slope component of the weight of the water is exactly equal to the total force of bed resistance.
2. The resisting force of the flow per unit bed area varies with the square of the velocity: $\tau_b = ku^2$. With k being the roughness coefficient.

Rewriting Equation B.56:

$$ku^2 = R\rho gS \tag{B.57}$$

Rearranging:

$$u = \sqrt{\frac{R\rho gS}{k}} \tag{B.58}$$

The Chezy equation:

$$u = \sqrt{\frac{\rho g}{k}}\sqrt{RS} = C\sqrt{RS} \tag{B.59}$$

With:

$$C = \sqrt{\frac{\rho g}{k}} \tag{B.60}$$

With Chezy coefficient C. The average velocity in the channel should increase with square root of the gradient. The square root of the hydraulic radius, for wide shallow channels this is equal to the average depth. A coefficient that reflects the smoothness (inverse roughness) of the channel. Many empirical relations have been created. For this several empirical investigations have been done in which the simultaneous measurements of u, R and S in experimental flumes indicated that C varied slighlty with R in any given channel. From this new proportionalities were defined by Manning, Chezy, Darcy Weisbach, Soulsby etc etc. Each of them have there pro's and con's...

In this case the Darcy-Weisbach equation is used that is a fit for frictional losses in circular pipes that is modified for open channel in the form of:

$$f_f = \frac{8gRS}{u^2} \tag{B.61}$$

The Darcy Weisbach equation has the advantage that it is suitable for open channel flow
Rewritting:

$$u = \sqrt{\frac{8}{f}gRS} \tag{B.62}$$

The gravitational acceleration is modified to express the gravitational force exerted by the density difference $\Delta\rho$Assuming the current is also driven by a density difference the equation can be rewritten in the following form:

$$u = \sqrt{\frac{8}{f} g' R S} \tag{B.63}$$

with

$$g' = \frac{\rho_s - \rho_a}{\rho_a} \tag{B.64}$$

with:

$$\Delta\rho = \rho_s - \rho_a \tag{B.65}$$

An assumption for the friction factor is that of darcy weissbach that gives an empirical equation for the friction along a given length of the pipe to the average velocity of the fluid flow for an incompressible fluid. To describe the velocity of the turbidty current the chezy equation is used, this equation contains a dimensionless friction factor by darcy weisbach and the reduced gravity. This equation is proposed as an estimate for the velocity of a turbid density current, by Morris and Fan 1992 in the Reservoir sedimentation handbook [46] or by Middleton 1966 or Lofquist 1960 [43]:

$$u_c = \sqrt{\frac{8}{f} g' R g S_f} \tag{B.66}$$

$$-g'(S_f - S_0) = 0 \tag{B.67}$$

with

$$S_f = \frac{f}{8g'R} u^2 \tag{B.68}$$

$$-g'(\frac{f}{8g'R} u^2 - So) = 0 \tag{B.69}$$

$$g' So - \frac{f}{8R} u^2 = 0 \tag{B.70}$$

B.5.2. Deposition

The deposition flux(D):

$$D = \rho_s v_s \phi (1 - \alpha\phi)^n \tag{B.71}$$

With ρ_s sediment density, v_s particle settling velocity, ϕ particle concentration, n exponent depending on turbulence and α is 1 for hindered settling and 0 for non-hindered settling depending on the concentration of the flow. Within literature it is not clearly specified when one make a distinction between non-hindered and hindered settling. Within this study it is chose to always assume hindered settling.

Deposition of sediment grains is depended on the current velocity, grain settling velocity, turbulence and concentration. For a single grain the settling velocity in a stationary water column can be determined with:

$$v_s = \sqrt{\frac{4\Delta g d}{3C_D}} \tag{B.72}$$

For river flow the water is not stationary and settling is depended on the turbulence regime. The drag coefficient(C_D) depends on the flow regime which is related to the particle Reynolds number. There are three different turbulence regimes described for the particle Reynolds number(Re_p):

$$Re_p = \frac{w_0 d}{\nu} \tag{B.73}$$

$$C_D = \begin{cases} \frac{24}{Re_p} & Re_p < 1 \quad \text{Laminar regime} \\ \frac{24}{Re_p} + \frac{3}{\sqrt{Re_p}+0.34} & 1 < Re_p < 2000 \quad \text{Transition regime} \\ 0.34 & Re_p > 2000 \quad \text{Turbulent regime} \end{cases} \tag{B.74}$$

To determine the settling velocity one should determine if the flow is laminar, transitional or turbulent. Within the transitional regime an iteration is required to determine the settling velocity. It should be accounted for that particles have a certain grain size distribution over different diameters. Within this study it is assumed that particles have a median diameter(d_{50}). The iterative process is avoided by using the settling velocity by Ferguson and Church 2004, which is valid for a wide range of particle Reynolds numbers(Re_p):

$$v_s = \frac{\Delta g d_{50}^2}{C_1 v + \sqrt{0.75 C_2 \delta g d_{50}^3}} \tag{B.75}$$

In a turbidity current a certain concentration of particles is present. Due this concentration interaction with both the fluid and particles the settling velocity decreases compared to settling a stationary water column. The phenomenon is referred to as hindered settling. A relation for hindered settling is proposed by Richardson & Zaki (1954)[55]:

$$v_{s,h} = v_s(1-\phi)^n \tag{B.76}$$

The exponent n is determined by Rowe(1987). Where v_s is the settling velocity of a single grain and n is calculated with the method of Rowe (1987):

$$n = \frac{4.7 + 0.41 Re_{p,w}^{0.75}}{1 + 0.175 Re_{p,w}^{0.75}} \tag{B.77}$$

The Deposition flux (D) for hindered settling:

$$D = \rho_s v_s \phi (1 - \alpha\phi)^n \tag{B.78}$$

Introducing α equal to 0 if non hindered settling occurs or 1 hindered settling occurs.

B.5.3. Erosion

For particles to be eroded from the bed the the threshold of motion should be exceeded and partilces start to move and erode from the bed. Many studies have been done to quantify the process of erosion(pick-up) from the sediment bed. Many pick up functions are available such as those by Cao 2004, van Rijn 1984, Hu Cao 2008 Van Rhee 2010. Most of these pick up functions are based upon experimental result. The main focus of these studies was to improve the function for certain flow regimes. Within this study the flow is in the lower flow velocity regime, in which the van Rijn 1984 pick up function has provide to provide reasonable predictions. The van Rijn pick-up function denotes:

$$E_p = 0.00033 D_*^{0.3} (\frac{\theta - \theta_{cr}}{\theta_{cr}})^{1.5} \rho_s \sqrt{\Delta g d_{50}} \tag{B.79}$$

Since the mass, momentum and particle equation do not contain the sediment density one should devide by the density. The pick up function by van Rijn 1984 is used in the following form:

$$E = 0.00033 D_*^{0.3} (\frac{\theta - \theta_{cr}}{\theta_{cr}})^{1.5} \sqrt{\Delta g d_{50}} \tag{B.80}$$

with E being the pick up flux in [m/s] and the dimensionless grain size diameter (D_*):

$$D_* = (\frac{g\Delta}{v^2})^{1/3} d \tag{B.81}$$

With the critical shield number (θ_{cr}):

$$\theta_{cr} = \frac{0.30}{1 + 1.2 D_*} + 0.055[1 - exp(-0.020 D_*)] \tag{B.82}$$

B.5.4. Erosion by Cao 2004

Erosion capacity by Hu and Cao Concentration

$$\phi_i^n = c(1 + 31.5(\frac{u_{*,i}^n}{v_s})^{-1.46}) \tag{B.83}$$

with c = 0.6

$$E_{s,i}^n = \begin{cases} 0.3 & Z_i^n > Z_m \\ 3 \cdot 10^{-12} Z^{10} (1 - \frac{Z_c}{Z}) & Z_c < Z_i^n < Z_m \\ 0 & Z_i^n < Z_c \end{cases} \tag{B.84}$$

$$Z_i^n = (\frac{u_{*,i}^n}{v_s})(\frac{\sqrt{\Delta_{Rk} g d_{50}}^3}{\nu})^{0.6} \tag{B.85}$$

$$u_{*,i}^n = \sqrt{C_{D,i}^n u_i^n u_i^n} \tag{B.86}$$

$$C_{D,i}^n = (\frac{\kappa}{1 + ln(\frac{z_o}{h_i^n})}) \tag{B.87}$$

$z_{0=}$ 0.06

Settling velocity by Ferguson and Church

$$v_s = \frac{\Delta g d_{50}^2}{C_1 \nu + \sqrt{0.75 C_2 \Delta g d_{50}^3}} \tag{B.88}$$

$$\phi_i^{n+1} = \frac{[\phi h]_i^{n+1}}{h^{n+1}} \tag{B.89}$$

Erosion and Deposition by Cao 2004 Computational Dam-Break[18]

$$D = v_s (1 - C_a)^m C_a \tag{B.90}$$

$$C_a = \alpha c \tag{B.91}$$

α = min [2, (1-p)/c]
m = 2.0
n = 0.03
p = 0.4
s = 1.65
v = 1.2E-6
θ_{cr} = 0.045

$$E = \frac{160}{R^{0.8}} \frac{(1-p)}{\theta_{cr}} \frac{(\theta - \theta_{cr}) d_{50} U_\infty}{h} \tag{B.93}$$

Can be written as:

$$D = \alpha \phi v_s (1 - \alpha \phi)^m \tag{B.94}$$

$$D = \alpha \phi_i^n v_s (1 - \alpha \phi_i^n)^m \tag{B.95}$$

$$E = \begin{cases} \Phi(\theta - \theta_c) u h^{-1} d^{-0.2} & \theta \geq \theta_{cr} \\ 0 & else \end{cases} \tag{B.96}$$

$$E_i^n = \begin{cases} \Phi(\theta_i^n - \theta_{cr}) u_i^n (h_i^n)^{-1} d_{50}^{-0.2} & theta \geq \theta_{cr} \\ 0 & else \end{cases} \tag{B.97}$$

$$u_{*,i}^n = \sqrt{c_d u_i^n u_i^n} \tag{B.98}$$

$$\theta_i^n = \frac{u_{*,i}^n u_{*,i}^n}{S_o g d_{50}} \tag{B.99}$$

B.6. Model overview: check what to do with it

B.6.1. 1D SWE for Particle Driven Turbid Density Current: Friction, Gravity, Deposition and Erosion

- Equilibrium situation =0
- Friction and Gravity
- Deposition and Erosion

Continuity equation:

$$\frac{\partial h}{\partial t} + \frac{\partial uh}{\partial x} = 0 \tag{B.100}$$

Momentum equation with friction and gravity

$$\frac{\partial uh}{\partial t} + \frac{\partial u^2 h}{\partial x} + g'(\phi)\frac{1}{2}\frac{\partial h^2}{\partial x} = g'(\phi)So - \frac{f}{8R}u^2 \tag{B.101}$$

h is height, u is velocity, t is time, x is directional coordinate

Particle conservation equation with Deposition and Erosion:

$$\frac{\partial \phi h}{\partial t} + \frac{\partial u\phi h}{\partial x} = D - E \tag{B.102}$$

with f the friction coefficient by darcy weissach and equal too 0.025. D is the deposition and E the erosion.

R is the hydraulic radius:

$$R_{trapezoidal} = \frac{A_c}{P} = \frac{W_b h_c + 2h_c}{W_b + 2h_c\sqrt{5}} \tag{B.103}$$

with A_c = channel dimension, P the wet perimeter. W_b the bottom width, h_c the channel height. It is assumed that the channel is Trapezoidal with a natural sloping of the walls of 30 degrees.

Reduced gravity(g'):

$$g^{'}(\phi) = g\frac{\rho_m(\phi) - \rho_w}{\rho_w} \tag{B.104}$$

With ρ_w = 1000 kg/m^3 and rho_m the density of the mixture of water and sand:

$$\rho_m(\phi) = (1-\phi)\rho_w - (\phi)\rho_s \tag{B.105}$$

with ρ_s = 2650 kg/m^3 the density of sand. And ϕ the concentration. The deposition and erosion for a turbid density current over an erodible bed are proposed by Hu an Cao 2009 [33] For D the deposition and E the erosion:

$$D = v_s c_b \tag{B.106}$$

$$E = v_s E_s \tag{B.107}$$

With c_b the near bed concentration and the settling/fall velocity equal to that of ferguson and churche:

$$v_s = \frac{\Delta g d_{50}^2}{C_1 \nu + \sqrt{0.75 C_2 \Delta g d_{50}^3}} \tag{B.108}$$

With $d_5$0 the median grain size, C_1 = 18, C_2 = 1.
c_b

$$c_b = c(1 + 31.5(\frac{u_*}{v_s})^{-1.46}) \tag{B.109}$$

E_s friction coefficient, c the layer averaged volumetric sediment concentration (approximatly 0.6)

$$E_s = \begin{cases} 0.3 & Z > Z_m \\ 3 \cdot 10^{-12} Z^{10} (1 - \frac{Z_c}{Z}) & Z_c < Z < Z_m \\ 0 & Z < Z_c \end{cases} \tag{B.110}$$

With Z [33]:

$$Z = (\frac{u_*}{v_s})(\frac{\sqrt{R_k g d_{50}}^3}{\nu})^{0.6} \tag{B.111}$$

with v the kinematic viscosity of water (1.3*10-6 water at 10 degrees), R_k = the submerged specific gravity of sediment Z_c = 5.0 a critical value for the onset of significant suspension, Z_m = 13.2 denotes the maximum value of Z. [33]

$$R_k = \frac{\rho_s - \rho_w}{\rho_w} = 1.65 \tag{B.112}$$

$$u_*^2 = C_D u^2 \tag{B.113}$$

With C_D the drag coefficient as proposed by Soulsby 1997[61]:

$$C_D = (\frac{\kappa}{B + ln(\frac{z_o}{h})}) = (\frac{0.40}{1 + ln(\frac{z_o}{h})}) \tag{B.114}$$

with κ the von Karman constant and $B = 1$. z_o is obtained from the table below:

B.6.2. 1D SWE for Kinematic wave

For the numerical discretisation of the continuity, momentum and particle conservation equation a Forward in time Central in Space(FTCS) scheme is used.

- Explaination of method used
- stability criterion
- flux limiters
- convergence

Continuity equation:

$$\frac{\partial h}{\partial t} + \frac{\partial}{\partial x}(uh) = 0 \tag{B.115}$$

Discretisation continuity equation:

$$\frac{h_i^{n+1} - h_i^n}{\Delta t} + \frac{[uh]_{i+1}^n - [uh]_{i-1}^n}{2\Delta x} = 0 \tag{B.116}$$

$$h_i^{n+1} = h_i^n - \frac{\Delta t}{2\Delta x}([uh]_{i+1}^n - [uh]_{i-1}^n) \tag{B.117}$$

Momentum equation:

$$\frac{\partial uh}{\partial t} + \frac{\partial u^2 h}{\partial x} = -\frac{1}{2}g'(\phi)\frac{\partial h^2}{\partial x} \tag{B.118}$$

$$\frac{[uh]_i^{n+1} - [uh]_i^n}{\Delta t} + u\frac{[uh]_{i+1}^n - [uh]_{i-1}^n}{2\Delta x} + \frac{1}{2}g'(\phi)\frac{h_{i+1}^n h_{i+1}^n - h_{i-1}^n h_{i-1}^n}{2\Delta x} = 0 \tag{B.119}$$

$$u_i^{n+1} = \frac{[uh]_i^{n+1}}{h_i^{n+1}} \tag{B.120}$$

Particle equation:

$$\frac{\delta}{\delta t}(\phi h) + \frac{\partial}{\partial x}(u\phi h) = -v_s\phi \tag{B.121}$$

$$\frac{[\phi h]_i^{n+1} - [\phi h]_i^n}{\Delta t} + u\frac{[\phi h]_{i+1}^n - [\phi h]_{i-1}^n}{2\Delta x} + v_{s,i}\phi_i = 0 \tag{B.122}$$

$$\phi_i^{n+1} = \frac{[\phi h]_i^{n+1}}{h^{n+1}} \tag{B.123}$$

The particle settling velocity is described by Ferguson and Church:

$$v_s = \frac{\Delta g d_{50}^2}{C_{1v} + \sqrt{0.75 C_2 \Delta g d_{50}^3}} \tag{B.124}$$

Reduced gravitational force

$$g'(\phi)_i^n = \frac{\rho_m(\phi)_i^n - \rho_w}{\rho_w} \tag{B.125}$$

$$\rho_{m,i}^n = (1 - \phi_i^n)\rho_w + \phi_i^n \rho_s \tag{B.126}$$

B.6.3. Model Overview

This paragraph provides the model overview of the 1D Shallow Water Equations for a Particle driven Turbid Density Current with gravity, friction, Particle Settling and Erosion.

continuity

$$h_i^{n+1} = h_i^n - \frac{\Delta t}{2\Delta x}([uh]_{i+1}^n - [uh]_{i-1}^n) \tag{B.127}$$

momentum

$$[uh]_i^{n+1} = [uh]_i^n - \Delta t \frac{u_{i+1}^n [uh]_{i+1}^n - u_{i-1}^n [uh]_{i-1}^n}{2\Delta x} - \frac{1}{2}\Delta t \frac{g'(\phi)_{i+1}^n h_{i+1}^n h_{i+1}^n - g'(\phi)_{n-1}^n h_{i-1}^n h_{i-1}^n}{2\Delta x} + \Delta t g'(\phi)_i^n S_o - \Delta t \frac{f}{8R} u_i^n u_i^n \tag{B.128}$$

$$u_i^{n+1} = \frac{[uh]_i^{n+1}}{h_i^{n+1}} \tag{B.129}$$

Particle conservation equation:

$$[\phi h]_i^{n+1} = [\phi h]_i^n - \Delta t \frac{u_{i+1}^n [\phi h]_{i+1}^n - u_{i-1}^n [\phi h]^n + i - 1}{2\Delta x} - \Delta t v_{s,i}^n \phi_i^n + \Delta t v_{s,i}^n E_{s,i}^n \tag{B.130}$$

$$\phi_i^{n+1} = \frac{[\phi h]_i^{n+1}}{h^{n+1}} \tag{B.131}$$

Reduced gravitational force

$$g'(\phi)_i^n = \frac{\rho_m(\phi)_i^n - \rho_w}{\rho_w} \tag{B.132}$$

$$\rho_{m,i}^n = (1 - \phi_i^n)\rho_w + \phi_i^n \rho_s \tag{B.133}$$

Concentration

$$\phi_i^n = c(1 + 31.5(\frac{u_{*,i}^n}{v_s})^{-1.46}) \tag{B.134}$$

with c = 0.6

Erosion capacity by Hu and Cao:

$$E_{s,i}^n = \begin{cases} 0.3 & Z_i^n > Z_m \\ 3 \cdot 10^{-12} Z^{10}(1 - \frac{Z_c}{Z}) & Z_c < Z_i^n < Z_m \\ 0 & Z_i^n < Z_c \end{cases} \tag{B.135}$$

$$Z_i^n = (\frac{u_{*,i}^n}{v_s})(\frac{\sqrt{\Delta_{Rk} g d_{50}}^3}{\nu})^{0.6} \tag{B.136}$$

$$u_{*,i}^n = \sqrt{C_{D,i}^n u_i^n u_i^n} \tag{B.137}$$

$$C_{D,i}^n = (\frac{\kappa}{1 + ln(\frac{z_o}{h_i^n})}) \tag{B.138}$$

$z_{0=}$ 0.06

Settling velocity by Ferguson and Church

$$v_s = \frac{\Delta g d_{50}^2}{C_1 \nu + \sqrt{0.75 C_2 \Delta g d_{50}^3}} \tag{B.139}$$

$$\phi_i^{n+1} = \frac{[\phi h]_i^{n+1}}{h^{n+1}} \tag{B.140}$$

Erosion and Deposition by Cao (2004) Computational Dam-Break

$$D = v_s(1 - C_a)^m C_a \tag{B.141}$$

$$C_a = \alpha c \tag{B.142}$$

α = min [2, (1-p)/c]
m = 2.0
n = 0.03
p = 0.4
s = 1.65
v = 1.2E-6
θ_{cr} = 0.045

$$E = \frac{160}{R^{0.8}} \frac{(1-p)}{\theta_{cr}} \frac{(\theta - \theta_{cr}) d_{50} U_\infty}{h} \tag{B.144}$$

Can be written as:

$$D = \alpha\phi v_s(1 - \alpha\phi)^m \tag{B.145}$$

$$D = \alpha\phi_i^n v_s(1 - \alpha\phi_i^n)^m \tag{B.146}$$

$$E = \begin{cases} \Phi(\theta - \theta_c) u h^{-1} d^{-0.2} & \theta \geq \theta_{cr} \\ 0 & else \end{cases} \tag{B.147}$$

$$E_i^n = \begin{cases} \Phi(\theta_i^n - \theta_{cr}) u_i^n (h_i^n)^{-1} d_{50}^{-0.2} & theta \geq \theta_{cr} \\ 0 & else \end{cases} \tag{B.148}$$

$$u_{*,i}^n = \sqrt{c_d u_i^n u_i^n} \tag{B.149}$$

$$\theta_i^n = \frac{u_{*,i}^n u_{*,i}^n}{S_o g d_{50}} \tag{B.150}$$

h = water depth
Δt = time step size
Δx = space step size
u = velocity
κ = 0.4 von Karman constant
C_D = Drag coefficient
u_* = friction velocity
E_s = erosion capacity
$g'(\phi)$ = reduced gravity m/s2
S_o = slope of the channel
R = Hydraulic radius of trapezoidal channel
ρ_m = mixture density depended on concentration
ρ_s = 2650 kg/m3 (density sand)
ρ_w = 1000 kg/m3 (density water)
$v = 1.3 \cdot 10^{-6}$ kinematic viscosity
$\phi_{initial}$ = 0.02 (2 percent volume concentration ≈ 1030 kg/m3)
z_0 = 0.06 (Table 7 Soulsby)
c = 0.6
d_{50} = 60 - 400 um median sediment diameter(??)
g = 9.81
Δ_{rk} = 1.65
C_1 = 18
C_2 = 1
Z = ...

Physical parameters																
d_{50} [μm]	h [m]	u [m/s]	ϕ [-]	L [m] ϕ [-]	W_b [m]	t[s]	S [-]	m [-]	ν_s [m/s]	Δ	D_*	R [m]	ν	θ	θ_{cr}	g
1	2	3	4	5	6	7	8	9	10	11	12	13	14	15	16	17

Table B.1: Physical parameters to test the influence of grid size on the numerical model

C

Python Code

C.1. Steady State

```
#!/usr/bin/env python3
# -*- coding: utf-8 -*-
"""
Created on Mon Feb 25 11:47:51 2019

@author: koos
"""
import numpy as np
import matplotlib.pyplot as plt
from sympy.solvers import solve
from sympy import Symbol
from sympy import roots, solve_poly_system

class Turbidity:
    def __init__(self, U_r, A_r,rho_w,rho_rw,rho_r,f,A_c, S, g, rho_c, W_b, H, H_trap, Wb_trap):
        self.U_r = U_r
        self.A_r = A_r #100.0
        self.rho_w = rho_w
        self.rho_rw = rho_rw# 1000.0
        self.rho_r = rho_r #1050.0
        self.f = f #0.025
        self.A_c = A_c# 20.0
        self.S = S #0.001
        self.g = g #9.81
        self.rho_c = rho_c #1100#1160.3
        self.W_b = W_b
        self.H = H
        self.H_trap = H_trap
        self.Wb_trap = Wb_trap


    def set_values(self,U_r):
        self.U_r = U_r

    def calc_R_hydraulic_radius(self):
        self.R = self.A_c / (2*(np.sqrt(self.A_c)+np.sqrt(self.A_c)))
        return (self.R)
```

```
def calc_u_channel(self):
    self.U_c = np.sqrt((8/self.f)*((self.rho_c - self.rho_w)/(self.rho_w))*self.R * self.S *
    #print("U_c_square = ", self.U_c)

def calc_rho_channel(self):
    self.rho_channel = (1.0 - (self.U_r * self.A_r)/(self.U_c*self.A_c))* self.rho_rw + self
    #print("Rho_channel =", self.rho_channel)


def calc_R_trapezoidal_30_degree(self, afdrukken = False):
    self.labda_trap     = self.H_trap* np.sqrt(5)
    self.kappa          = 2 * self.H_trap
    self.Wt_trap        = self.Wb_trap + 2* self.kappa
    self.A_trac         = self.Wb_trap * self.H_trap + self.kappa * self.H_trap
    self.P_trac         = self.Wb_trap  + (2*self.labda_trap) #+ self.Wt_trap
    self.R_trac         = self.A_trac / self.P_trac


def calc_u_channel_trap(self):
    self.U_c_trap = np.sqrt((8/self.f)*((self.rho_c - self.rho_w)/(self.rho_c))*self.R_trape
    #print("U_c_trap =",self.U_c_trap)

def calc_rho_channel_trap(self):
    self.rho_channel = (1.0 - (self.U_r * self.A_r)/(self.U_c_trap*self.A_c))* self.rho_rw +
    #print("Rho_channel_trap = ", self.rho_channel)


def determine_rho_channel(self):
    self.calc_R_hydraulic_radius()
    current_guess_rho_c = 1100
    #print("Slope", self.S)

    for i in range(100):
        guess_U = np.sqrt((8/self.f)*((current_guess_rho_c - self.rho_w)/(current_guess_rho_c
        next_guess_rho_c = (1.0 - (self.U_r * self.A_r)/(guess_U*self.A_c))* self.rho_rw + s

        if abs(current_guess_rho_c - next_guess_rho_c) < 0.5:
            return (next_guess_rho_c, guess_U)
        else:
            current_guess_rho_c = next_guess_rho_c
    print("Iteration limit reached!!!")



def determine_rho_channel_trapezoidal(self):
    self.calc_R_trapezoidal_30_degree()
    current_guess_rho_c_2 = 1080
    #print("Trap slope = ", self.S)
    for i in range(10):
        guess_U_2 = np.sqrt((8/self.f)*((current_guess_rho_c_2 - self.rho_w)/(current_guess_r
        next_guess_rho_c_2 = (1.0 - (self.U_r * self.A_r)/(guess_U_2*self.A_trac))* self.rho_


        if abs(current_guess_rho_c_2 - next_guess_rho_c_2) < 0.5:
            return (next_guess_rho_c_2, guess_U_2)
```

```
            else:
                current_guess_rho_c_2 = next_guess_rho_c_2
        print("Iteration limit reached!!!")

    def plot_dens_slope_higher_density_rectangle(self):
        self.A_c_list = [100, 225, 400, 625, 900]
        self.Colour_list = ['b','g', 'r', 'c', 'm', 'y', 'k', 'w']
        self.zipped = zip(self.A_c_list, self.Colour_list)

        for (self.A_c, self.colour) in self.zipped:

            self.outputs = []

            for self.S in np.arange(0.001, 0.05, 0.001):
                #T = Turbidity(self.U_r, self.A_r, self.rho_w, self.rho_rw,self.rho_r,self.f,self.A_c,
                self.result = self.determine_rho_channel()
                self.outputs.append((self.result[0], self.result[1], self.S))


            self.slope_list = []
            self.density_list = []
            self.velocity_list = []
            for self.triplet in self.outputs:
                self.slope_list.append(self.triplet[2])
                self.density_list.append(self.triplet[0])
                self.velocity_list.append(self.triplet[1])
        #fig = plt.figure()
        #ax1 = fig.add_subplot(211)
            plt.figure(1)
            Title = "Slope_Density"
            plt.plot(self.slope_list, self.density_list, self.colour ,  label= "W = H = " + str(np.sqr
            plt.title("Rectangular Channel; Slope, Density" + " (A_river = " + str(self.A_r)+"m2" + "
            plt.xlabel("Slope [-]")
            plt.ylabel("Density channel [kg/m3]")
            plt.legend()
            plt.savefig("Rectangular_Channel_" + str(Title)+'.pdf', bbox_inches="tight", pad_inches=0)

            plt.figure(2)
            Title = "Slope_Velocity"
            plt.plot(self.slope_list, self.velocity_list, self.colour, label = "A_c = " + str(self.A_c
            plt.title("Rectangular Channel; Slope, Velocity" + " (A_river = " + str(self.A_r)+"m2" + "
            plt.xlabel("Slope channel [-]")
            plt.ylabel("Velocity channel [m/s]")
            plt.legend()
            plt.savefig("Rectangular_Channel_" + str(Title)+'.pdf', bbox_inches="tight", pad_inches=0)

        self.Wb_trap = 10
        self.H_trap_list = [10, 15, 20, 25, 30]
        self.Colour_list = ['b','g', 'r', 'c', 'm', 'y', 'k', 'w']
        self.zipped = zip(self.H_trap_list, self.Colour_list)

        for (self.H_trap, self.colour) in self.zipped:
            self.outputs = []
            #for self.H_trap in self.H_trap_list:
            for self.S in np.arange(0.001, 0.05, 0.001):
                #T = Turbidity(self.U_r, self.A_r, self.rho_w, self.rho_rw,self.rho_r,self.f,self.A_c,
```

```
            self.result = self.determine_rho_channel_trapezoidal()
            self.outputs.append((self.result[0],self.result[1], self.S))

        self.slope_list = []
        self.density_list = []
        self.velocity_list = []
        self.H_trap_list = []

        for self.triplet in self.outputs:
            self.slope_list.append(self.triplet[2])
            self.density_list.append(self.triplet[0])
            self.velocity_list.append(self.triplet[1])
            #self.H_trap_list.append(self.triplet[3])

        plt.figure(3)
        Title= "Slope_Density_Changing_denst"
        plt.plot(self.slope_list, self.density_list, self.colour, label = "A_trac = " + str(
        plt.title("Trapezoidal channel: Slope, Density"+ " (A_river = " + str(self.A_r)+"m2"
        plt.xlabel("Slope [-]")
        plt.ylabel("Velocity channel [m/s]")
        plt.legend()
        plt.savefig("Trapezoidal_channel_" + str(Title)+'.pdf', bbox_inches="tight", pad_inc


        plt.figure(4)
        Title= "Slope_Velocity_Changing_Denst"
        plt.plot(self.slope_list, self.velocity_list, self.colour, label = "A_trac = " + str
        plt.title("Trapezoidal channel: Slope, Velocity" + " (A_river = " + str(self.A_r)+"m
        plt.xlabel("Slope channel [-]")
        plt.ylabel("Velocity channel [m/s]")
        plt.legend()
        plt.savefig("Trapezoidal_channel_" + str(Title)+'.pdf', bbox_inches="tight", pad_inc



    def calc_hydr_rect_radius_vs_slope(self): #WITHOUT RESERVOIR RETURNFLOW
        self.outputs = []
        for self.S_1 in np.arange(0.001, 0.05, 0.001):
            self.A_c_123 = ((3*self.rho_c * self.f * self.U_r**2 * self.A_r**2) / (8 * self.g *
            self.A_c = self.A_c_123
            self.result = self.calc_R_hydraulic_radius()
            self.W_H = np.sqrt(self.A_c_123)

            self.R = self.A_c / (2*(np.sqrt(self.A_c)+np.sqrt(self.A_c)))
            self.Uc_rect = np.sqrt((8 *(self.rho_c - self.rho_w) * self.R * self.g * self.S_1)/(


            self.outputs.append((self.A_c_123, self.S_1, self.result, self.W_H, self.Uc_rect))
            #print(self.W)
        self.slope_list = []
        self.surface_list = []
        self.hydr_radi_list = []
        self.W_H_list = []
        self.Uc_rect_list = []

        for self.duplet in self.outputs:
```

```
            self.slope_list.append(self.duplet[1])
            self.surface_list.append(self.duplet[0])
            self.hydr_radi_list.append(self.duplet[2])
            self.W_H_list.append(self.duplet[3])
            self.Uc_rect_list.append(self.duplet[4])
        plt.figure(5)
        Title = "Slope_Surface_Height_equals_Width"
        plt.plot(self.slope_list, self.surface_list, label = "A_rect" + " for rho_c = " + str(self.rho
        plt.xlim(0,0.05)
        plt.ylim(0,1000)
        plt.title("Rectangular channel(h=W): Slope, Cross-sectional area")
        plt.ylabel("Area [m2]")
        plt.xlabel("Slope [-]")
        plt.legend()
        plt.savefig("Rectangular_channel_" + str(Title)+'.pdf', bbox_inches="tight", pad_inches=0)

        plt.figure(6)
        Title = "Slope_hydraulic_radius"
        plt.plot(self.slope_list, self.hydr_radi_list, label = "Radius" + " for rho_c = " + str(self.r
        plt.xlim(0,0.05)
        plt.ylim(0,8)
        plt.title("Rectangular Channel(h=W): Slope, Hydraulic Radius")
        plt.xlabel("Slope[-]")
        plt.ylabel("Hydraulic radius [m]")
        plt.legend()
        plt.savefig("Rectangular_channel_" + str(Title)+'.pdf', bbox_inches="tight", pad_inches=0)


        plt.figure(16)
        Title = "Flow_Velocity_Slope"
        plt.plot(self.slope_list, self.Uc_rect_list, label =" for rho_c = " + str(self.rho_c))
        plt.xlabel("Slope [-]")
        plt.ylabel("Flow velocity [m/s]")
        plt.title("Rectangular Channel(h=W): Flow velocity, Slope")
        plt.legend()
        plt.savefig("Rectangular_channel_" + str(Title)+'.pdf', bbox_inches="tight", pad_inches=0)


        plt.figure(15)
        plt.plot(self.slope_list, self.W_H_list, label = "W=H= " + "for rho_c = " + str(self.rho_c))
        #plt.xlim(0,0.05)
        #plt.ylim(0,8)
        Title = "Width_Height_Hydraulic_radius"
        plt.title("Rectangular Channel(h=W): Width, Height and Hydraulic radius")
        plt.xlabel("Slope[-]")
        plt.ylabel("Hydraulic radius [m]")
        plt.legend()
        plt.savefig("Rectangular_channel_" + str(Title)+'.pdf', bbox_inches="tight", pad_inches=0)


    def calc_hydr_trap_radius_vs_slope(self): #WITHOUT RESERVOIR RETURNFLOW

        self.W_b_list = [5, 20, 40, 60, 80, 160, 320] #, 15, 20, 25, 30]
        self.Colour_list = ['b','g', 'r', 'c', 'm', 'y', 'k', 'darkgrey', 'k', 'skyblue', 'cyan']
        self.zipped = zip(self.W_b_list, self.Colour_list)
```

```
for (self.W_b, self.colour) in self.zipped:
    self.outputs = []
    for self.H in np.arange(1.0, 50.0, 1.0):
        self.A_c_trap = self.W_b * self.H + 2*self.H**2

        #print(self.A_c_trap)
        self.p = self.W_b + 2 *self.H* np.sqrt(5)
        self.R_trap = self.A_c_trap / self.p
        self.S_12 =  (self.p / self.A_c_trap**3) * ((3*self.f*self.rho_c*self.U_r**2 * s

        self.U_c_22 = np.sqrt(((8*(self.rho_c - self.rho_w) * self.g * self.R_trap * sel
        self.outputs.append((self.H, self.A_c_trap, self.p, self.R_trap, self.S_12, self


    self.H_list = []
    self.A_c_trap_list = []
    self.p_list = []
    self.R_trap_list = []
    self.S_12_list = []
    self.U_c_22_list = []


    for self.fiveplet in self.outputs:
        self.H_list.append(self.fiveplet[0])
        self.A_c_trap_list.append(self.fiveplet[1])
        self.p_list.append(self.fiveplet[2])
        self.R_trap_list.append(self.fiveplet[3])
        self.S_12_list.append(self.fiveplet[4])
        self.U_c_22_list.append(self.fiveplet[5])

    plt.figure(7)
    Title = "Hydraulic_radius_Slope"
    plt.plot(self.S_12_list, self.R_trap_list, self.colour, label = "W_b = " + str(self.W
    plt.xlim(0,0.05)
    plt.xlabel("Slope [-]")
    plt.ylabel("Hydraulic radius [m]")
    plt.title("Trapezoidal Channel: Hydraulic radius, Slope")
    plt.legend()
    plt.savefig("Trapezoidal_Channel_" + str(Title)+'.pdf', bbox_inches="tight", pad_inch

    plt.figure(8)
    Title = "Depth_Slope"
    plt.plot(self.S_12_list, self.H_list, self.colour, label = "W_b = " + str(self.W_b) +
    plt.xlim(0,0.05)
    plt.ylim(0,40)
    plt.xlabel('Slope[-]')
    plt.ylabel('Depth [m]')
    plt.title("Trapezoidal Channel: Depth, Slope")
    plt.legend()
    plt.savefig("Trapezoidal_Channel_" + str(Title)+'.pdf', bbox_inches="tight", pad_inch


    plt.figure(9)
    Title = "Velocity_Slope"
    plt.plot(self.S_12_list, self.U_c_22_list, self.colour, label = "W_b = " + str(self.W
```

```
            plt.xlim(0,0.05)
            plt.ylim(0,5)
            plt.xlabel("Slope [-]")
            plt.ylabel("Flow velocity [m/s]")
            plt.title("Trapezoidal Channel: Velocity vs Slope")
            plt.legend()
            plt.savefig("Trapezoidal_Channel_" + str(Title)+'.pdf', bbox_inches="tight", pad_inches=0)

            plt.figure(10)
            Title = "Cross_section_Slope"
            plt.plot(self.S_12_list, self.A_c_trap_list, self.colour, label = "W_b = " + str(self.W_b)
            plt.xlabel("Slope [-]")
            plt.ylabel("Surface area [m2]")
            plt.xlim(0,0.01)
            plt.title("Trapezoidal Channel: Cross-sectional area, Slope")
            plt.legend()
            plt.savefig("Trapezoidal_Channel_" + str(Title)+'.pdf', bbox_inches="tight", pad_inches=0)


    def calc_1040(self): #WITHOUT_RESERVOIR_RETURN_FLOW_CHANGING_WIDTH
        self.calc_R_trapezoidal_30_degree()
        self.rho_c = 1040
        #self.W_b = 10


        self.W_b_list = [5, 10, 20, 30, 40, 50, 60, 70, 80, 90] #, 15, 20, 25, 30]
        self.Colour_list = ['b','g', 'r', 'c', 'm', 'y', 'k', 'darkgrey', 'k', 'skyblue', 'cyan']
        self.zipped = zip(self.W_b_list, self.Colour_list)
        for (self.W_b, self.colour) in self.zipped:
            self.outputs = []
            for self.H in np.arange(5.0, 30.0, 1.0):
                self.A_c_5 = (self.W_b * self.H) + (2*self.H**2)
                self.p = (self.W_b*self.H) + (2 *self.H* np.sqrt(5))
                self.R_5 = self.A_c_5 / self.p
                self.rho_r = self.rho_c
                self.U_c = ((self.U_r * self.A_r * self.rho_rw) - (self.rho_r * self.U_r *self.A_r))
                self.S_123 = (self.U_c**2) * ((self.f*self.rho_c)/(8* (self.rho_c - self.rho_w)* self

                self.U_c_123 = np.sqrt(((8*(self.rho_c - self.rho_w) * self.g * self.R_5 * self.S_123
                self.outputs.append((self.S_123, self.R_5, self.H, self.U_c, self.A_c_5))
                #print(self.U_c)

                #print(self.U_c_123)
                #print(self.S_123)
                #print(self.A_c_5)
            self.S_123_list = []
            self.U_123_list = []
            self.R_5_list = []
            self.H_list = []
            self.U_c_list = []
            self.A_c_5_list = []

            for self.oneplet in self.outputs:
                self.S_123_list.append(self.oneplet[0])
                #self.U_123_list.append(self.oneplet[1])
                self.R_5_list.append(self.oneplet[1])
```

```
            self.H_list.append(self.oneplet[2])
            self.U_c_list.append(self.oneplet[3])
            self.A_c_5_list.append(self.oneplet[4])



        plt.figure(11)
        Title = "Hydraulic_radius_Slope"
        plt.plot(self.S_123_list, self.R_5_list, self.colour, label = "W_b = " + str(self.W_
        plt.xlim(0,0.05)
        plt.ylim(0,8)
        plt.xlabel("Slope [-]")
        plt.ylabel("Hydraulic radius [m]")
        plt.title("Trapezoidal Channel with Reservoir-Returnflow: Hydraulic Radius, Slope" )
        plt.legend()
        plt.savefig("Trapezoidal_Channel_with_Returnflow_" + str(Title)+'.pdf', bbox_inches=


        plt.figure(12)
        Title = "Velocity_Slope"
        plt.plot(self.S_123_list, self.U_c_list, self.colour, label = "W_b = " + str(self.W_
        plt.xlim(0,0.05)
        plt.ylim(0,5)
        plt.xlabel("Slope [-]")
        plt.ylabel("Channel velocity [m/s]")
        plt.title("Trapezoidal Channel with Reservoir-Returnflow: Velocity, Slope" )
        plt.legend()
        plt.savefig("Trapezoidal_Channel_with_Returnflow_" + str(Title)+'.pdf', bbox_inches=

        plt.figure(13)
        Title = "Depth_Slope"
        plt.plot(self.S_123_list, self.H_list, self.colour, label = "W_b = " + str(self.W_b)
        plt.xlim(0,0.05)
        plt.ylim(0,30)
        plt.xlabel("Slope [-]")
        plt.ylabel("Channel depth")
        plt.title("Trapezoidal Channel with Reservoir-Returnflow: Depth, Slope")
        plt.legend()
        plt.savefig("Trapezoidal_Channel_with_Returnflow_" + str(Title)+'.pdf', bbox_inches=

        plt.figure(14)
        Title = "Cross_section_Slope"
        plt.plot(self.S_123_list, self.A_c_5_list, self.colour, label = "W_b = " + str(self.
        plt.xlim(0,0.05)
        plt.ylim(0,1000)
        plt.xlabel("Slope [-]")
        plt.ylabel("Channel surface area [m2]")
        plt.title("Trapezoidal Channel with Reservoir-Returnflow: Cross-sectional area, Slop
        plt.legend()
        plt.savefig("Trapezoidal_Channel_with_Returnflow_" + str(Title)+'.pdf', bbox_inches=


#print(self.H_1)
```

```
    def dimensieloos(self):
        self.rho_c = 1040
        #self.Q = 1000
        self.W_b = 10
        self.U_river_1 = [0.1, 0.2, 0.4, 0.6, 0.8, 1.0, 2.0, 3.0, 4.0, 5.0]


        for self.U_river in self.U_river_1:
            self.outputs = []
            for self.A_c in np.arange(0.001,500, 10):
                #print("2", self.A_c)
                self.H_1 = (- self.W_b + np.sqrt(self.W_b**2 - (4 * 2 * (-self.A_c)) )) / 4
                #print(self.H_1)
                self.P = self.W_b + 2 * self.H_1 * np.sqrt(5)
                self.R = self.A_c / self.P
                self.S = (self.U_river**2 * self.f * self.rho_c) / (8 * (self.rho_c - self.rho_w) * se

                self.Q = self.U_river * self.A_c

                self.outputs.append((self.S, self.H_1, self.A_c, self.Q, self.U_river, self.R))
                #print(self.S)
                #print(self.P)


            self.S_list         = []
            self.H_1_list       = []
            self.A_c_list       = []
            self.Q_list         = []
            self.U_river_list   = []
            self.R_list         = []
            for self.plet in self.outputs:
                self.S_list.append(self.plet[0])
                self.H_1_list.append(self.plet[1])
                self.A_c_list.append(self.plet[2])
                self.Q_list.append(self.plet[3])
                self.U_river_list.append(self.plet[4])
                self.R_list.append(self.plet[5])
            #print(self.S_list)

            plt.figure(34)
            plt.plot(self.S_list, self.A_c_list)
            plt.xlim(0,0.05)
            plt.ylim(0,500)
            plt.xlabel("Slope [-]")
            plt.ylabel("Surface [m2]")


            plt.figure(35)
            plt.plot(self.S_list, self.Q_list, label = "U = " + str(self.U_river_1))
            plt.xlim(0, 0.05)
            plt.ylim(0, 2000)
            plt.xlabel("Slope[-]")
            plt.ylabel("Discharge [m3/s]")

            plt.figure(36)
            plt.plot(self.S_list, self.R_list)
```

```
            plt.xlim(0, 0.05)
            plt.ylim(0,7.0)
            plt.xlabel("Slope [-]")
            plt.ylabel("Hydraulic radius")

    def Voor_H_en_Wb(self):
        self.rho_c = 1040
        #self.Q = 1000
        self.W_b_1 = [20, 30, 40, 50, 60]
        self.H_1_1 = np.arange(1, 40, 1)
        self.U_river_1 = [1, 2, 3, 4, 5]

        for self.U_river in self.U_river_1:

            for self.W_b in self.W_b_1:
                self.outputs = []
                for self.H_1 in self.H_1_1:
                    #print("2", self.A_c)
                    #self.H_1 = (- self.W_b + np.sqrt(self.W_b**2 - (4 * 2 * (-self.A_c)) )) / 4
                    #print(self.H_1)
                    self.A_c = self.W_b * self.H_1 + 2 * (self.H_1)**2
                    self.P = self.W_b + 2 * self.H_1 * np.sqrt(5)
                    self.R = self.A_c / self.P
                    self.S = (self.U_river**2 * self.f * self.rho_c) / (8 * (self.rho_c - self.rh

                    self.Q = self.U_river * self.A_c
                    #print(self.S)
                    self.outputs.append((self.S, self.H_1, self.A_c, self.Q, self.U_river, self.
                    #print(self.S)
                    #print(self.P)


                self.S_list         = []
                self.H_1_list       = []
                self.A_c_list       = []
                self.Q_list         = []
                self.U_river_list   = []
                self.R_list         = []
                for self.plet in self.outputs:
                    self.S_list.append(self.plet[0])
                    self.H_1_list.append(self.plet[1])
                    self.A_c_list.append(self.plet[2])
                    self.Q_list.append(self.plet[3])
                    self.U_river_list.append(self.plet[4])
                    self.R_list.append(self.plet[5])
                    #print(self.S_list)

            plt.figure(30)
            Title = "Surface_Slope_Equal_Rho_U_A"
            plt.plot(self.S_list, self.A_c_list)# label = "U = " + str(self.U_river_1[n])) #self
            plt.xlim(0,0.05)
            plt.ylim(0,4000)
            plt.title("Trapezoidal Channel: Surface, Slope. Equal U, A, rho")
            plt.xlabel("Slope [-]")
            plt.ylabel("Surface [m2]")
            plt.legend( ['u = 1 m/s', 'u = 2 m/s', 'u = 3 m/s','u = 4 m/s','u = 5 m/s'])
```

```
            plt.savefig("Trapezoidal_Channel_Equal_Parameters_" + str(Title)+'.pdf', bbox_inches="tigh

            plt.figure(31)
            Title = "Discharge_Slope"
            plt.plot(self.S_list, self.Q_list)#, label = "U = " + str(self.U_river_1))
            plt.xlim(0, 0.05)
            plt.ylim(0, 10000)
            plt.title("Trapezoidal channel: Discharge, Slope. Equal U, A, rho")
            plt.xlabel("Slope[-]")
            plt.ylabel("Discharge [m3/s]")
            plt.legend(['u = 1 m/s', 'u = 2 m/s', 'u = 3 m/s','u = 4 m/s','u = 5 m/s'])
            #plt.legend()
            plt.savefig("Trapezoidal_Channel_Equal_Parameters_" + str(Title)+'.pdf', bbox_inches="tigh


            plt.figure(32)
            Title = "Hydraulic_Radius_Slope"
            plt.plot(self.S_list, self.R_list) #, label = "U = " + str(self.U_river_1))
            plt.xlim(0, 0.05)
            plt.title("Trapezoidal channel: Hydraulic radius, Slope. Equal U, A, rho")
            plt.xlabel("Slope [-]")
            plt.ylabel("Hydraulic radius")
            plt.legend(['u = 1 m/s', 'u = 2 m/s', 'u = 3 m/s','u = 4 m/s','u = 5 m/s'])
            plt.savefig("Trapezoidal_Channel_Equal_Parameters_" + str(Title)+'.pdf', bbox_inches="tigh



def main():
    U_r = 2.0 #bovenstroomse snelheid
    A_r = 550 #oppervlakte
    rho_rw = 1000 #dichtheid rivier water (word nu niet gebruikt)
    rho_w = 1000 #dichtheid water
    rho_r = 1040.0 #dichthied inkomende rivier
    f = 0.025 #friction coefficient
    #A_c = 170 #Oppervlakte channel
    #S = 0.01 #Slope channel
    g = 9.81 #fall velocity
    rho_c = 1040 #rho channel die gelijk moet zijn aan Rho_channel
    H_trap = 5
    Wb_trap = 5
    W_b = 10 #breedte van de bodem van trapezoidal kanaal
    H = 10    #diepte van trapezoidal kanaal
    A_c = 1
    S = 0.001

    T = Turbidity(U_r, A_r, rho_w, rho_rw,rho_r,f,A_c, S, g, rho_c, W_b, H, H_trap, Wb_trap)


    #T.plot_dens_slope_higher_density_rectangle()
    #T.calc_hydr_rect_radius_vs_slope() #WITHOUT RESERVOIR RETURNFLOW

    #T.calc_hydr_trap_radius_vs_slope() # WITHOUT RESERVOIR RETURNFLOW
    #T.calc_hydr_rect_radius_vs_slope()
    #T.calc_hydr_trap_radius_vs_slope()
    #T.calc_1040()
```

```
    #T.calc_Ur_Uc()
    T.Voor_H_en_Wb()
    #T.dimensieloos()

if __name__ == '__main__':
        main()
```

C.2. Numerical Model

C.2.1. Simulator

```
import math
import numpy as np

def simulate(simulated_time, simulated_length, cell_size, u, h_in, d, phi_in, W_b, g, Delta, C_1
    d_50        = d * 10**-6
    nx          = math.ceil(simulated_length/cell_size) + 1     # number of cells / spatial reso
    l           = simulated_length                              # total length of simulated doma
    dx          = cell_size                                     # cell size, step size...
    dt          = 0.01 * (2* dx / u)                            # dt according to cfl condition =
    nt          = math.ceil(simulated_time / dt)                # number of time steps
    H           = h_in
    D_star      = d_50 * (((g*Delta)/((vis)**2))**(1/3))
    theta_cr    = (0.30 / (1+(1.2* D_star))) + (0.055 * (1-(np.exp(-(0.020*D_star)))))
    #theta_cr  = 0.045
    #Hydraulic radius dependend op height H
    R           = (W_b*H + 2* H** 2) / (W_b + 2 * H * np.sqrt(5))
    # fall velocity ferguson and church:
    v_s         = (Delta * g * (d_50)**2) / (C_1 * (vis) + np.sqrt(0.75 * C_2 * g * (d_50)**3))



    print('vs                          = ', v_s)
    print('cell size(dx)               = ', cell_size)
    print('time step (dt)              = ', dt)
    print('simulated time(t)           = ', simulated_time)
    print('number of time steps(nt)    = ', nt)
    print('number of cells (nx)        = ', nx)
    print('D_star                      = ', D_star)
    print('theta_cr                    = ', theta_cr)
    print('h_in                        = ', h_in)
    print('u_in                        = ', u)
    print('R(hydraulic radius)         = ', R)
    #zero lists
    h           = np.zeros(nx) #array with zeros
    u_list      = np.zeros(nx)
    uh          = np.zeros(nx)
    phi_list    = np.zeros(nx)
    phi_h       = np.zeros(nx)
    rho_mn_list = np.zeros(nx)
    gn          = np.zeros(nx)
    phi_hn      = np.zeros(nx)
    U_star      = np.zeros(nx)
    theta       = np.zeros(nx)
    E_s         = np.zeros(nx)
    hn          = h.copy()
```

```
un          = u_list.copy()


#INITIAL CONDITIONS

#initial conditions van h
hn[int(0) : ]           = 0.001

for n in range(nt + 1): #looping accros a number of time steps
    ### Boundary conditions
    hn[-1]          = hn[-2] #neumann boundary
    h[-1]           = h[-2] #neumann boundary
    h[0]            = h_in
    hn[0]           = h_in

    u_list[0]       = u
    u_list[-1]      = u_list[-2] #
    un[0]           = u
    un[-1]          = un[-2] #

    uh[0]           = u*h_in

    phi_hn[0]       = phi_in * h_in
    phi_h[0]        = phi_in * h_in
    phi_list[0]     = phi_in
    phi_hn[-1]      = phi_hn[-2] #
    phi_list[-1]    = phi_list[-2] #

    E_s[0]          = 0
    E_s[-1]          = E_s[-2] #


    ### input van WID
    #hn[70:80]          = 1.2
    #h[70:80]           = 1.2
    #u[70:80]           = 1.2

    #un[70:80]          = 1.1
    #u_list[70:80]      = 1.1
    #phi_h[70:80]       = 0.09
    #phi_hn[70:80]      = 0.09
    #phi_list[70:80]    = 0.09
    #hn[70:80]          = 1.2
    #h[70:80]           = 1.2

    h[1:-1] = (A* hn[2:] +  B * hn[1:-1] + C * hn[:-2]) / (A+B+C)\
    - (dt / (2*dx)) * (un[2:]* hn[2:] - un[:-2] * hn[:-2])

    rho_mn_list[1:-1] = phi_list[1:-1] * rho_s + (1 - phi_list[1:-1] ) * rho_w

    gn[1:-1] = g * (rho_mn_list[1:-1] - rho_w) / rho_w

    if source_gravity:
        source_gravity_value = (dt * gn[1:-1]*S *hn[1:-1])
    else:
        source_gravity_value = 0
```

```
        if source_friction:
            source_friction_value = ((dt * f)/ (8*R)) * un[1:-1] * un[1:-1] *hn[1:-1]
        else:
            source_friction_value = 0
        #de discretisatie van uh Momentum Equation
        uh[1:-1] = ((A* un[2:]* hn[2:] + B * un[1:-1] * hn[1:-1] + C * un[:-2]* hn[:-2]) /(A+B+C
        - (dt / (2 * dx)) * (un[2:] * un[2:] * hn[2:] - un[:-2] * un[:-2] * hn[:-2])\
        - (1.0/2.0) * (dt/(2*dx)) * (gn[2:] * hn[2:]*hn[2:] - gn[:-2]*hn[:-2]*hn[:-2]) \
        + source_gravity_value - source_friction_value
        #+ (dt * gn[1:-1]*S *hn[1:-1]) - ((dt * f)/ (8*R)) * un[1:-1] * un[1:-1] *hn[1:-1]
\

        # u bepalen
        u_list[1:-1] = uh[1:-1]/ (h[1:-1]) # epsilon divide by zero

        # phiH bepalen op nieuwe tijdsstap
        #U_star[1:-1] =  np.sqrt(C_d * un[1:-1] ** 2)
        #theta[1:-1] = (U_star[1:-1]**2) / (Delta * g * d_50)

        #simplified form of the above:
        #theta = (C_d * u ** 2) / (Delta * g * d_50)
        #print('theta              = ', theta)
        #theta[1:-1] = ((C_d * ((un[1:-1]) ** 2)) / (Delta * g * d_50))


        theta = (C_d * (un**2)) / (Delta * g * d_50)

        critical_cells = theta > theta_cr
        E_s = ((0.00033*D_star**0.3) * ( (((theta-theta_cr)/theta_cr) * critical_cells) **1.5) *

        #E_s = (0.00033*1.0618**0.3) * (((theta-theta_cr)/theta_cr)**1.5) * np.sqrt(Delta * g *
        #print(E_s)
        #print(E_s)
        '''
        for i in range(len(theta[1:-1])):
            E_s[i] = 0
            if theta[i]  > (theta_cr + 0.05):
                E = (0.00033*D_star**0.3) * (((theta[i]-theta_cr)/theta_cr)**1.5) * np.sqrt(Delta
                #E = phi_constant * (theta[i] - theta_cr) * (7/6)*un[i] * (hn[i]**-1) * (d_50 **
                E_s[i] = E
                #E_s[i] = A * E_s[i] + B * E_s[i-1] / A+ B


#                 print(i)
#                 print(E_s[i])
#                 print(un[i])
         '''
        if source_sedimentation:
            source_sedimentation_value = dt * v_s * phi_list[1:-1]
        else:
            source_sedimentation_value = 0

        if source_erosion:
            source_erosion_value = dt * E_s[1:-1]
        else:
```

```
            source_erosion_value = 0

        if hindered_erosion:
            hindered_erosion_value = (1 - ((phi_list*3)/(1 - 0.6)))**1.38
        else:
            hindered_erosion_value = np.ones(nx)
        #'''settling of particles due to v, ferguson and churge'''
        #'''Erosion capacity of the flow'''
        phi_h[1:-1] =  (A* phi_hn[2:] +  B * phi_hn[1:-1] + C * phi_hn[:-2]) / (A+B+C)\
        - (dt / (2*dx)) * (un[2:]* phi_hn[2:] - un[:-2] * phi_hn[:-2])\
        + source_erosion_value * hindered_erosion_value[1:-1] - source_sedimentation_value

        #+dt * E_s[1:-1] #- dt * v_s * phi_list[1:-1] +
        #- dt * v_s * phi_list[1:-1] * (1-phi_list[1:-1] )**4

        # phi bepalen door te delen door h van de nieuwe tijdstap
        phi_list[1:-1] = (phi_h[1:-1]) / (h[1:-1])

        # limiting the concetration to 100% otherwise (+-infinity solutions)
        phi_list_max = phi_list < 0.30
        phi_list = phi_list * phi_list_max + np.invert(phi_list_max) * 0.30

        hn[-1]          = hn[-2] #neumann boundary
        h[-1]           = h[-2] #neumann boundary
        h[0]            = h_in
        hn[0]           = h_in

        u_list[0]       = u
        u_list[-1]      = u_list[-2] #
        un[0]           = u
        un[-1]          = un[-2] #

        uh[0]           = u*h_in

        phi_hn[0]       = phi_in * h_in
        phi_h[0]        = phi_in * h_in
        phi_list[0]     = phi_in
        phi_hn[-1]      = phi_hn[-2] #
        phi_list[-1]    = phi_list[-2] #

        E_s[0]          = 0
        E_s[-1]          = E_s[-2] #

        hn      = h.copy()
        un      = u_list.copy()
        phi_hn  = phi_h.copy()


    return (h, u_list, phi_list)



if __name__ == '__main__':
    print('This is not a stand-alone python file!\nImport it in your main file and call the simulate f
```

C.2.2. Plotting Scripts

```
#!/usr/bin/env python3
# -*- coding: utf-8 -*-
"""

@author: koos2
"""
import numpy as np
import matplotlib.pyplot as plt
import math
import time

start = time.clock()
print('Simulation Started')

import simulator_WID as sim

def plot_full_model(simulated_time, simulated_length, cell_size, u, W_b, g, Delta, C_1, C_2, vis
    #PRESET CONDITONS

    #Start of plotting part
    output_list_phi     = []
    output_list_u       = []
    output_list_h       = []
    output_list_d       = []
    output_list_s       = []

    for h_in in input_values_h_in:
        for S in input_values_S_in:
            for phi_in in input_values_phi_in:
                for d in input_d_50_values:
                    (h, u_list, phi_list) = sim.simulate(simulated_time, simulated_length, cell_s
                    output_list_phi.append(phi_list)
                    output_list_u.append(u_list)
                    output_list_h.append(h)
                    output_list_d.append(d)
                    output_list_s.append(S)

            print('Simulation for              =  cell size = ' + str(cell_size)+ ' d_50 = ' +
            print('Finished, phi_in = ', str(phi_in))
    l               = simulated_length
    nx              = math.ceil(simulated_length/cell_size) + 1
    #plotting figures
    for i in range(len(output_list_phi)):
            nx2 = math.ceil(simulated_length/input_cell_sizes[0]) + 1
            #plt.plot(np.linspace(0,l, nx2), output_list_phi[i], label = "cell size = "+str(inpu
            plt.figure(51)
            plt.plot(np.linspace(0,(l), nx2), output_list_phi[i]/0.01, label = "t: " + '%.1f'
% (simulated_time) + ' [s]')# + '%d'  % (output_list_d[i]) +'$\mu$m' ) #str(output_list_d[i]) +
            plt.figure(52)
            plt.plot(np.linspace(0,(l), nx2), output_list_u[i], label = 't: ' + '%.1f'
%  (simulated_time) + ' [s]') #+ '%d' % (output_list_d[i])+ '$\mu$m')
            plt.figure(53)
            plt.plot(np.linspace(0,(l), nx2), output_list_h[i], label = "t: "+ '%.1f'
%  (simulated_time) + ' [s]') #+ '%d' % (output_list_d[i])+ '$\mu$m')
```

```
    Title = "Full_Model_WID_case_study_0_1"
    Title_plot =  '$h_{in}$ = ' + str(h_in) + ', $u_{in}$ = ' + str(u) + ', $\phi_{in}$ = '+ str(phi_i
+   ', Slope = ' + str(S) + ', $\Delta$t = 0.007 ' + ', $\Delta$x = ' + '0.1'

    plt.figure(51)
    plt.xlim(0,(l))
    plt.ylim(0,40.0)
    plt.grid(b=bool, which='major', axis='both')
    plt.grid(which='minor', linestyle='-')
    plt.minorticks_on()
    #plt.rcParams["axes.titlesize"] = 8
    plt.title(str(Title_plot)) # + str(u) + ', h_in = ' + str(h_in)+ ', d_50 =' + str(d)+ ', Time '+ s
    plt.ylabel('Concentration [%]') #Height [m] , , Velocity [m/s]
    plt.xlabel('Distance [m] ')
    plt.legend(loc ='upper right', prop={'size': 8})
    plt.savefig("Concentration_" + str(Title)+'.pdf', bbox_inches="tight", pad_inches=0)
    plt.savefig("Concentration_" + str(Title)+'.png', bbox_inches="tight", pad_inches=0)

    plt.figure(52)
    plt.xlim(0,(l))
    plt.ylim(0,1.7)
    plt.grid(b=bool, which='major', axis='both')
    plt.grid(which='minor', linestyle='-')
    plt.minorticks_on()
    plt.title(str(Title_plot)) # + str(u) + ', h_in = ' + str(h_in)+ ', d_50 =' + str(d)+ ', Time '+ s
    plt.ylabel('Velocity [m/s]') #Height [m] , , Velocity [m/s]
    plt.xlabel('Distance [m] ')
    plt.legend(loc ='upper right', prop={'size': 8})
    plt.savefig("Velocity_" + str(Title)+'.pdf', bbox_inches="tight", pad_inches=0)
    plt.savefig("Velocity_" + str(Title)+'.png', bbox_inches="tight", pad_inches=0)

    plt.figure(53)
    plt.xlim(0,(l))
    plt.ylim(0,4.0)
    plt.grid(b=bool, which='major', axis='both')
    plt.grid(which='minor', linestyle='-')
    plt.minorticks_on()
    plt.title(str(Title_plot)) # + str(u) + ', h_in = ' + str(h_in)+ ', d_50 =' + str(d)+ ', Time '+ s
    plt.ylabel('Height [m]') #Height [m] , , Velocity [m/s]
    plt.xlabel('Distance [m] ')
    plt.legend(loc ='upper right', prop={'size': 8})
    plt.savefig("Height_" + str(Title)+'.pdf', bbox_inches="tight", pad_inches=0)
    plt.savefig("Height_" + str(Title)+'.png', bbox_inches="tight", pad_inches=0)



    end = time.clock()
    print('Simulation time              =  '+ str(end - start) + ' [s]')
    print('Simulation Complete')



if __name__ == '__main__':
    g                   = 9.81              # Gravitational acceleration [m/s2]
```

```
Delta                = 1.65              #
vis                  = 1.3 * 10**-6      #Kinematic viscosity at 10 degrees celcius [m2/s]
rho_w                = 1000              #density water [kg/m3]
rho_s                = 2650              #density sediment [kg/m3]
f                    = 0.025             #darcy weissbach friction factor [-]
C_d                  = f/8               #drag coefficient according to darcy weisbach [-]
#n                   = 0.03
p                    = 0.4
phi_constant         = 0.015
#RICHARDSON AND ZAKI SETTLING
C_1                  = 18
C_2                  = 1


#Channel parameters
W_b                  = 10
input_values_S_in    = [0.001]
m                    = 4.0
#h_in                 = [1.0, 2.0, 3.0, 4.0]
input_values_h_in    = [1.0]
u                    = 0.3
#phi_in               = 0.02 # rho_w * %water + rho_s * %sediment
input_d_50_values    = [50]
input_values_phi_in = [0.02] #, 0.03, 0.04, 0.05, 0.06, 0.07, 0.08]
#Nummerical aspects
input_cell_sizes     = [1.0]
cell_size            = 1.0               # size of the cells in meters; lower value = more de
simulated_time       = 8000
#input_values_simulated_time =[100]          # total simulated time in seconds 2000
simulated_length     = 1000              # total simulated domain length in meters 700
# numerical scheme
A                    = 0.1           #0.01 standaard
B                    = 1.0           #1.0 standaard
C                    = 0.1           #0.01 standaard
#WID PARAMETERS
Delta_p              = 100000        #kpa pressure drop
D_nozzle             = 0.05          #nozzle diameter
L_wid                = 5.0             #wid influence length
n_0                  = 0.4
n_i                  = 0.6
u_wid                = 14.14
C_k                  = 1.0


#Sourceterms: If true it is taken into account, if false its not taken into account
source_gravity              = True
source_friction             = True
source_sedimentation        = True
source_erosion              = True
hindered_erosion            = True # default = false
source_wid_height           = True
source_wid_concentration    = True

plot_full_model(simulated_time, simulated_length, cell_size, u, W_b, g, Delta, C_1, C_2, vis
```